INVESTIGATION OF COMBINED BIOLOGICAL ROLES OF NEURAMINIDASE 1 AND GD3 SYNTHASE IN GLYCOLIPID METABOLISM

A Thesis Submitted to
the Graduate School of
Izmir Institute of Technology
in Partial Fulfillment of the Requirements for the Degree of

MASTER OF SCIENCE

in Molecular Biology and Genetics

by
Berkay DAĞALP

July 2020
İZMİR

ACKNOWLEDGMENTS

For giving me the opportunity to play a minor part in the projects of his lab, I would like to thank my supervisor Prof. Dr. Volkan SEYRANTEPE who always supported me and showed great patience throughout my studies. His endless ambition and enthusiasm towards this field have made a great impact on me therefore motivated me to always look for the perfect in my studies as well as in my personal life.

I am truly honored to be able to experiment on the mice that was gifted to our lab from one of the greatest scientists in this research field, Dr. Alessandra d'Azzo and Dr. Roger Sanhoff.

My special thanks to Prof. Dr. Yusuf BARAN and Prof. Dr. Bünyamin AKGÜL for letting me to use their equipment for my experiments.

I'm very grateful for "The Scientific and Technological Research Council of Turkey (TÜBITAK)" (117Z259) for financially supporting our project. Also Intensified cooperation (IntenC) of German-Turkish bilateral agreement provided us the mice.

I appreciate my current members as well as the ones graduated, who taught me many important aspects of this profession. Seçil A. DEMİR, Zehra K. TIMUR, O. Yipkin CALHAN, Nurselin ATEŞ, Orhan Kerim Inci, Melike CAN, Hande Hatice Basırlı, Tugçe SENGUL. I also appreciate the undergraduate students who helped during this period. Selman Yanbul, Berkan Kanmaz, Betülay KUS, Buket YILANCIOGLU, Sena SEVİNDİ, Ebru ADA, Tekin Can SOBACI, Özlem BOZDEMIR.

To have such a valuable veterinarian for our work was a great privilege for us there for I want to thank Guzin Savran IPLIKCI.

My deepest gratitude belongs to my beloved family. They never stopped supporting me in every case and always backed me up. I would like to thank them for the many sacrifices they made throughout my life.

ABSTRACT

INVESTIGATION OF COMBINED BIOLOGICAL ROLES OF NEURAMINIDASE 1 AND GD3 SYNTHASE IN GLYCOLIPID METABOLISM

Neuraminidases or sialidases are classified enzymes hydrolases the sialic acid residues from the glycoconjugates. In vertebrates, so far four different neuraminidases have been identified having distinct roles besides degradation of glycoconjugates. Neuraminidases differ in subcellular locations where Neuraminidase 1 is mainly localized in lysosomes having crucial regulatory roles and forms a multienzyme complex with protective protein/cathepsin A and ß-galactosidase. Only Neu1 is recognized when its functions or a component from the complex they together forged are defected, resulting two severe lysosomal storage disorders, sialidosis and galactosialidosis. To shed light on these disorders, Neu1-/- mice model lacking the enzyme was generated. By addition of sialic acid residue to the structure of Glycosphingolipids (GSLs), complex sugars in the membrane surface that provide special properties to cell, gangliosides are generated that further processed into 0-, a-, -b, -c series. Since the function of Neu1 in Glycosphingolipid pathway is unclear, to investigate the role of Neu1in this pathway, Neu1-/- mice crossed with the mice lacking b-and c- series of gangliosides, the GD3S-/- mice are used to generate Neu1-/-GD3S-/- mice. Even though mice showed indifferent ganglioside profile with a thin layer chromatography, they displayed decreased apoptotic signals and ER-stress markers with RT-PCR. However, western blotting and immunohistochemical studies revealed severe cell death in the brain. Moreover severe behavioral deficits were observed with open field and rotarod tests. The effects of b- and c- series of gangliosides on double knock-out mice still require further research that might reveal important roles in terms of cell death mechanism.

ÖZET

NÖROMİNİDAZ 1 VE GD3 SENTAZ ENZİMLERİNİN GLİKOLİPİT METABOLİZMASINDAKİ BİRLEŞİK BİYOLOJİK ROLÜNÜN ARAŞTIRILMASI

Nöraminidazlar, diğer bir ismi ile siyalidazlar, siyalik içeren şekerlenmiş konjuge yapılardaki siyalik asit moleküllerini hidrolize eden enzimler olarak sınıflandırılmışlardır. Günümüzde omurgalılarda birbirlerinden farklı işlevlere sahip olan dört adet siyalidaz keşfedilmiştir. Nöraminidazlar, işlevleri açısından hücre içi konumlanmasında farklılık göstermektedir. Nöraminidaz 1 (Neu1), lizozomlarda bulunan ve işlev görebilmesi için iki farklı yapı olan katepsin A (PPCA) ve ß-galaktosidaz (ß-gal) ile multienzimkompleksi oluştururlar. Siyalidazlar arasında sadece Neu1 eksikliğinde veya oluşturduğu enzim kompleksinde meydana gelen bozukluklar sonucunda iki farklı lizozomal depo hastalığı olan siyalidoz ve galaktosiyalidoz hastalığı görülmektedir. Hastalıklar meydana gelen mutasyonlara göre farklılık gösterebilmektedirir. Neu1 enziminin işlevlerinin öğrenilmesi için farelerde işlevsiz olan Neu1-/- fare modeli yaratılmıştır. Glikosifingolipitler (GSL) bir çeşit kompleks şekerler olan hücre yüzeyinde gerçekleşen rastgele yaşanan olaylara iletişim sağlayarak hücreye derinlik katan moleküllerdir. Bu yapılara siyalik asit eklenmesi ile gangliyositler meydana gelmektedir ve daha sonrasında 0-, a-, b-, c- serisi gangliyositler olarak özelleşmektedirler. Neu1 enziminin GSL yolağındaki görevi ile sınırlı sayıda kanıt bulunmaktadır. Dolayısıyla Neu1 enziminin GSL yolağındaki rolünün araştırılması için Neu1-/- fare modeli ile yapısında –b ve c-gangliyositlerinden yoksun GD3S-/- faresi ile Neu1-/-GD3S-/- faresi elde edilmiştir. Yapılan araştırmalar sonucu farenin GSL yolağında ince tabaka kromatografisi ile belirgin bir fark görülmezken, mRNA düzeyinde apoptoz ve ER-stres bağlantılı belirteçler azalırken protein ve imminohistokimyasal analizler ile ciddi hücre ölümüne rastlanılmıştır. Bu sonuçlara ek olarak rotarod ve açık alan testleriyle ciddi derecede davranış bozuklukları sergilemişlerdir. Bu sonuçlar, b- ve c- gangliyositlerin Neu1-/-GD3S-/- faresindeki biyolojik belirteçlerin aydınlanması için başka araştırmalara da ihtiyaç duyulduğunu belirtirken, hücre ölümü mekanizmasının aydınlanmasında önemli bir potansiyel oluşturmaktadır.

TABLE OF CONTENTS

LIST OF FIGURES

Figure **Page**

Figure **Page**

LIST OF TABLES

CHAPER 1

INTRODUCTION

1.1. Discovery of Sialidases

Sialidases or neuramizidases are classified as exoglycosyl hydrolases that by cleaving the α-glycosidically bound N-terminal sialic acids from glycoconjugates such as glycoproteins, oligosaccharides and glycolipids. Discovery of these enzymes were linked to the experiments on microorganisms such as influenza virus and bacterial cultures, experimented on human blood cells proposed a name for these enzymes as "receptor-destroying enzymes"(Burnet, McCrea, and Stone 1946). Firstly purified enzyme from the Vibrio cholera bacteria, showed similar catalytic activity with the "receptor-destroying enzymes" (Ada and French 1959). These searches in this field led these enzymes to be studied on other organisms.

1.2. Mammalian Sialidases

Sialic acids comprise a structure composed of 9-carbon containing carboxylated sugars that tend to form at the N-terminus of glycoconjugates. There are various isoforms of sialic acids with diverse structures that seemed to play important biological events such as ligands and interaction molecules involved in recognition (Varki 1997; Saito and Yu 1995). Removal of the sialic acid compounds from sugar, the sugar residues is an important step for the degradation of various oligosaccharides (Cantz and Ulrich-Bott 1990). The findings of complex sugars revealed that these structures are more than immobile structures which can store biological information (Laine 2008). To sum up, sialyated molecules are important in cell signaling but their degradation is also important for the stability of the cell where sialidases are important in this step. In vertebrates, sialidases are involved in many important biological processes. Cell proliferation and differentiation, stability of cell adhesion, degradation of complex sugar such as gangliosides and glycoproteins, and modification of cell receptors are the crucial roles of sialidases (Monti et al. 2010). Mammalian sialidases/neuraminidases include four

different enzymes that are encoded by different genes which are Neu1, Neu2, Neu3, and Neu4. Localization of these enzymes inside the cell differs, as Neu1 enzyme functions in the lysosomes, Neu2 in the cytosol, Neu3 in the plasma membrane and NEU4 can be seen in the mitochondria, endoplasmic reticulum and in lysosomes. Although some studies revealed that these enzymes are found in different subcellular locations rather than their usual localizations. Evidences indicated that Neu1 was present in the outer membrane whereas Neu3 was observed in the inner membrane of the nuclear envelope (Jianfeng Wang et al. 2009). Another exception was also reported for Neu2 enzyme where its presence was observed in the nucleoplasm of muscle fibers in rat (Hidari et al. 1994). Besides their subcellular localization, mammalian sialidases have different functions.

Human Neu4 can be seen in 2 isoforms; either in short or long form which indicates a 12 amino acid difference at the N-terminus (Yamaguchi et al. 2005). Demonstration of the long isoform of Neu4 (NEU4L) was described by Seyrantepe *et al.*, 2004, and further, localization was showed by Yamaguchi *et al.*, 2005. The localization of the short isoform, NEU4S, was related with intracellular membranes (Yamaguchi et al. 2005). Further experiments towards NEU4 revealed that in the outer membrane of mitochondria NEU4L were localized whereas in the endoplasmic reticulum NEU4S were present (Bigi et al. 2009). Neu4 was reported to have variety in its functions including degradation of gangliosides, oligosaccharides, and sugar containing proteins (Hasegawa et al. 2007), as well as neuronal cell differentiation (Shiozaki et al. 2009). Neu4 deficient mice? displayed storage of GM2 gangliosides (Seyrantepe et al. 2008). Further studies on Neu4 demonstrated important aspects towards neurodegenerative disorders such as Tay-Sachs disease, a type of lysosomal storage disorder, accumulating abnormal amounts of GM2 due to lack of ß-Hexosaminidase A (HexA) enzyme. Mice model lacking HexA enzyme was created and did exhibit some symptoms resembling the Tay-Sachs disease phenotype but did not show any severe phenotype (Yamanaka et al. 1994). This model, crossed with Neu4 deficient mice forming a double knock-out mice demonstrated important features of Tay-Sachs disease (Seyrantepe et al. 2010).

Sialidase Neu3 is an enzyme where functions in the plasma membrane and featuring catabolic activities against gangliosides (Miyagi et al. 1999). Further studies on Neu3 revealed more about its functions and defined as a membrane bound enzyme possessing both cis -and trans-activity on the cell surface modulating gangliosides (Papini et al. 2004). Its important roles in the cell membrane made scientists to think that Neu3 might play important roles on cell differentiation. Studies revealed that the

overexpression of Neu3 showed rapid neurite branching in mouse neuroblastoma cells (Hasegawa et al. 2000). One of the major properties of Neu3 was discovered recently, possessing specific activity against GM2 ganglioside in mice which was demonstrated by generation of the double knock-out HexANeu3 mice (Pan et al. 2017). Later on, double knock-out HexANeu3 mice was studied in a more detailed aspect and showed a very severe progressively increasing pathology within age very similar to the Tay-Sachs patients and being suggested as the most suitable mice to study the pathology of Tay-Sachs disease in-vivo (Seyrantepe et al. 2018).

Similar to other sialidases, Sialide 2 (Neu2) was shown to have a role in cell differentiation which was shown firstly in the muscle cells of rats (Sato and Miyagi 1996). Later on, studies showed that Neu2 was related with the muscle regeneration which was shown with the down-regulation of Neu2 in a mouse model of human dysferlinopathy (Suzuki et al. 2005). In addition to the functions of Neu2, in vitro studies with Neu2 showed catalytic activity against oligosaccharides, glycoproteins and gangliosides under neutral pH(Miyagi et al. 1999).

1.3. Sialidase 1 / Neuraminidase 1

Hydrolysis of N-terminally linked sialic acids of sialyated complex sugars is one of the major tasks of sialidase 1 (Neu1). It is expressed almost in all of the tissue and cell types of vertebrates and successfully isolated from placenta, mammary gland, brain, kidney, liver, testis, and thyroid (Saito and Yu 1995). It functions together with two other hydrolases named ß-galactosidase and serine carboxypeptidase protective protein/cathepsin A (PPCA) and forms a multienzyme complex. PPCA plays a crucial role, by forming interactions when Neu1 is recruited to lysosomes, activating the catalytic properties of Neu1. Acidic environment is present in the lysosomes, the multienzyme complex, catalytic activity of Neu1 is enhanced. Transport and the process of the forming of multienzyme complex is unclear although there are speculations of the recruitment of Neu1 to the lysosomes. One introduces Neu1 as a non-soluble enzyme which acts like an integral membrane protein and formed intracellular activity with its C-terminal domain formed interactions with the adaptor protein complexes (AP-3) (Lukong et al. 2001). Another speculation of Neu1 is based on the interactions with PPCA. Right after the synthesis of Neu1 proteins forms a strong complex with PPCA, acting a chaperone like

structure, it is directed to the lysosomes with mannose 6 phosphate pathway where this complexed did not formed in the absence of PPCA and Neu1 was either remained in the ER or degraded (Van Der Spoel, Bonten, and D'Azzo 1998; Bonten and D'Azzo 2000)

1.4. Human Neu1 Deficiency

Among sialidases, only the absence or defective form of sialidase 1/ neuraminidase1 (Neu1) can cause two clinically associated neurodegenerative lysosomal storage disorder in the human. Mutations in the human NEU1 gene results sialidosis and galactosialidosis (GS) GS occurs when the component of the multienzyme complex of Neu1, PPCA is missing resulting non-functioning Neu1 and ß-GAL. GS and sialidosis are phenotypically similar disorders because of the malfunctioning or absence of Neu1(Cantz and Ulrich-Bott 1990; Caciotti et al. 2013).

1.4.1. Galactosialidosis

In GS, patients suffer various defects such as coarse facies, macular cherry-red spots, vertebral changes, and altered bone marrow structure. GS patients are classified into three groups based on the severity of the disease phenotype and named as early infantile, late infantile, and juvenile/adult (Annunziata and d'Azzo 2017). Early infantile patients start to show the clinical features between birth and 3-months of age. They suffer from very harsh features such as neonatal edema, altered facial futures, skeletal dysplasia, hearth failures, kidney abnormalities, visual defects and variable neurological abnormalities. Patients suffering such harsh symptoms mostly cannot withstand for long due to function loses of crucial organs such as heart and kidney. Late infantile GS includes a variety of patients categorized in terms of their cognitive abilities. Phenotypes seen in late infantile group also include coarse facies, enlarged spleen and liver, muscular atrophy, altered heart features, hearing loss. This group of patients have longer lifespan and can reach up to adulthood. A patient in this category who suffered kidney failure and with the renal transplantation made at 2.5 years old, which was to be the first in the field of GS, provided at least 6 years of life (Kiss et al. 2008). The juvenile/adult form of GS disease includes most of the GS patients. They show similar physical features like in the other forms of the GS patients such as coarse facies, vertebral changes, cherry-red spots

and corneal clouding. In addition these patients tend to show severe neurological abnormalities including cerebella ataxia, seizures, progressive cognitive impairment and mental retardation(Mochizuki et al. 2000). These patients can live even longer, they seem to have normal sized organs and absence of angiokeratoma(Annunziata and d'Azzo 2017; Sewell et al. 1987).

1.4.2. Sialidosis

Like described earlier, sialidosis shows close clinical abnormalities with GS patients. Sialidosis is divided in to two groups, type I and II. Type I sialidosis is the mild form of the disease and clinical features are seen in their second decade of life are mostly restricted to show myoclonus, visual defects, ataxia, tonic-clonic seizeures. Type II sialidosis is the severe form of the disease and classified in to three groups like in the GS patients which are classified as congenital onset, infantile onset and juvenile onset. Congenital is the most severe form of the sialidosis type II and patients mostly die right after birth. Infantile onset phenotypes appear between birth and 1 year and juvenile onset form shows after 2 years. All patients in the type II sialidosis shows progressive increase in their phenotypes which includes macular red-spot, enlarged organs, mental retardation, coarse features. Phenotype of the disease is associated in the mutations in the NEU1 gene.(Monti et al. 2010). Sialidosis patients show distinct biologically altered manifestions such as altered oligosaccharide profile in the urine which is an important indication for the diagnosis of these patients (Mütze et al. 2017).

Studies showed that Neu1also has crucial roles for the tissue homeostasis within the cell besides of the desialyation oligosaccharides. Elastin fiber assembly is one of the important processes which supports the tissues and especially organs by providing elastic properties required to maintain healthy and remain unharmed (Yanagisawa and Davis 2010) The multienzyme complex formed with Neu1,ß-GaL and PPCA are required to form this assembly with their interactions (Hinek et al. 2006; Privitera et al. 1998)

1.5. Sialidosis Mouse Model – Neu1-/- Mice

Sialidosis mice model the Neu1-/- mice was created by the insertion of the (LacZ/PGK/neo) cassette in to the SacII site within exon 1. Homologous recombination at the Neu1 locus resulted to translate a non-functional neurominidase protein(N. de Geest 2002).

Mice lack of Neu1 enzyme exhibited severe pathology resembling the sialidosis type II patients. Neu1-/- mice displayed similar phenotypes that the sialidosis patients suffered. Mice showed low-molecular chained oligosaccharide in their urine which was diagnostic for the GS and sialidosis patients. Edema in various tissues such as, limbs, penis, forehead, eyelids at the early stages of age (4-6 weeks). Disease phenotype progressively increases with age. Its bone structure is altered with age and lordosis was prominent at the 6 months of age. And their life span was estimated to be around 6-9 months. Further studies on Neu1-/- mice demonstrated that absence of Neu1 had a negative effect on the lysosomal exocytosis. Absence of Neu1 resulted the accumulation sialyated LAMP-1 remained in the surface of macrophages (Yogalingam et al. 2008). Same group also showed more pathological features such as muscle degeneration (Zanoteli et al. 2010) and important roles the Neu1 in the aspect of muscle regeneration (Neves et al. 2015). Most recent finding in Neu1-/- mice, linked a lysosomal storage disorder related enzyme with a common disease fibrosis seen in human (van de Vlekkert et al. 2019).

1.6. Glycosphingolipid Pathway

Glycosphingolipids (GSLs) are type of lipid molecules and has a ceramide (Cer) backbone with various glycans bound with glycosidic bonds to its structure. GSLs are found abundant on the cellular membrane and implicated to have various roles in the cell (Van Meer, Voelker, and Feigenson 2008). GSLs are generated in the Endoplasmic Reticulum (ER) by various enzymes. Production of GSLs requires base sphingoids as a base structure combined together with an acyl-CoA processed with ceramide synthesis, forms the Cer molecule (T. D. Mullen, Hannun, and Obeid 2012). Fate of the Cer can differ, which either be galactosylated in the ER which forms the GalCer or can be transferred to Golgi for further processes (Holthuis et al. 2001). Inside the trans-Golgi

network (TGN) GalCer can be converted to glucosylceramide (GlcCer) with the addition of glucose to its structure (Gault, Obeid, and Hannun 2010). Generation of complex GSLs are derived from GalCer and GlcCer by various enzymes (MacCioni, Quiroga, and Ferrari 2011). Addition of sialic acid residues with certain sialyltransferases to the LacCer backbone, produces GM3, GD3 and GT3 gangliosides which and differ in terms of the sialic residues are can be defined as small/simple gangliosides and the precursor of o-, a, b and c series of gangliosides O- series of gangliosides are absent in terms of sialic acids and called neutral gangliosides due to their non-charged group where as a, b and c series have sialic acids and are being called as acidic gangliosides (Breiden and Sandhoff 2018). Synthesis of the complex GSLs are listed within the Figure 1.1.

1.7. Gangliosides

Synthesis of the gangliosides occurs in the intraluminal face of the Golgi apparatus and transported to the external side of the plasma membrane where their sugar components faces the towards the extracellular space (Demarco and Woods 2009; Schnaar 2019). In addition, they have associations spontaneously through the outer leaflet of lateral lipid structure including other molecules such as sphingolipids, GPI-anchored proteins, transmembrane. They are distributed ubiquitously among the tissues, body fluids and especially in the brain (Yu, Tsai, and Ariga 2012). To think that, there are various types of gangliosides in the surface of the plasma membrane, being together with the spontaneous reactions, they have contribution to many important cellular event for the cell. During the in the early stages of the neurodevelopment, levels in terms of the gangliosides were expressed differently (Ngamukote et al. 2007).

1.8. GD3 Synthase Deficient Mice Model

GD3 synthase (GD3S) mice was created with the insertion of a LacZ-neo cassette in to the BamHII site of the fifth exon, GD3S gene was disrupted. This mice only possessed a- series of gangliosides due to lack of GD3S, generation of GM3 to GD3 ganglioside was prohibited and all of the complex gangliosides linked were depleted (Figure 4). Mice lack of GD3S displayed no severe phenotype and a normal life span(Kawai et al. 2001). Other studies in this mice model demonstrated that, neural repair

mechanism was impaired and related with b- and c- series of gangliosides (Okada et al. 2002).

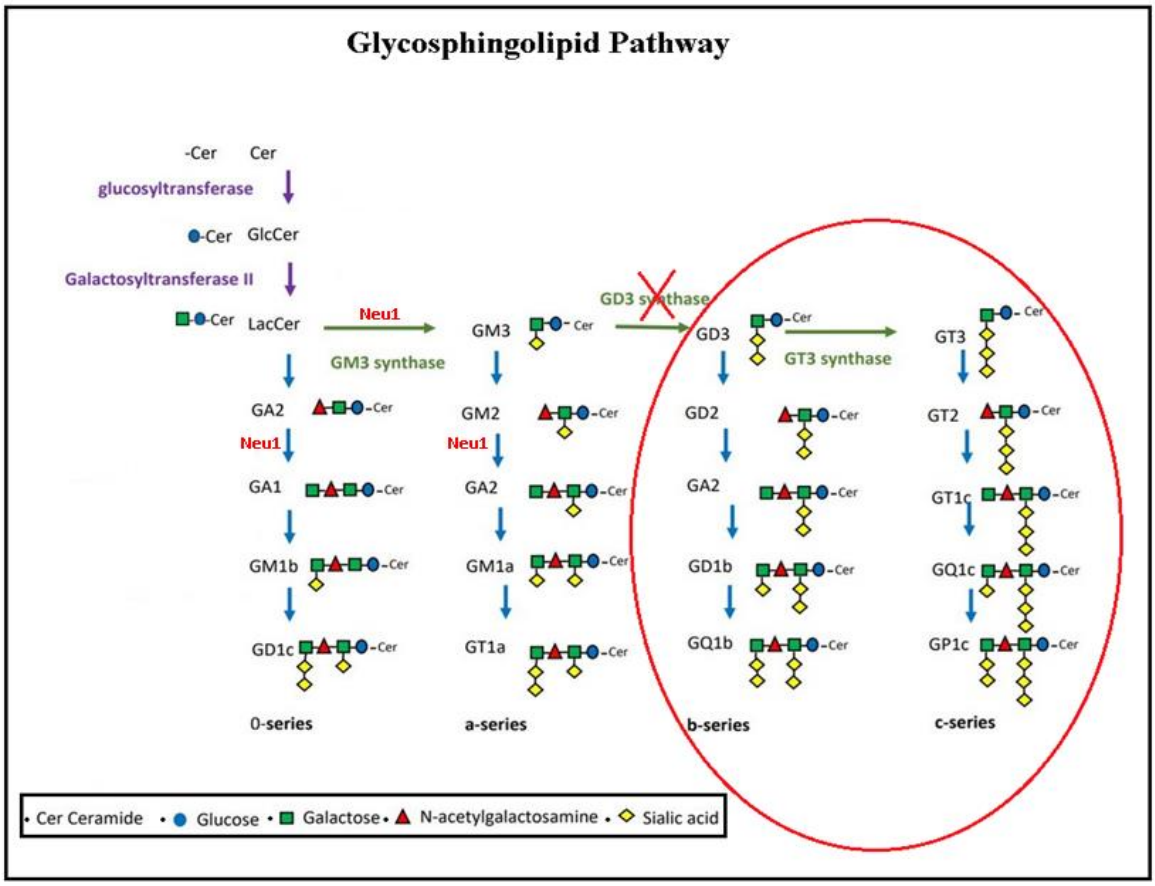

Figure 1. 1. Representative figure showing the affected gangliosides due to the lack of GD3S in the Glycosphingolipid pathway (Source: Pasquel-Dávila et al. 2019).

Simple gangliosides, such as GD3 and GM3 were observed in the brain embryonic stages of the vertebrates and complex gangliosides such as GM1, GD1a, GD1b and GT1b substituted these simple gangliosides after the development of the brain (Yu, Nakatani, and Yanagisawa 2009; Ngamukote et al. 2007). Specific expressions of the gangliosides during development suggests that they contribute to regulation of such cellular events like neuritogenesis, axonogenesis and synaptogenesis (Wu et al. 2001; Bieberich et al. 2001).

To understand more about the functions of the GSL, mice models were used lack of in terms of the enzymes related with the GSL pathway. Gangliosides in terms of -0, - a, -b and –c series were targeted and by the deletion of specific enzymes these mice were generated. Some examples includes a mice model lack of ST-1 enzyme resulting

the absence of all -a, -b and- c series displayed neurodevelopmental abnormalities (Proia 2003).

1.9. Aim of the Study

Neu1 which is a critical enzyme that has many crucial roles in the cell especially in the lysosomes and its disturbance with mutations resulted severe phenotypes in human (Sialidosis and Galactosialidosis) and mice (Neu1-/- mice model). Besides its catalytic activity many regulatory roles of Neu1 has been found. Although its functions in the glycosphingolipid pathway is still unclear. In this study, to understand the role of Neu1 in the glycosphingolipid pathway we demonstrated a unique double-knock out mice model, the Neu1-/-GD3S-/- mice possessing absent in terms of Neu1 possessing only a-series of gangliosides.

CHAPTER 2

MATERIALS AND METHODS

2.1. Animals

Neu1 mice were donated by Dr. Alessandra d'Azzo (St. Jude Children's Research Hospital, Tennesse, USA) and GD3S deficient mice was present in our lab which is donated Dr. Roger Sanhoff (Hochschule Mannheim - Mannheim University of Applied Sciences, Germany). Mice were bred and housed with the groups of five per cage and kept under constant temperature with a 12-h light.dark cycle. Water and food were available ad libitum. All animal experiments were performened in accordance with the Turkish Institute of Animal Health guide for the care and use of laboratory animals. The experiments made with animals were approved by the Institutional Animal Care and Use Committee of Izmir Institute of Technology.

2.2. Tissue Handling

In this study, two- and four-month old mice were used for the experiments. For the biochemical analysis mice were sacrificed with CO2 when they were at their targeted age. From two and four month old WT, GD3S-/-, Neu1-/- and Neu1-/-GD3S-/- mice, cortex, cerebellum thalamus brain regions were obtained. Brains were cut into half and their regions were dissected into Eppendorf tubes which were immediately frozen with dry ice. Samples were kept at -80°C until usage. For immunohistochemical and histopathological analysis, brain tissues were fixed with cardiac perfusion.

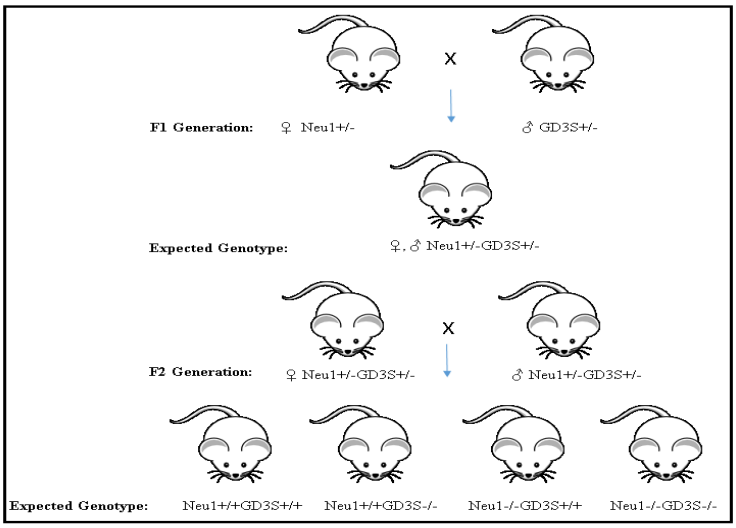

Figure 2. 1. Breeding plan made for to obtain the desired mice.

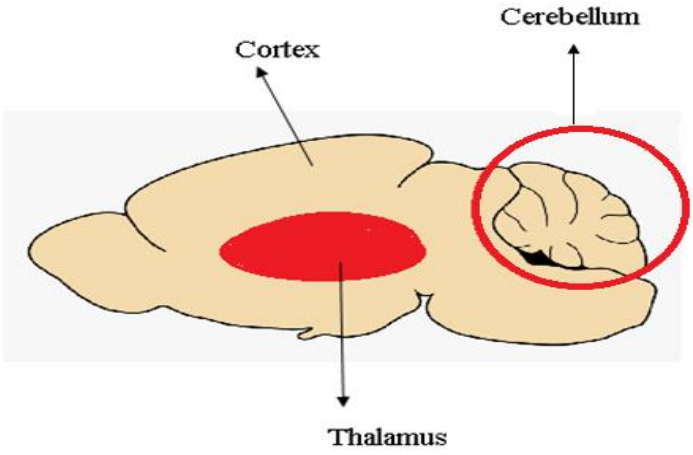

Figure 2. 2. Mouse brain dissection.

2.3. Fixation of Mice brain

To perform pathological and immunohistochemical analysis from mice brain, fixation of the mice brain is required. In order to perform transcardial perfusion, mice were ksilazol and basilazin were used for mouse anesthesia. After being sure that the mice lost their consciousness, through their abdomen, an incision was made to open the rib cage. After rib cage was visible, it was bent to reveal the heart of the mice. From the left ventricle, a serum needle was inserted and its position was secured. After securing the needle, a sharp cut was made to the right atrium and right after the cut, from the secured

needle, saline (0.9% NaCl aqueous solution, pH. 7.4) was circulated to eradicate the blood out. After circulating the blood out, ice-cold 4% paraformaldehyde dissolved in PBS (pH. 7.6) was replaced with saline to fix the organs. 15-20 ml of fixative solution was used for each mice. Later on, the brains were excised and placed in to falcons which contained fixative solution and incubated overnight at +4ºC. Next day, paraformaldehyde was discarded and then the brains were subjected to sucrose gradient (sucrose dissolved in PBS solution pH. 7.6). Firstly, brains were incubated for 2 hours with the concentration of 10% of sucrose at +4ºC, then with 2 hours with the concentration of 20% sucrose at +4ºC and finally overnight incubation at +4ºC was performed with the concentration of 30% sucrose. Following day, the brains were embedded into cryomolds with OCT (optimal cutting temperature) solution and slowly frozen with a right angle with the help of dry ice. Cryofrozen tissues were kept at -80ºC until usage. With the help of Leica Cryostat machine, 10µm brain sections were obtained and placed onto adhesive-coated slides (Marienfeld, Germany). Collected slides were stored inside the slide boxes and kept at -80ºC until usage.

2.4. DNA Isolation

After one months, the mice were weaned and small piece from the mice tail was used to obtain their DNA for genotyping. The following steps are used to obtain the genomic DNA from mice(R). Tails obtained from mice were put in an Eppendorf tubes which consisted of 250µl of lysis buffer (10% 1M Tris pH 7.6, 2.5% 0.2M EDTA, 20% SDS, 4% 5M NaCl) and 6µl of Proteinase K (25µg/ µl solution). Samples were incubated overnight in the incubator at 55˚Cat 70 rpm. On the following day, samples were centrifuges at 13.000 rpm for 10 minutes. The supernatants were transferred into new tubes containing equal volumes of %100 isopropanol. DNAs were collected using pipette tips and transferred in to new tubes containing 250µl of 70% ethanol. Tubes were then centrifuged for 1 minutes at 15.000 rpm and discarded the 70% ethanol. Samples were air-dried for 10-20 minutes then dissolved in 50-100 µl of distilled water, and incubated for 30-60 minutes at 55˚C.

Table 2.1. Primer sequences used for the genotyping of the mice.

Allel	Primers	Primer Sequence
GD3S (WT)	GD3S-F	5'-CTTCAGAGGACTGGGTGAGC-3’
GD3S (WT)	GD3S-R	5'-AAGGGCCAGAAGCCATAGAT-3'
GD3S (Mutant)	koRLP29-	5'-TCGCCTTCTTGACGAGTTCTTCTGAG-3'
Neu1 (WT)	Neu1-F	5’-CCGGAGATACAATGATACAG-3’
Neu1 (WT&Mutant)	Neu1-R	5’-CTGTCCGAATACTCTCCCCACAT-3’
Neu1 (Mutant)	Neo-R	5’-CACCTTTTAAAGGGAGCCGGT-3’

2.5. PCR Reaction

PCR reactions were carried to amplify the alleles of GD3S and Neu1 from the genomic DNA isolated from the mice tail. Primers described in the table X were for the PCR reactions.

For Neu1 PCR, 1cycle 3 minutes at 94℃; 35 cycles 30 seconds at 94℃, 30 seconds at 58℃, 40 seconds at 72℃; 1 cycle 5 minutes at 72℃. The reaction mixture of the Neu1 PCR was 50 µl at total which contained 100 ng genomic DNA, 50 pmol of each primer, 10 mM of dNTPs, 2.5 units of Taq polymerase (GeneDirex), 10X reaction buffer containing 2mM $MgCl_2$.For GD3S PCR, 1cycle 3 minutes at 94℃; 30 cycles 30 seconds at 94℃, 30 seconds at 58. 1℃, 2 minutes at 72℃; 1 cycle 5 minutes at 72℃. The reaction mixture of the GD3S PCR was 50 µl at total which contained 100 ng genomic DNA, 50 pmol of each primer, 10 mM of dNTPs, 0.3 mM $MgCl_2$, 2.5 units of Taq polymerase (GeneDirex), 10X reaction buffer containing 2mM $MgCl_2$.

2.6. Thin-Layer Chromatograpy

In order to observe acidic and neutral gangliosides, thin layer chromatography was used. Cortex and cerebellum brain regions were obtained from two-and four-month old mice for this experiment.

2.6.1. Isolation of Neutral and Acidic Gangliosides from Brain

25 mg of brain tissue from each mice were weighted and then added in to a borosilicate glass tubes containing 2ml of distilled water. Brains inside the borosilicate tubes were then homogenized with ultra turax homogenizer (IKA t10, Sigma, Darmstadt, Germany) for 30 seconds at 6000 rpm. After homogenization, samples were sonicated (Bandelin-sonopuls, Berlin, Germany) for 4 minutes. Samples were then placed in to Reacti-Therm Heating module with N_2 flow to dry, (Thermo, Massachusetts, USA) which was filled with water and heated up to 55°C in order to speed up the evaporation. After the water is completely evaporated, extraction was proceeded with 3ml of %100 acetone. The samples were vortexed and centrifuged at 2000rpm for 5 minutes and the supernatants were discarded which contained phospholipids and other small membrane lipids. This step was repeated twice. After that, each pellet containing tube were washed with a 1.5ml of chloroform.methanol.water (10.10.1) solution, vortexed and centrifuged at 2000rpm for 5 minutes, and their supernatants are collected into new neutral glass tubes. This step was repeated twice. Next, 2ml of chloroform.methanol.water (30.60.8) solution was added to the tubes, vortexed and centrifuged at 2000rpm for 5 minutes, and their supernatants are collected into same tubes mentioned above. This step was repeated twice. Collected supernatants contain both neutral and acidic gangliosides which are then separated with DEAE Sephadex A-25. DEAE Sephadex A-25 columns were freshly prepared before usage. Collected supernant which containing both acidic and neutral gangliosides were then loaded to DEAE Sephadex A-25 columns and washed with 4 ml of methanol. After loaded and washed with methanol, the flow through was collected in to new tubes which were the neutral glycosphingolipids whereas the acidic glycosphingolipids were held on the DEAE Sephadex A-25 columns. In order to collected the acidic glycosphingolipids, 4 ml of 500 mM potassium acetate dissolved in methanol was eluted from the columns and collected in to new tubes.

Acidic glycosphingolipid containing extract were then desalted by using Supelclean™ LC-18 SPE columns (Sigma-Aldrich, USA) which were placed on the Chromabond Vacuum manifold (MachereyNagel) and the pressure was fixed to 3-4Hg. First the Supelclean™ LC-18 SPE columns were washed with 2 ml of methanol and 2 ml of 500 mM potassium acetate in methanol. Then acidic glycosphingolipid containing extract was loaded on the columns and washed with 10 ml of distilled water. At this point

columns contains desalted acidic glycosphingolipids. Columns were eluted with 4 ml of methanol and 4 ml of methanol.chloroform (1.1) and collected in to new tubes which contained acidic glycosphingolipids. Both neutral and acidic glycosphingolipid containing extracts were evaporated by using N_2 gas which was explained earlier in this method. After evaporation samples were ready to load on silica gel plates (CAMAG, Switzerland).

Acidic and neutral glycosphingolipids were separated with a running solvent composed of chloroform. methanol. 0.2%aqueous $CaCl_2$ (60.35.8). In order to form a vaporous environment inside the tank (CAMAG, Switzerland), tank containing the running solvent was incubated at room temperature for 2 hours.

Neutral and acidic glycosphingolipids were dissolved in chloroform. methanol. distilled water (10.10.1) solution and loaded on to silica gel with Linomat V (CAMAG, Switzerland). Each evaporated extract was isolated from 25mg of brain tissue which was then dissolved in 100ul of chloroform. methanol. distilled water (10.10.1) solution and loaded 50ul on the silica gels containing the half of the extract (12.5 mg of brain). Lipids were separated until there was 5 cm between the samples and the end of the plate.

2.6.2. Preperation of DEAE Sephadex A25 Ion Exchange Columns

In order to separate the acidic and neutral glycosphingolipids into different tubes DEAE Sephadex A-25 columns were prepared fresh (BURNET, McCREA, and STONE 1946). 1g of resin was weighted and washed three times with 10ml of methanol. chloroform. 0.8 M sodium acetate (60.30.8) solution. Then with the same solution resins were incubated overnight. With this treatment, the chloride ions on the resins were converted into acetate ions. Next day, resins were washed three times with 10ml of methanol. chloroform. distilled water (60.30.8) and kept inside with the methanol. chloroform. distilled water (60.30.8) solution until usage.

Glass wool (Sigma-Aldrich, USA) was washed with methanol. chloroform. distilled water (60.30.8) solution and placed inside to 225mm glass Pasteur pipette. Glass wool will keep the resins inside the column.

2.6.3. Visualization of Glycosphingolipids with Orcinol Staining

0.04 g of orcinol was dissolved in 10ml of 25% sulphiric acid in distilled water was freshly prepared. After the separation of lipids the silica gel plates were dried off from the running solvent and then with the help of TLC sprayer (Sigma-Aldrich, USA) orcinol solution was sprayed to the plates. Plates were then heated on the TLC plate heater (CAMAG, Switzerland) at 100^{o}C until the bands were visible. Images were taken with a scanner.

2.7. Analysis of Urinary Oligosaccharides with Thin Layer Chromatography

Urines from mice were collected from two and four month old WT, GD3S-/-, Neu1-/- and Neu1-/-GD3S-/- mice. Mice were gently grabbed and the belly of the mice were gently rubbed until urines were collected to the Eppendorf tubes. Collected urines were stored at -80°C until usage. Urinary creatine content was used to normalize the creatine in each Urine sample. Creatinine Assay kit (Creatinine Assay kit Colorimetric/ Fluorometric, Abcam, UK) was used to detect the creatine levels according to the manufacturer's instructions. Creatine levels of the urine samples were adjusted to 500ng and loaded to 20 cm x 20 cm silica TLC plates (Merck, USA) with Linomat V (CAMAG, Switzerland).1,5 μg of sugar standards (D+ Lactose Monohydrate, D+ Mannose,D+ Glucose, Sucrose, D+ Xylose and D+ Raffinose Pentahidrat (Sigma-Aldrich, Germany)) were loaded to plates. Urinary oligosaccharides were separated with a 3 hours pre-incubated butanol.water.acetic acid (50.25.25) solution for 5 hours, stained with orcinol and heated at 100^{o}C until the bands were visible. Images were obtained with a scanner.

2.8. Real-Time PCR

RNAs were isolated from cortex, cerebellum thalamus brain regions obtained from two and four month old WT, GD3S-/-, Neu1-/- and Neu1-/-GD3S-/- mice. After obtaining the total RNA isolate, it was converted to cDNA and with the primers specially designed for ER-stress, Oxidative Stress and Apoptosis markers were used for RT-PCR.

2.8.1. Isolation of Total RNA from Brain

50 mg of brains were weighted and placed into 2ml Eppendorf containing with 500ul GeneZol (GeneAid) with RNase free beads. With the help of tissue homogenizator (Retsch MM100) tissues were homogenized and incubated for 5 minutes at room temperature. After the incubation, 100ul chloroform was added to the samples and the tubes were vigoursly shaked. Samples were then centrifuged for 15 minutes at 15.000g, +4^{o}C to separate into phases. After the centrifugation, samples showed 3 layer, which were the colourless phase (RNAs), white phase (DNAs) and the bottom phase (proteins). The colourless phase were carefully transferred into new 1.5ml Eppendorf tubes and incubated for 10 minutes with isopropanol equal to their volumes. Samples were centrifuged for 10 minutes at 15.000g, +4^{o}C to precipitate the RNAs. After the precipitation, 70% ethanol was used to wash the RNA pellets. Samples were inverted couple times after adding the 70% ethanol and centrifuged for 5 minutes at 15.000g, +4^{o}C. Supernatants were discarded and the RNA pellets were left to for drying at room temperature until the pellet became invisible. After the RNA pellets were dried fully, 35-50ul RNase free water was used to dissolve the pellet. Pellets were incubated in water bath at 50^{o}C for 10 minutes and after RNAs were full dissolved, their concentration was measured with NanoDrop Spectrophotometer (ND-1000)

2.8.2. cDNA Conversion

High-Capacity cDNA Reverse Transcription Kit (Applied Biosystems) was used to convert the isolated RNAs. 50ng/ul cDNA was prepared according to manufacturer's instroduction. The reaction mixture contained 1 x RT buffer, 1 x Random primers, 4mM dNTP, 50 units MultiScribe Reverse Transccriptase combined with calculated amounts of RNA and RNase free water. Each sample volume was optimized to 20ul. The reaction conditions were conducted with following condidtions. 1 cycle for 10 minutes at 25 ˚C, 1 cycle for 120 minutes at 37 ˚C, 1 cycle for 5 minutes at 85 ˚C.

2.8.3. RT-PCR Reaction

Apoptosis, ER-Stress and Oxidative stress markers were designed and listed on the table 2. LightCycler 96 (Roche, Switzerland) was used to measure the expression levels of the genes. 20ul of reaction mixture was used (0.4uM for each primer, 1 X Roche LightCycler 480 SYBR Green I Master Mix and 50ng cDNA). Reaction was conducted with three step amplification. First step is for 1 cycle for 600 seconds at 95˚C, second step is for 45 cycles for 20 seconds at 95˚C, and then follows 15 seconds at 61˚C and the third step is for 22 seconds at 72˚C. Samples were loaded with three copies each and average of these values were obtained. Expressions of the genes were normalized to GAPDH gene expression levels. For the statistical analysis, with the help of Graph Pad Prism, two-way ANOVA was used.

2.9. Western Blot Analysis

Proteins were isolated from cortex, cerebellum thalamus brain regions obtained from two and four month old WT, GD3S-/-, Neu1-/- and Neu1-/-GD3S-/- mice.

2.9.1. Protein Isolation

Brain tissue samples were homogenized with RIPA buffer (1% TritonX100, 50mM

Hepes, 150mM NaCl, 10%Glycerol, and 50mM Tris-Base, 1% PMSF, 1% protease inhibitor). After samples were homogenized nicely, samples were incubated on ice for 1 hour and a briefly vortexed at every 10 minutes. At the en of 1 hours of incubation, samples were centrifuged at 14.000 rpm for 15 minutes at 4^{o}C. Supernatants were carefully transferred into new tubes which were containing the proteins isolated from the brain tissues.

Table 1.2. Primer sequences & the length of their products are given below.

Gene	**Primer Sequence**	**Product length**
ATF6	F.5'- TGGAAGTGGGAAGATCGGGA -3' R.5'- AGGACAGAGAAACAAGCTCGG -3'	354bp
Calnexin	F.5'- ATTGCCAACCCCAAGTGTGA -3' R.5'- TCCAGCATCTGCAGCACTAC -3'	362bp
XBP1	F.5'- TCCGCAGCACTCAGACTATG -3' R.5'- GACTCTCTGTCTCAGAGGGGA -3'	360bp
SOD2	F.5'- GTGTCTGTGGGAGTCCAAGG -3' R.5'- CCCCAGTCATAGTGCTGCAA -3'	339bp
Catalase	F.5'- TTCGTCCCGAGTCTCTCCAT -3' R.5'- GAGGCCAAACCTTGGTCAGA -3'	351bp
Ttase1	F.5'- CTGCAAGATCCAGTCTGGGAA -3' R.5'- CTCTGCCTGCCACCCCTTTTAT -3'	322bp
Bcl2	F.5'- CGCAGAGATGTCCAGTCAGC -3' R.5'- TATGCACCCAGAGTGATGCAG -3'	369bp
BclXL	F.5'- TCAGCCACCATTGCTACCAG -3' R.5'- GTCTGAGGCCACACACATCA -3'	356bp
Bax	F.5'- AGGATGCGTCCACCAAGAA-3' R.5'- CTTGGATCCAGACAAGCAGC -3'	306bp
GAPDH	F.5'- CCCCTTCATTGACCTCAACTAC-3' R.5'- ATGCATTGCTGACAATCTTGAG-3'	347 bp

2.9.2. Bradfod Assay and Sample Preperation

Isolated proteins were diluted with the ratio of 1.100 (4 ul of protein and 396ul of distilled water). Standart curve was created by diluting BSA (Bovine Serum Albumin Sigma-Aldrich, USA) with different concentrations (1, 0.8, 0.6, 0.4, 0.2, 0.1mg/ml). Samples were loaded into 96-well plate. 5ul of diluted proteins and BSA standart were incubated with 250 ul of Bradford reagent (Sigma-Aldrich, USA) for 5 minutes. At 595nm absorbance of the samples were obtained with spectrophotometer (Biorad).

Samples were calculated according to the equation obtained from the standard curve of the BSA. 20ug of proteins were determined for usage.

After determination protein concentrations, desired amount of proteins were completed with water to make a volume of 9ul (protein+ distilled water). 3ul of 4x loading buffer (40% Glycerol, 240mM Tris-HCl pH 6.8, 8%SDS, 0.04%Bromophenol Blue, 5% β-mercaptoethanol) was added to protein sample which made the final volume of 12 ul of protein mixture. Samples containing 4x loading buffer were heated up to 95 ^{o}C for 10 minutes and the kept at 4 ^{o}C until usage.

2.9.3. SDS-PAGE Gel Electrophoresis

Table 2.3. Materials used to hand cast gels used for SDS-PAGE electrophoresis

	10% Resolving Gel	5% Stacking Gel
Lower Buffer(1.5M Tris-HCL pH.8.8)	3 ml	-
Upper Buffer(1.5M Tris-HCL pH.6.8)	-	1.5 ml
%30 Acrylamide	4 ml	1 ml
dH_2O	5 ml	3.5 ml
10%APS (ul)	60 µl	60 µl
10% SDS (ul)	60 µl	60 µl
TEMED (ul)	6 µl	6 µl

Glass plates were cleaned with 95% ethanol and their setup was prepared on gel casting stand. Resolving gel was prepared according to table 1 and poured into the gap between glass plates about 5 ml for each gel being cast. 2-propanol was used to seal the top and waited about 15-20 minutes for the polymerization of resolving gel. After resolving gel is polymerized, stacking gel was poured and the combs were placed with an angle to avoid air bubbles to form next to wells. After 15-20 minutes the gels were ready to be used for the SDS-PAGE gel electrophoresis.

After the gels are casted according to table 1, gels were placed on the running apparatus and the inner chamber is filled with running buffer (0.25M Tris-Base, 1.92M Glycine, 1%SDS). Proteins were separated at 80V for approximately 1 hours until the

loading dye left the gel. Next, gels were transferred to nitrocellulose membrane (Biorad) with transfer buffer (48mM Tris-Base, 39mM Glycine, 20%Methanol, and pH 9.2) at 0.25A for 75 minutes. After transfer of proteins, the membranes were blocked with 5% non-fat dry milk dissolved in PBS-T (%0.005 tween 20) for 1 hour at room temperature. After blocking, membrane was washed for 5 minutes with PBS-T for 3 times and incubated with Caspase 9 (1.1000, Cell signalling) ,Caspase 3 (1.1000, Cell signalling), BIP (1.1000, Cell signalling), Fas-Ligand (1.1000, Cell signalling) and Beta-actin (1.1000, Cell signalling). Primary antibodies were diluted with red solution (5%BSA, 0.02% NaAzide, Phenol Red, in PBS-T pH 7.5) which extended the durability and the using amount of the antibodies. After primary anti body incubation, blots were washed 3 times with PBS-T for 5 minutes and incubated with HRP-conjugated secondary antibodies (Jackson ImmunoResearch Lab) for 1 hour at room temeperature diluted with 5% non-fat dry milk (PBS-T). At the end of secondary antibody incubation, blots were washed 3 times with PBS-T for 5 minutes. Images were taken by incubating LuminataTM Forte Western HRP Substrate (Millipore) for 5 minutes directly applied to membranes and visualized with digital imaging system, Fusion SL, Vilber. Intensity of the bands were calculated with ImageJ and normalized to the beta actin intensity. For the statistical analysis, with the help of Graph Pad Prism, two-way ANOVA was used.

2.10. DNA Fragmentation Analyses

DNA fragmentation analysis is a method used for detection of fragmentated DNAs which is correlated with apoptosis. Fragmentated DNAs isolated from cortex, cerebellum and thalamus brain regions obtained from two and four month old WT, GD3S-/-, Neu1-/- and Neu1-/-GD3S-/- mice, were abtained with phenol-chloroform method. Isolated DNAs were run on gel electrophoresis and visulized under UV-light.

To briefly explain this procedure, brain regions were left for overnight incubation inside the 1.5ml Eppendorf tubes containing 500µl of tissue lysis buffer (10% 1M Tris pH 7.6, 2.5% 0.2M EDTA, 20% SDS, 4% 5M NaCl) with 12µl Proteinase K solution with gentle shaking at 37℃. Next day, 1 volume of phenol.chloroform.isoamyl alcohol (25.24.1) was added to the samples and tubes were rapidly inverted for several times then centrifuged at 13000rpm for 10minutes at room temperature. After centrifugation, supernatants were collected to new tubes, s, the same procedure was repeated twice, and

totally supernatants were collected for 3 times. After the supernatants were collected, 1 volume of chloroform was added to the samples and centrifuged for 10minutes at 13000rpm and room temperature. This steps was repeated once more. Later on, in order to precipitate the DNA molecules, 0.1 volume of 3M sodium acetate of collected samples were added to the samples and 100% ethanol was added after about the 2.5 volumes of the total volume sample and a brief shake was given to visualize the DNA. Mixture containing DNA was placed in to -80℃ for at least 1hour. Next, samples were centrifuged for 30 minutes at13000rpm at +4℃ for 30minutes. Supernatant was discarded the the DNA pellet was washed with 150µl of 70% ethanol followed with centrifugation at 13000 rpm at +4℃ for 10minutes. This step was repeated once more. After the second supernatant was discarded DNA pellet was left for air-drying for 10-15minutes at room temperature. Samples were dissolved in 50-100ul of TE buffer and concentration was measured with nano drop spectrophotometer. 2µg of DNA was adjusted for loading on to %2 agarose gel and run at 40V for about 2 hours.

2.11. Immunohistochemical Analysis

To reveal the loss of neurons in the brain regions, NeuN was used for the immunohistochemical analysis.

2.11.1. Anti - NeuN Staining

In order to detect the neurons in the brain sections, NeuN protein marker was used. Primary anti-NeuN antibody (1.50, Cell Signaling, Netherlands) and Goat anti-rabbit Alexa Flour 568 (1.500, Abcam, UK) secondary antibody was used for the detection.

Slides were defrosted on ice and washed with 1XPBS for 10 minutes. Inside a humidified blocking chamber, tissues were blocked for 1 hour at room temperature with 5% goat serum and 0.3% Triton X-100 in 1X PBS. After blocking, tissues were overnight incubated at 4 °C with anti-NeuN antibody (diluted in blocking buffer) inside the humidified chamber. Next day after primary antibody incubation, slides were washed with 1X PBS for 15 minutes. Later on, secondary antibody incubation was performed at room temperature for 1 hour inside the humidified chamber. Because the secondary

antibody is highly sensitive to light, incubation was performed in a dark environment. After the secondary antibody incubation, slides were washed with 1X PBS for 15 minutes and then mounted wigh Fluoeroshield mounting medium DAPI (Abcam, UK). Images were taken with fluorescence microscopy (Olympus, Germany). Statistical analysis were obtained via Graphpad with one-way anova analysis

2.12. Histopathological Analysis

Pathological and immunohistochemical analysis were demonstrated to the mice brain sections. From 10µm coronal sections cortex obtained from from two and four month old WT, GD3S-/-, Neu1-/- and Neu1-/-GD3S-/- mice were used. Cortex, cerebellum, thalamus and hippocampus brain regions were visualized with light microscope (Olympus, Germany).

2.12.1. Hematoxylin & Eosin Staining

Gill's hematoxylin (Merck, Germany) was applied to sections for 3 minutes. After, sections were differentiated with 70% ethanol1.1N HCl (99.1, v/v) for 45 seconds. Sections were then washed with running tap water for 5 minutes and then stained with eosin Y (Merck, Germany) solution (0.5% alcoholic) for 45 seconds. Later on, sections were dehydrated 2 times with 95% and 100% ethanol respectively. Finally sections were dipped in to xylene for 2 minutes and sealed with Cytoseal™ XYL (ThermoFisher Scientific, UK) Sections were visualized under the light microscope (Olympus, Germany)

2.12.2. Cresyl Violet Staining

Slides were washed with distilled water for 1 minutes to clean off OCT. Then excess water was drained with tissue paper and stained with Cresyl Violet for 3 minutes. After, slides were briefly introduced to distilled water and then dehydrated with absolute ethanol with a quick rinse. Dehydrated slides were sealed with Cytoseal™ XYL (ThermoFisher Scientific, UK) and visualized under the light microscope. (Olympus, Germany)

2.13. Behavioral Analysis

To observe the behavioral changes between mice rotarod test and open field test was demonstraded on 2-and 4-month old WT, GD3S-/-, Neu1 and Neu1-/-GD3S-/- mice.

2.13.1. Rotarod Test

To assess the motor coordination, motor learning and balance in mice, rotarod test is widely used. Mice models resembling lysosomal storage disorder, such as Sandhoff mice(Gulinello, Chen, and Dobrenis 2008) and early on-set Tay - Sachs disease mice model(Seyrantepe et al. 2018) were also been tested with rotarod test. Firstly, selected individuals were introduced to the test with low speed. After they were successful at standing on the rod without falling, the actual test was started. Test starts with a low speed and slowly accelerates within time. Maximum time limit of the test was adjusted to 150 seconds. Each mice was tested for 3 times and the average fall time was calculated. Statistical analysis were obtained via Graphpad with 2-way anova analysis.

2.13.2. Open Field Test

Open field test is used for testing anxiety and locomotor activity in mice. Mice were placed inside a 40 X 40cm empty box like structure which prevents them escaping. Mice were released from the same spot and within 5 minutes, they were free to explore the empty area. This empty are is dived into sections such as periphery and the center area. Panlab SMART Video Tracking System (Harvard Apparatus, USA) was used to analyze the behavioral differences in mice. Statistical analysis were obtained via Graphpad with 2-way anova analysis

CHAPTER 3

RESULTS

3.1. Genotyping of the Mice

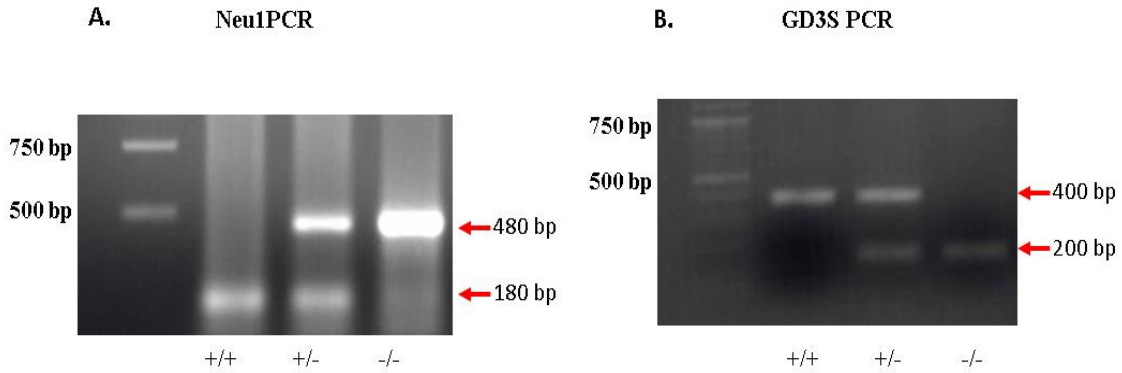

Figure 3. 1. Identification of (A) Neu1 and (B) GD3S PCR with specific primers

Genotype of the mice were identified with specific Neu1 and GD3S forward and reverse primers. Figure 4 is a representative result of Neu1 and GD3S PCR images obtained with gel-electrophoresis. PCR carried out with Neu1 primers, amplified product length of +/+ band was 200 bp and -/- band was 480bp long. For GD3S, +/+ band was seen at 400 bp and -/- band was at 200 bp long. (Figure 3.1 A and B)

3.2. Body Weight Measurement

Compared to WT mice, GD3S-/-, Neu1-/- and Neu1-/-GD3S-/- mice showed differences in terms of weight (Figure 3.2 A and B).Both Neu1-/- and Neu1-/-GD3S-/- mice showed similar gross appearance in terms of altered bone structure (data not shown) and weight except Neu1-/-GD3S-/- were even smaller. By measuring their weight every two weeks we observed that Neu1-/-GD3S-/- mice for male and female mice were smaller compared to Neu1-/- mice at the end of 20 week schedule. Whereas, GD3S-/- mice had slightly higher weight than WT mice for both gender (Figure 3.2 A and B).). Figure 3.2

C represents 4- month old WT, GD3S-/-, Neu1-/- Neu1-/-GD3S-/- mice where the severely under sized Neu1-/-GD3S-/- mice is clearly seen.

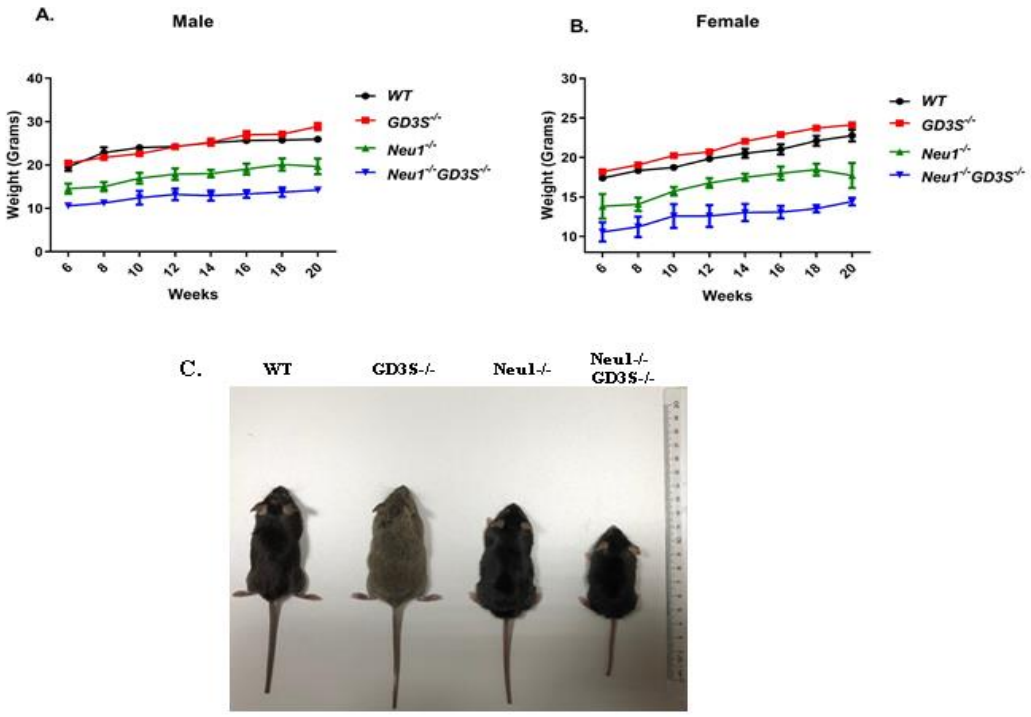

Figure 3. 2. Weight (grams) of (A) Male and (B) female WT (n=10), GD3S-/-(n=10), Neu1-/-(n=8), Neu1-/-GD3S-/- (n=7), mice starting from 6 weeks up to 20 weeks. (C) Physical appearances of 4- month old male WT, GD3S-/-, Neu1-/-, Neu1-/-GD3S-/- mice.

3.3 Glycosphingolipid Profile in the Brain

Thin layer chromatographic analysis was performed to demonstrate the ganglioside profile of 2- and 4 month-old WT, GD3S-/-, Neu1-/-, Neu1-/-GD3S-/-, mice isolated from cortex and cerebellum brain regions. In the cortex and cerebellum brain region GD1a, GM1, GT1b and GD1b and LacCer gangliosides were analyzed.

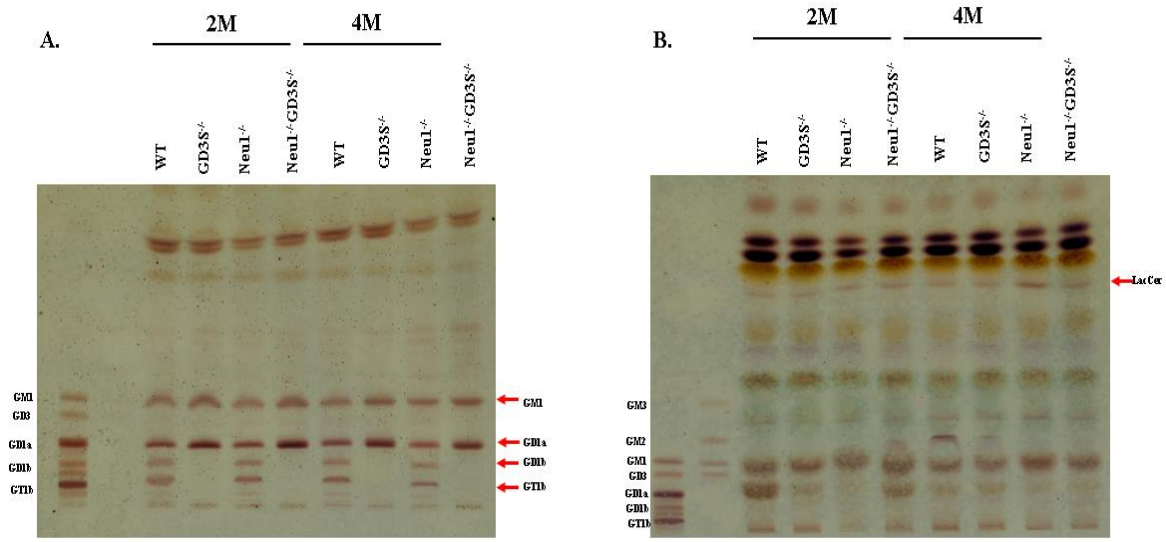

Figure 3.3. 1. Thin layer chromatography analysis visualized with orcinol staining, for acidic (A) and neutral (B) gangliosides isolated from cortex region of 2- and- 4 month-old WT, GD3S-/-, Neu1-/-,Neu1-/-GD3S-/-, mice (S1, total ganglioside standard; S2, mixed ganglioside standard, GM3, GM1 and GD3)(n=3).

Results for the GD3S-/- mice were expected however its effect was firstly going to be revealed with TLC method we looked for the different patterns in terms of acidic and neutral gangliosides. In cortex region, when compared to WT mice, GM1 ganglioside in 2- month old GD3S-/-(1.4 fold) and Neu1-/-GD3S-/-was increased (1.48 fold) compared to WT mice (Figure 3.3.1 A and Figure 3.3.2 A). 4- month old GD3S-/-(1.46 fold) and Neu1-/-GD3S-/-(1.54 fold) also showed an increase in the GM1 ganglioside (Figure 6A and Figure 7A). A significant increase was also seen for the GD1a ganglioside for 2- month old GD3S-/- (1.7 fold) and Neu1-/-GD3S-/- (1.8 fold) mice (Figure 3.3.1 A and Figure 3.3.2 A). Similar to 2 -month old mice, 4- month old GD3S-/-(1.5 fold) and Neu1-/-GD3S-/-(1.4 fold) showed a significant increase in GD1a ganglioside (Figure 3.3.1 A and Figure 3.3.2 B) Due to lack of GD3 synthase enzyme in both GD3S-/- and Neu1-/-GD3S-/- mice, GT1b and GD1b gangliosides were absent (Figure 3.3.1A) . 2- and 4- month old Neu1-/- mice showed 0.81 fold and 0.76 fold decrease respectively in GT1b ganglioside compared to WT mice (Figure 3.3.2 D). GD1b ganglioside was also decreased compared to WT mice in 2- and 4-month old Neu1-/- mice about 0.88 fold and 0.72 fold respectively (Figure 3.3.2 D).

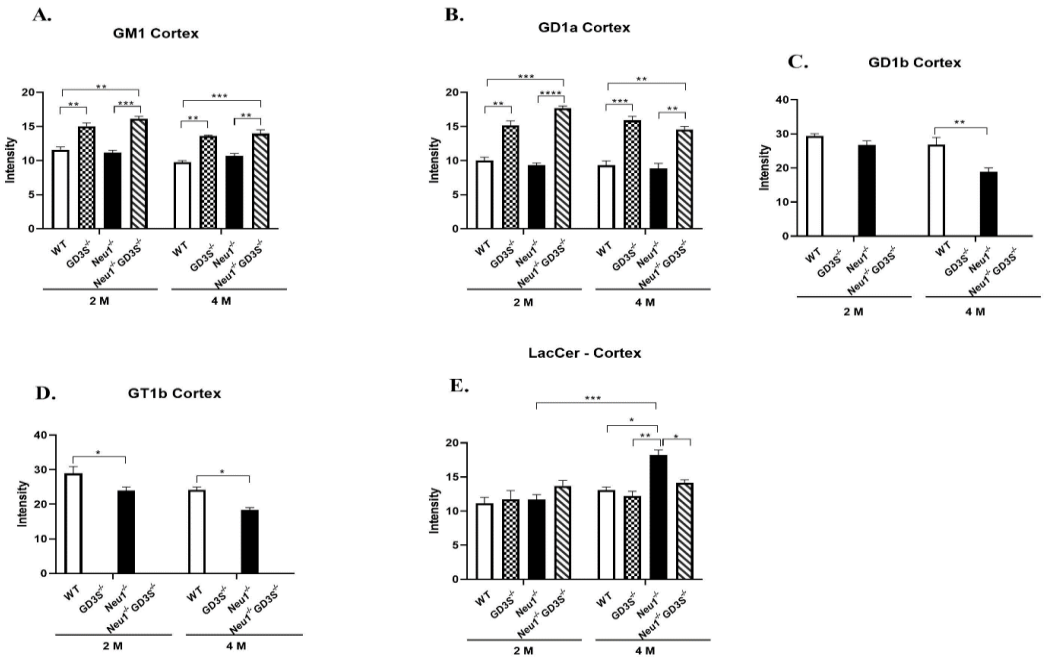

Figure 3.3. 2. Intensity analysis of (A) GD1a, (B) GM1, (C) GT1b and (D) GD1b, (E) LacCer glycosphingolipids isolated from cortex region of 2- and 4 month-old WT, GD3S-/-, Neu1-/-, Neu1-/-GD3S-/-, mice. (*p<.05, **p<.005, ***p<.001, ****p<.0001) (Band intensities were determined with ImageJ and p-values were determined with the 2-way-Anova analysis via GraphPad. Data were reported as means ± SE.)

When neutral gangliosides were compared in the cortex region, lactosyl ceramide (LacCer) was increased in 4- month oldNeu1-/- (Figure 3.3.1 B). 4 month old Neu1-/- mice showed a 1.48 fold to GD3S-/- mice and for Neu1-/-GD3S-/- mice 1.21 fold increase (Figure 3.3.1 B and Figure 3.3.2 E).

In cerebellum region, GM1 ganglioside for the 2- and 4 - month old mice, GD3S-/- and Neu1-/-GD3S-/- mice showed an increase compared to WT and Neu1 mice similar to the cortex region (Figure 3.3.3 A and Figure 3.3.4 A). GD1a ganglioside in 2 month GD3S-/- and Neu1-/-GD3S-/- mice showed a significant increase about 2.06 and 1.64 fold respectively compared to WT mice (Figure 3.3.4 B). In 4 months old GD3S-/- and Neu1-/-GD3S-/- mice, a 2.64 and 2.89 fold increase were observed respectively for the GD1a ganglioside compared to WT mice (Figure 3.3.3 A and Figure 3.3.4 B). GD1b and GT1b gangliosides did not show any significant change in both 2 and 4 months old GD3S-/- and Neu1-/-GD3S-/- mice (Figure 3.3.4 C and D).

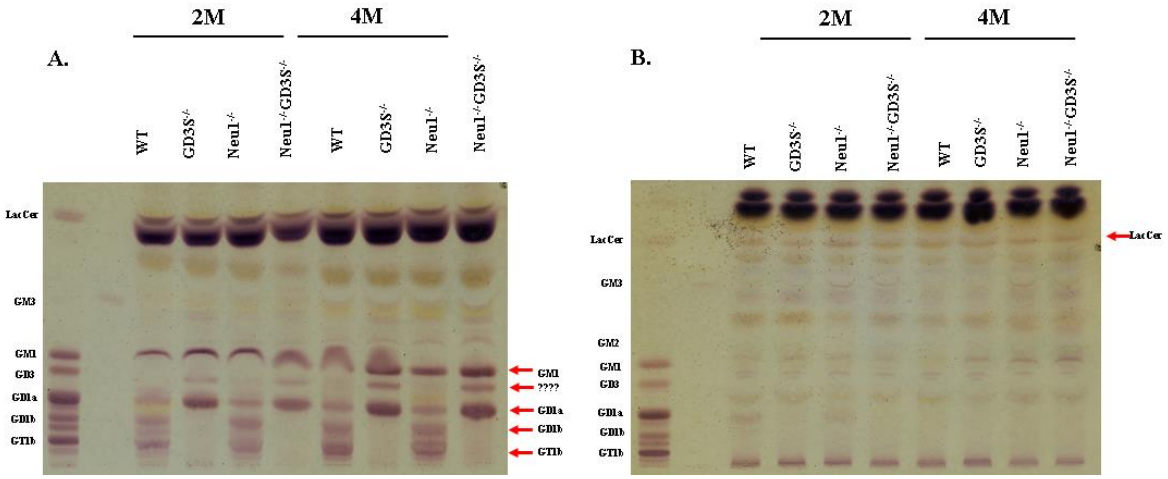

Figure 3.3. 3. Thin layer chromatography analysis visualized with orcinol staining, for acidic(A) and neutral (B) gangliosides isolated from cerebellum region of 2- and 4- month-old WT, GD3S-/-, Neu1-/-, Neu1-/-GD3S-/- mice (S1, total ganglioside standard; S2, mixed ganglioside standard, GM3, GM1 and GD3)(n=3).

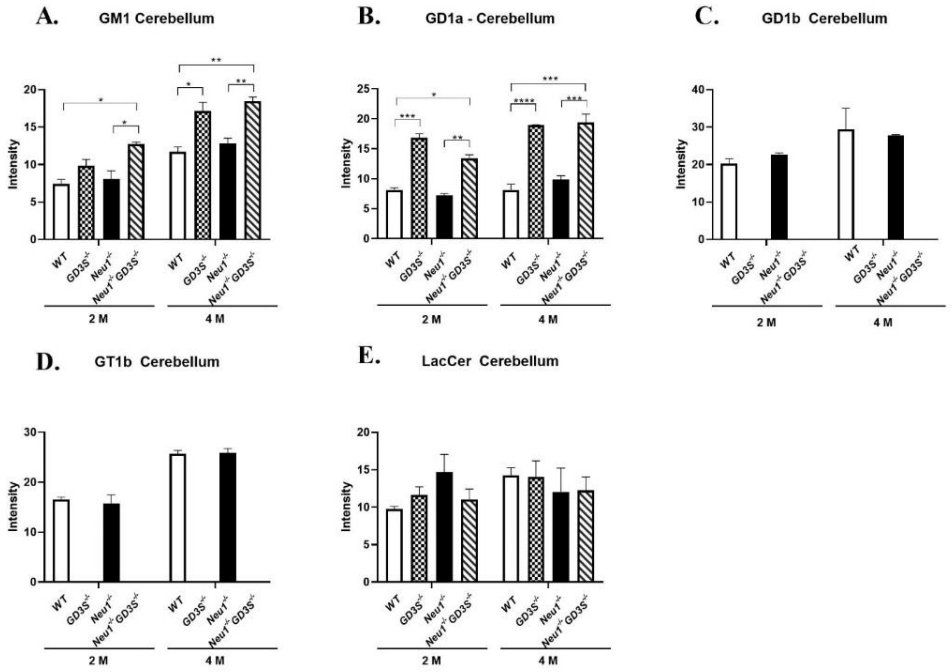

Figure 3.3. 4. Intensity analysis of (A) GD1a, (B) GM1, (C) GT1b and (D) GD1b (E) GalnacGM1b gangliosides isolated from cerebellum region of 2- and 4 month-old WT, GD3S-/-, Neu1-/-, Neu1-/-GD3S-/-, mice. (*p<.05, **p<.005, ***p<.001, ****p<.0001) (Band intensities were determined with ImageJ and p-values were determined with the 2-way-Anova analysis via GraphPad. Data were reported as means ± SE.)

When cortex and cerebellum brain regions were compared, most of the ganglioside patterns were similar (Figure 3.3.1 and Figure 3.3.3). However in the

cerebellum region, only in both 2- and 4- months old GD3S-/- and Neu1-/-GD3S-/- mice, a ganglioside was observed, between GD1a and GD3 ganglioside standards, which is probably a modified form of a ganglioside. This band was only seen in the mice which lacked GD3S enzyme and its intensity was increased within age (Figure 3.3.3 A).

3.4. Urinary Oligosaccharide Analysis

TLC analysis demonstrated with urine samples obtained from 2- and 4- month-old WT, GD3S-/-, Neu1-/-, Neu1-/-GD3S-/- mice to understand whether the urinary oligosaccharide content would alter with deficiency of the enzymes the mice possessed.

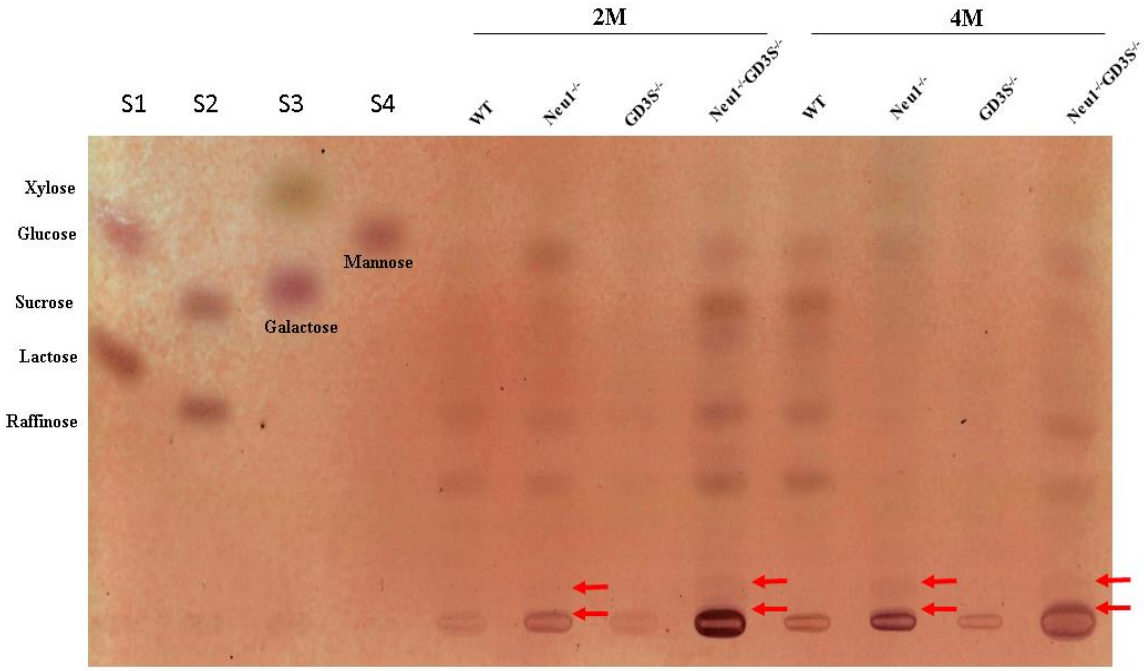

Figure 3.4. Urinary oligosaccharide profile by TLC analysis and visualized with orcinol staining of 2- and 4- month-old WT, GD3S-/-, Neu1-/-, Neu1-/-GD3S-/- mice. Standards are indicated with artificial sugars with the amount of (S1. Glucose and Lactose, S2. Sucrose and Raffinose, S3. Xylose and Galactose, S4. Mannose) (n=3).

Mice with the lacking of Neu1 enzyme, Neu1-/- and Neu1-/-GD3S-/- enzymes for both ages revealed a band close to loading point which was not visible for the other genotypes (Figure 3.4). In addition to this, 2 month old Neu1-/-GD3S-/- mice revealed more oligosaccharide content in the urine sample compared to other genotypes at 2-month old whereas GD3S-/- mice showed very low content of oligosaccharide in the urine

(Figure 3.4). However the urinary content of 4- month old Neu1-/-GD3S-/- mice was reduced compared to 2-month old Neu1-/-GD3S-/- mice (Figure 3.4). This type of decrease was also visible between 2- month old Neu1-/- and 4 month old Neu1-/- mice. Mice lacking GD3S-/- enzyme for both ages did not differ among each other and compared to other genotypes, their oligosaccharide content was the lowest (Figure 3.4).

3.5. Expression Analysis

Expression analysis was performed to 2- and 4-month-old WT, GD3S-/-, Neu1-/-, Neu1-/-GD3S-/-, mice from cortex, cerebellum and thalamus regions. With this method, apoptosis, (Bcl-2, Bcl-xl, Bax), oxidative stress (SOD-2, Ttase1, Catalase) and ER-stress (ATF-6, Calnexin, XBP1) related markers were studied.

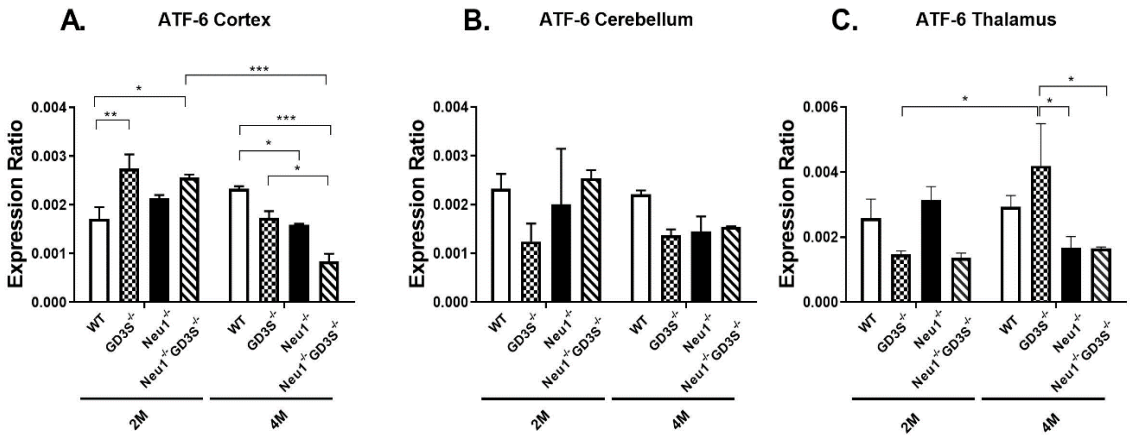

Figure 3.5. 1. Expression levels of ATF-6 gene for cortex (A), cerebellum (B), thalamus (C) from 2- and 4-month-old WT, GD3S-/-, Neu1-/-, Neu1-/-GD3S-/-, mice (Expression ratios were calculated with ΔCT method, normalized to GAPDH mRNA expression levels. P- values were determined with the 2-way-Anova analysis via GraphPad. Data were reported as means ± SE.) (*p<.05 and **p<.01, ***p<.001) (n=3)

For the cortex brain region ATF-6 gene expression levels were elevated in 2-month old GD3S-/- mice compared with 2- month old WT mice. 2- month old Neu1-/-GD3S-/- mice also showed higher rates of ATF-6 expression levels towards 2- month old WT mice (Figure 3.5.1 A). When 4- month old mice were compared for ATF-6 gene expression levels, the highest rates of expression were observed in the WT mice (Figure 3.5.1A). GD3S-/-, Neu1-/- and Neu1-/-GD3S-/- mice showed decrease in terms of ATF-6 gene expression compared with WT mice (Figure 3.5.1 A). Lowest expression of ATF-

6 gene was observed in the Neu1-/-GD3S-/- in 4- month old mice group. In addition to this, expression level of ATF-6 gene in 4- month old Neu1-/-GD3s-/- mice showed a significant decrease compared with 2 month old Neu1-/-GD3S-/- mice (Figure 3.5.1 A). In cerebellum region of 2- month old mice, no significant changes were observed although GD3S-/- mice showed the lowest expression level of ATF-6 gene (Figure 3.5.1 A). In cerebellum region expression levels of ATF-6 did not show a significant change although in GD3S-/- mice, expression of ATF-6 was reduced at 2- and 4- month old mice compared with other genotypes (Figure 3.5.1 B). In thalamus region no significant difference was observed although both GD3s-/- and Neu1-/-GD3S-/- mice showed lower expression levels compared with WT and Neu1-/- mice in 2- month old mice. In 4- month old mice, expression of ATF-6 was increased significantly in GD3S-/- compared to Neu1-/- and Neu1-/-GD3S-/- (Figure 3.5.1 C). In addition expression of ATF-6 was significantly increased between 2 -and 4- month GD3S-/-. (Figure 3.5.1 C).

Expression levels of Calnexin showed only significant change in cortex region for the 2- month old GD3S-/- mice compared with 2- month old WT and Neu1-/-GD3S-/- mice (Figure 3.5.2 A). Cerebellum and Thalamus region did show a change for Calnexin gene expression for any genotypes for both ages however in cerebellum when 4-month old mice were compared, WT mice showed an increase against the other genotypes (Figure 3.5.2 B and C).

Expression levels of XBP-1 did not show any significant change for any brain region for the mice regardless of age (Figure 3.5.3)

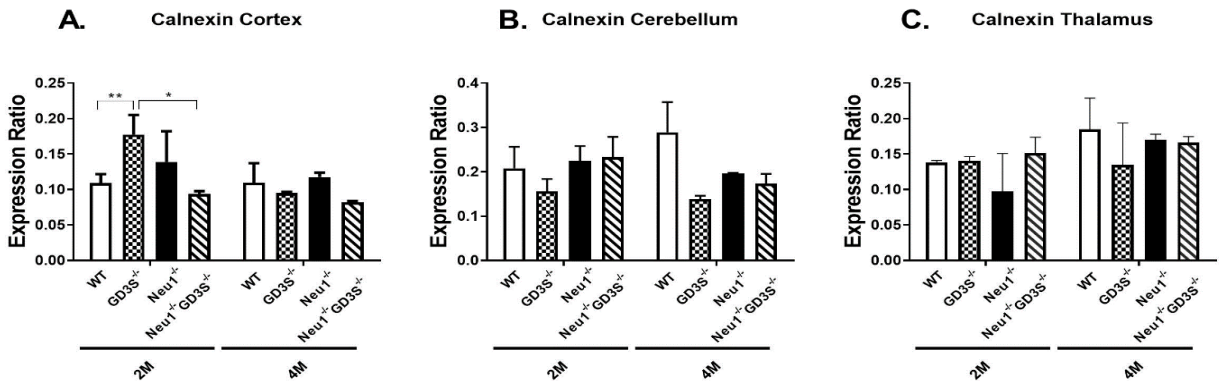

Figure 3.5. 2. Expression levels of Calnexin gene for cortex (A), cerebellum (B), thalamus (C) from 2- and 4-month-old WT, GD3S-/-, Neu1-/-, Neu1-/-GD3S-/-, mice (Expression ratios were calculated with ΔCT method, normalized to GAPDH mRNA expression levels. P- values were determined with the 2-way-Anova analysis via GraphPad. Data were reported as means ± SE.) (*p<.05 and **p<.01) (n=3)

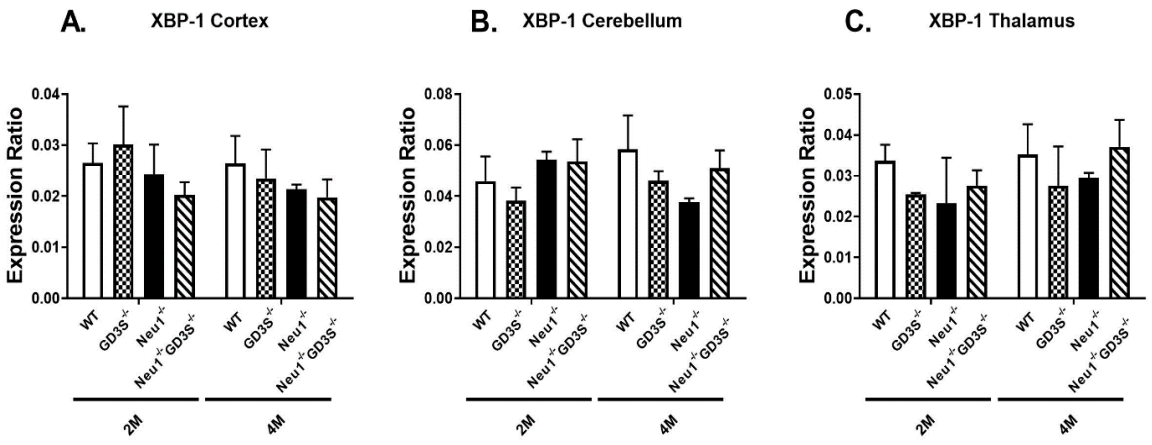

Figure 3.5. 3. Expression levels of XBP-1 gene for cortex (A), cerebellum (B), thalamus (C) from 2- and 4-month-old WT, GD3S-/-, Neu1-/-, Neu1-/-GD3S-/-, mice (Expression ratios were calculated with ΔCT method, normalized to GAPDH mRNA expression levels. P- values were determined with the 2-way-Anova analysis via GraphPad. Data were reported as means ± SE.) (n=3)

SOD-2 levels in cortex region did not show a significant change for the mice for the brain regions. Although, in the cortex and thalamus regions, 4- month old Neu1-/- and Neu1-/-GD3S-/- mice showed similar decrease, in the expression levels of SOD-2 compared to WT and GD3S mice (Figure 3.5.4 A and C)

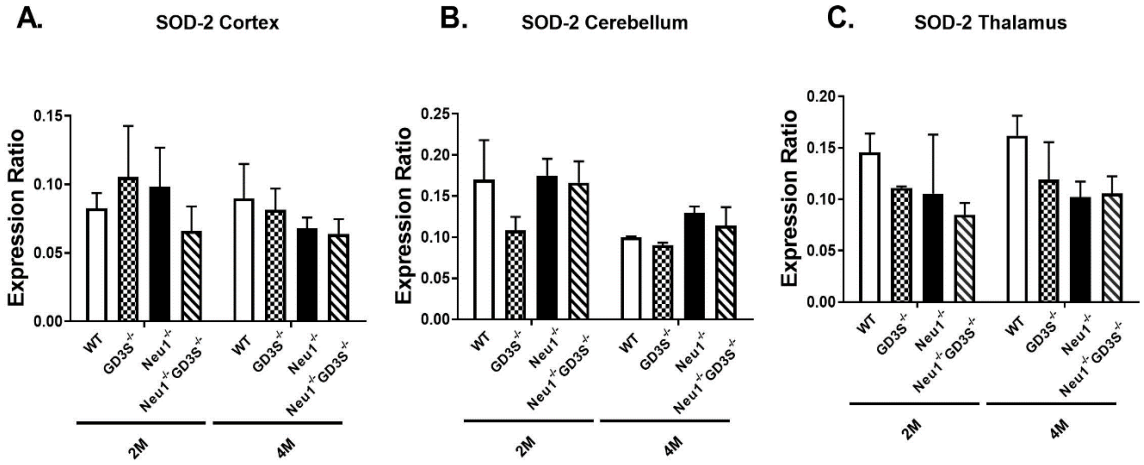

Figure 3.5. 4. Expression levels of SOD-2 gene for cortex (A), cerebellum (B), thalamus (C) from 2- and 4-month-old WT, GD3S-/-, Neu1-/-, Neu1-/-GD3S-/- mice.(Expression ratios were calculated with ΔCT method, normalized to GAPDH mRNA expression levels. P- values were determined with the 2-way-Anova analysis via GraphPad. Data were reported as means ± SE.)(n=3)

Expression levels of catalase in for all brain regions showed similar expression levels (Figure 3.5.5).

For the cortex region, Ttase 1 expressions were increased significantly for GD3S-/- mice compared to Neu1-/-GD3S-/- mice for the 2 -month old mice (Figure 3.5.6 A). In cortex region 4- month old GD3S-/- mice showed a significant decrease compared 2-month old littermates (Figure 3.5.6 A). Cerebellum expressions of Ttase 1 did not show a significant change for 2 -month and 4 -month old mice although a slight decrease was observed for the 4- month old GD3S-/-mice (Figure 3.5.6 B). In thalamus region, expression levels were similar for 2- and 4- month old mice in terms of Ttase1 expression levels (Figure 3.5.6 C).

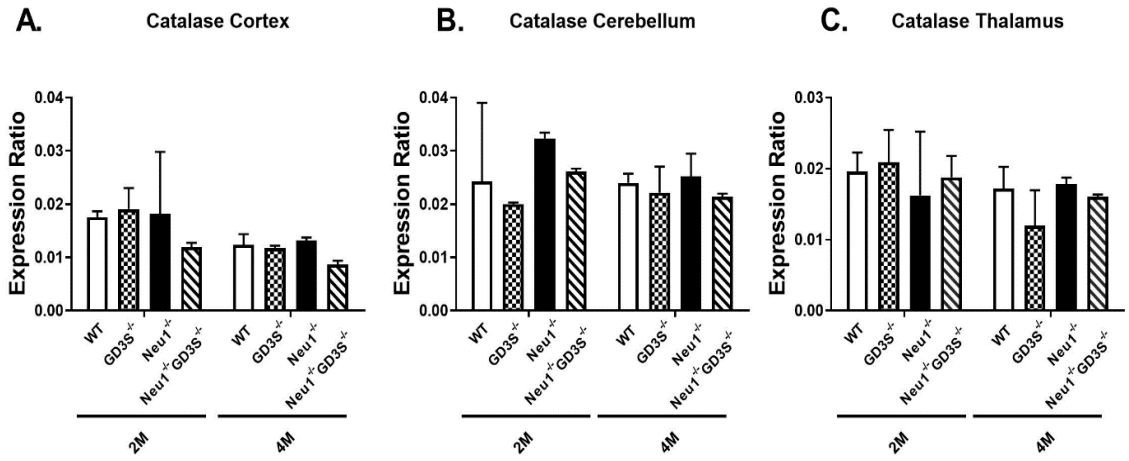

Figure 3.5. 5. Expression levels of Catalase gene for cortex (A), cerebellum (B), thalamus (C) from 2- and 4-month-old WT, GD3S-/-, Neu1-/-, Neu1-/-GD3S-/-, mice (Expression ratios were calculated with ΔCT method, normalized to GAPDH mRNA expression levels. P- values were determined with the 2-way-Anova analysis via GraphPad. Data were reported as means ± SE.)(n=3)

Bcl-2 expressions of cortex region for the 2 and 4- month old mice did not show a significant change although a decrease was observed for the 4- month old Neu1-/-GD3S-/- mice (Figure 3.5.7 A). In cerebellum region, 2- month old Neu1-/- mice showed significantly higher levels of Bcl-2 expression levels compared to GD3S-/- and WT mice (Figure 3.5.7 B). However, for the 4 month old mice in terms of Bcl-2 expression levels did not differ significantly but a slightly increase was observed for the Neu1-/- mice (Figure 3.5.7 B). In addition, expression of Bcl-2 was reduced at the 4- month old Neu1-/- mice compared to 2 -month old Neu1-/- mice (Figure 3.5.7 B). In thalamus region, Bcl-

2 levels for both ages did not show a significant increase although a slightly increase was observed in the 2- month old Neu1-/- mice (Figure 3.5.7C).

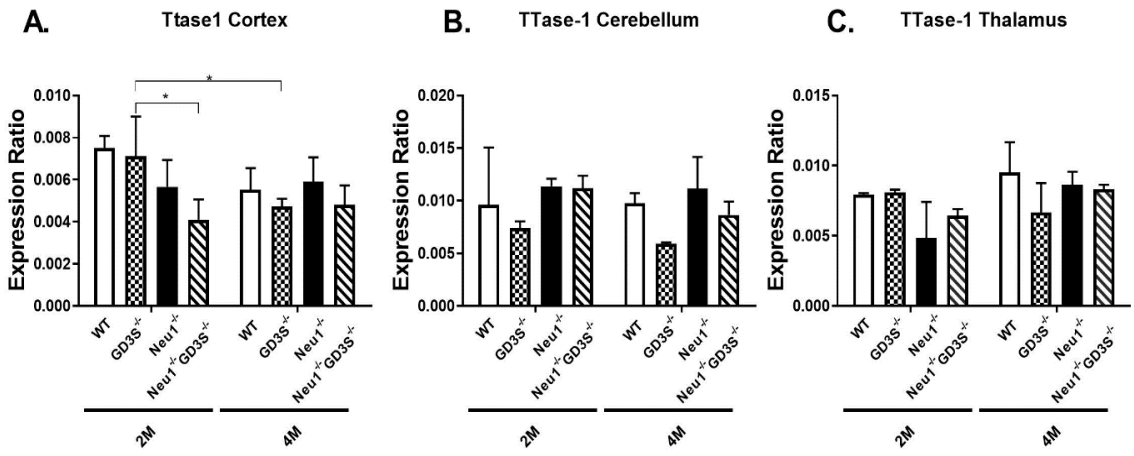

Figure 3.5. 6. Expression levels of Ttase1 gene for cortex (A), cerebellum (B), thalamus (C) from 2- and 4-month-old WT, GD3S-/-, Neu1-/-, Neu1-/-GD3S-/-, mice (Expression ratios were calculated with ΔCT method, normalized to GAPDH mRNA expression levels. P- values were determined with the 2-way-Anova analysis via GraphPad. Data were reported as means ± SE.) (*p<.05) (n=3)

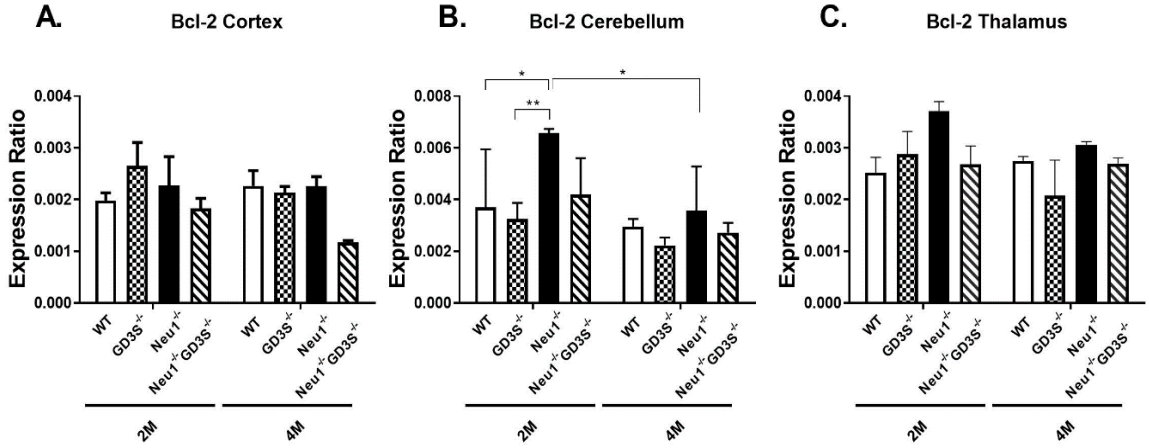

Figure 3.5. 7. Expression levels of Bcl-2 gene for cortex (A), cerebellum (B), thalamus (C) from 2- and 4-month-old WT, GD3S-/-, Neu1-/-, Neu1-/-GD3S-/-, mice (n=3). (Expression ratios were calculated with ΔCT method, normalized to GAPDH mRNA expression levels. P- values were determined with the 2-way-Anova analysis via GraphPad. Data were reported as means ± SE.) (*p<.05 and **p<.01) (n=3)

Neu1 -/- showed a significant increase in terms of Bcl-xl expression levels in cortex region compared to GD3S-/- mice (Figure 3.5.8 A). For the cortex region of 4-month old mice, no significant changes were observed for the Bcl-xl expression levels (Figure 3.5.8 B). In cerebellum region no significant change was observed for the 4-month old mice in terms of Bcl-xl expressions however, for GD3S-/- and Neu1-/- mice an increase was observed (Figure 3.5.8 B). Bcl-xl expression in thalamus region were similar between all mice regardless of age (Figure 3.5.8 C).

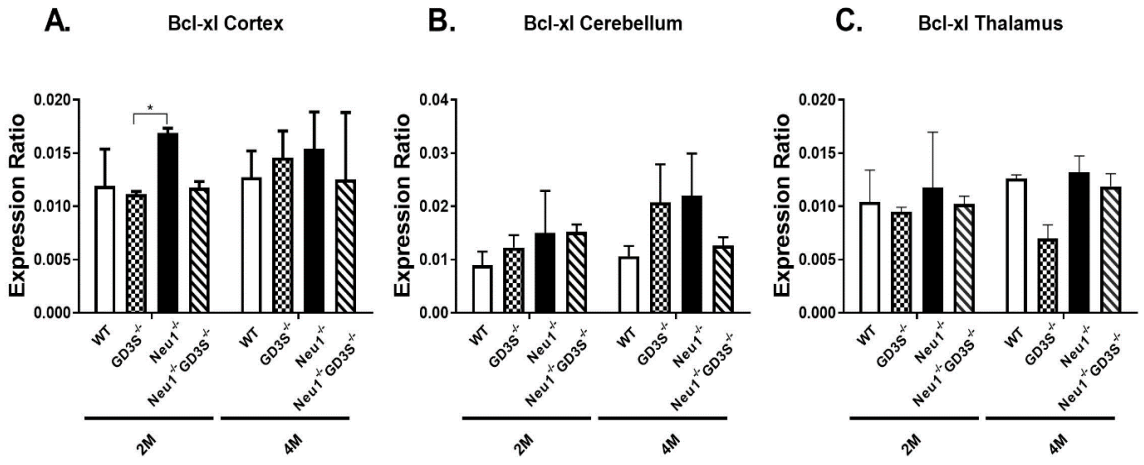

Figure 3.5. 8. Expression levels of Bcl-xl gene for cortex (A), cerebellum (B), thalamus (C) from 2- and 4-month-old WT, GD3S-/-, Neu1-/-, Neu1-/-GD3S-/-, mice (n=3). (Expression ratios were calculated with ΔCT method, normalized to GAPDH mRNA expression levels. P- values were determined with the 2-way-Anova analysis via GraphPad. Data were reported as means ± SE.)(*$p<0.05$) (n=3)

Bax gene expressions of 2- month old Neu1-/- elevated significantly compared to GD3S-/- mice in the cortex region. But for the 4- month old mice expression of Bax was reduced for the all mice which did not show any significant diffrence between genotypes for the 4- month old mice (Figure 3.5.9 A). Bax expression levels in cerebellum region, Neu1-/- mice showed a significant increase compared to WT (Figure 3.5.9 B). For 2-month old GD3S-/- and Neu1-/-GD3S-/- mice showed lower expression levels of Bax which was highly significant compared to Neu1-/- mice. Bax expression levels of 4-month old Neu1-/- mice significantly reduced compared to 2- month old Neu1-/- mice (Figure 3.5.9 B). Similar to cortex and cerebellum region, Bax expression levels of Neu1-/- mice were significantly increased in the thalamus region showed a significant decrease in the 4- months old littermates (Figure 3.5.9 C).

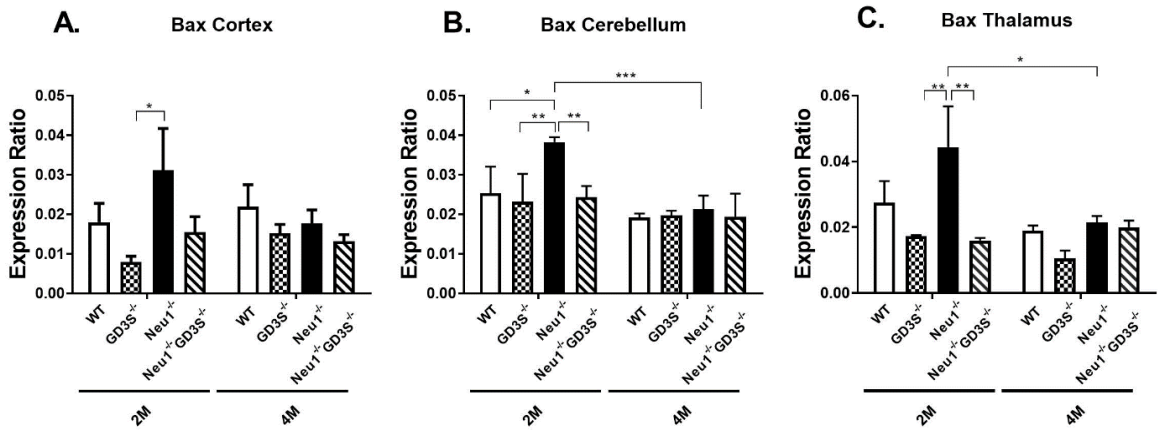

Figure 3.5. 9. Expression levels of Bax gene for cortex (A), cerebellum (B), thalamus (C) from 2- and 4-month-old WT, GD3S-/-, Neu1-/-, Neu1-/-GD3S-/-, mice (n=3). (Expression ratios were calculated with ΔCT method, normalized to GAPDH mRNA expression levels. P- values were determined with the 2-way-Anova analysis via GraphPad. Data were reported as means ± SE.) (*p<0.05 and **p<0.01, ***p<0.001) (n=3)

3.6. Western blot Analysis

Western blot analysis were performed with proteins isolated from cortex, cerebellum and thalamus brain regions to investigate the apoptotic pathways in 2- and 4-month-old WT, GD3S-/-, Neu1-/- and Neu1-/- mice. In addition some important components of extrinsic and intrinsic apoptotic pathways investigated by using Fas-Ligand, BIP, Caspase 9 and Caspase 3 anti-bodies to detect their protein expression levels

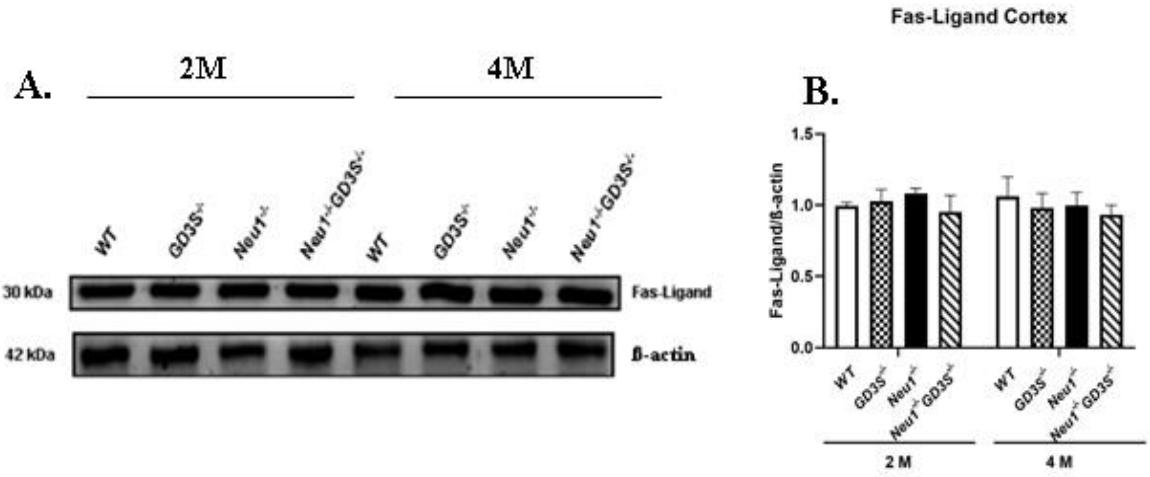

Figure 3.6. 1. (A) Western Blot image of Fas-Ligand antibody in the cortex region of 2- and 4-month-old WT, GD3S-/-, Neu1-/- and Neu1-/- mice. β-actin anti-body was used for control. (B) Protein bands were normalized with the ß-actin antibody. Significant levels in the data were presented by using the two-way ANOVA. (n=3)

In cortex, thalamus and cerebellum brain region, no significant change were observed in the protein levels of Fas-Ligand for the both 2- and 4- month old mice. (Figure 3.6.1, Figure 3.6.2 and Figure 3.6.3)

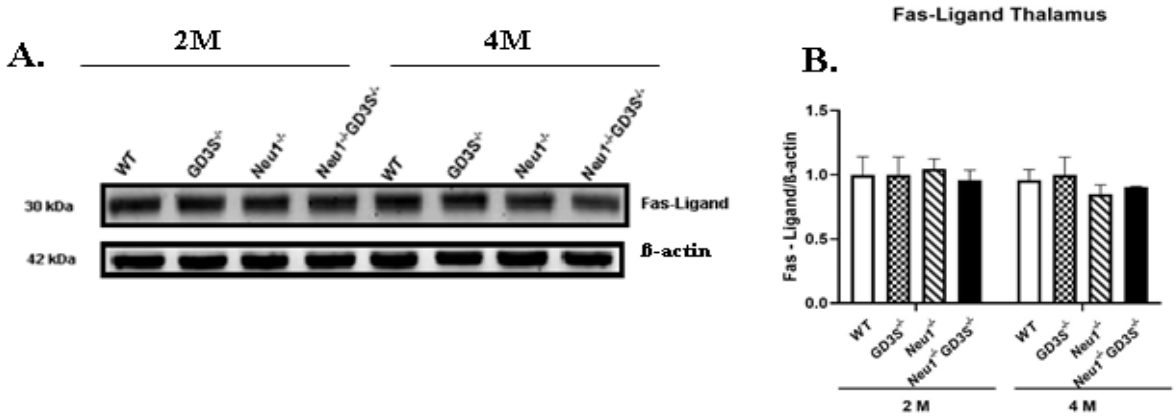

Figure 3.6. 2. (A) Western Blot image of Fas-Ligand antibody for the thalamus region of 2- and 4-month-old WT, GD3S-/-, Neu1-/- and Neu1-/- mice. β-actin anti-body was used for control. (B) Protein bands were normalized with the ß-actin antibody. Significant levels in the data were presented by using the two-way ANOVA. (n=3)

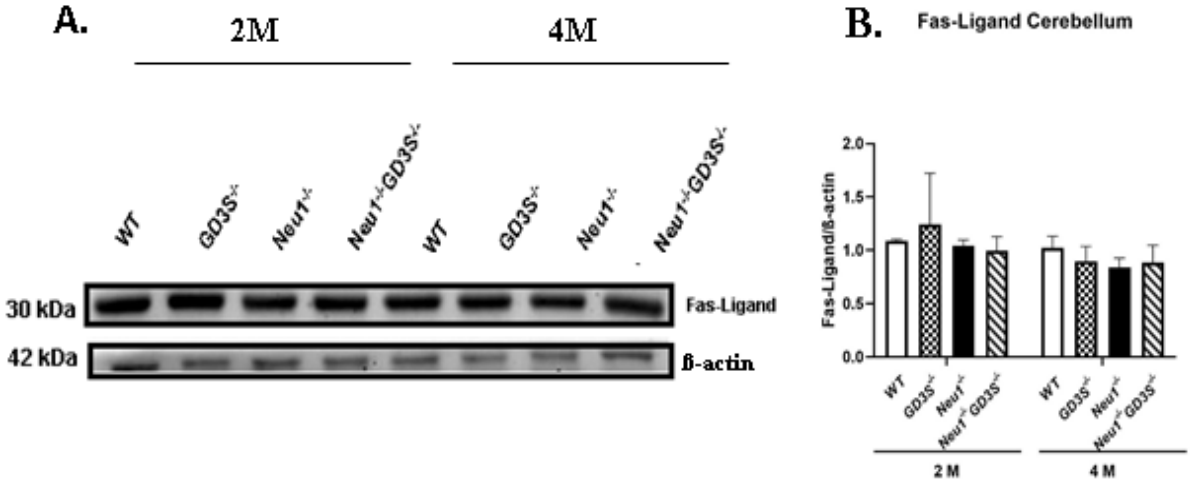

Figure 3.6. 3. (A) Western Blot image of Fas-Ligand antibody for the cerebellum region of 2- and 4-month-old WT, GD3S-/-, Neu1-/- and Neu1-/- mice. β-actin anti-body was used for control. (B) Protein bands were normalized with the ß-actin antibody. Significant levels in the data were presented by using the two-way ANOVA (n=3)

BIP protein cortex region showed a significant increase in the 2- month old Neu1-/-GD3-/- mice compared to WT mice at the same age. In addition, 2- month old Neu1-/-

mice also showed increased levels of BIP protein in the cortex region compared to other mice at the same age (Figure 3.6.4 A and B).

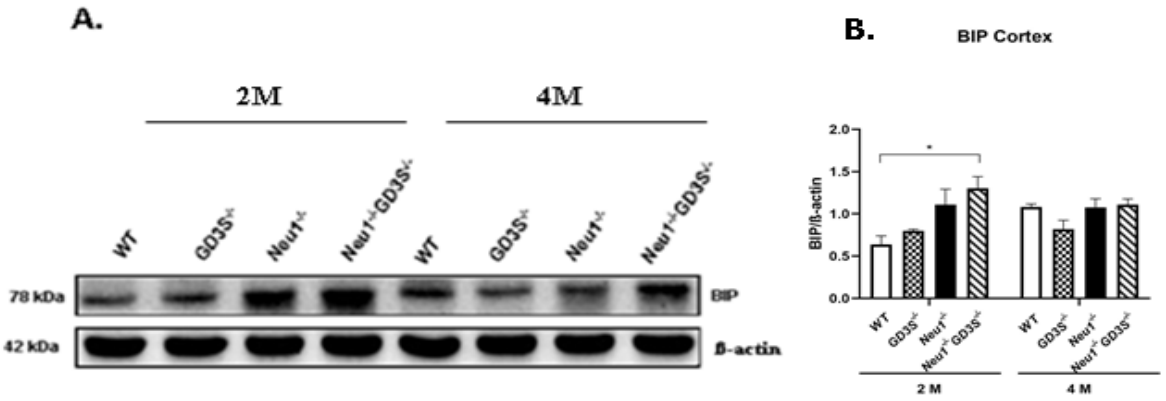

Figure 3.6. 4. Western Blot image of BIP antibody for the cortex region of 2- and 4-month-old WT, GD3S-/-, Neu1-/- and Neu1-/- mice. β-actin anti-body was used for control. (B) Protein bands were normalized with the ß-actin antibody. Significant levels in the data were presented by using the two-way ANOVA (*p<.05). (n=3)

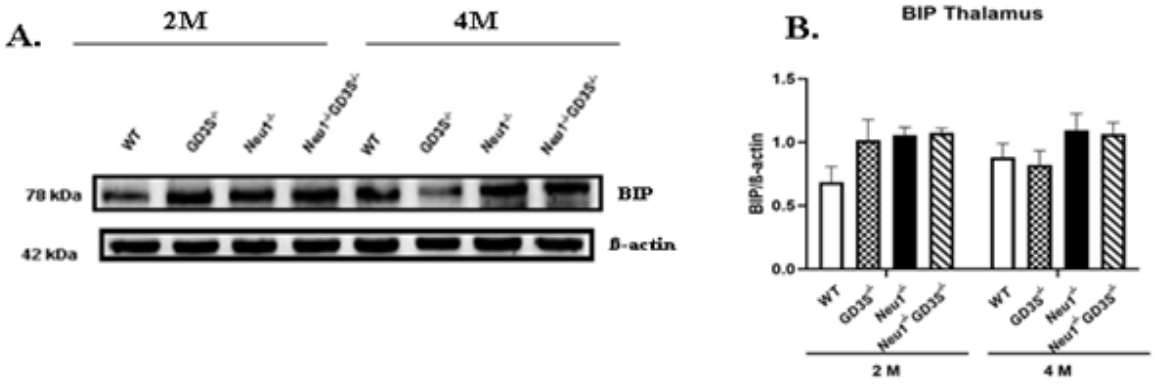

Figure 3.6. 5. Western Blot image of BIP antibody for the thalamus region of 2- and 4-month-old WT, GD3S-/-, Neu1-/- and Neu1-/- mice. β-actin anti-body was used for control. (B) Protein bands were normalized with the ß-actin antibody. Significant levels in the data were presented by using the two-way ANOVA (n=3)

BIP protein levels observed in thalamus region did not show a significant change for the mice (Figure 3.6.4 A and B). Although for the 2- month old WT mice, a slight decrease was observed (Figure 3.6.5A).

For the cerebellum region, no significant change were observed for the BIP protein levels (Figure 3.6.6)

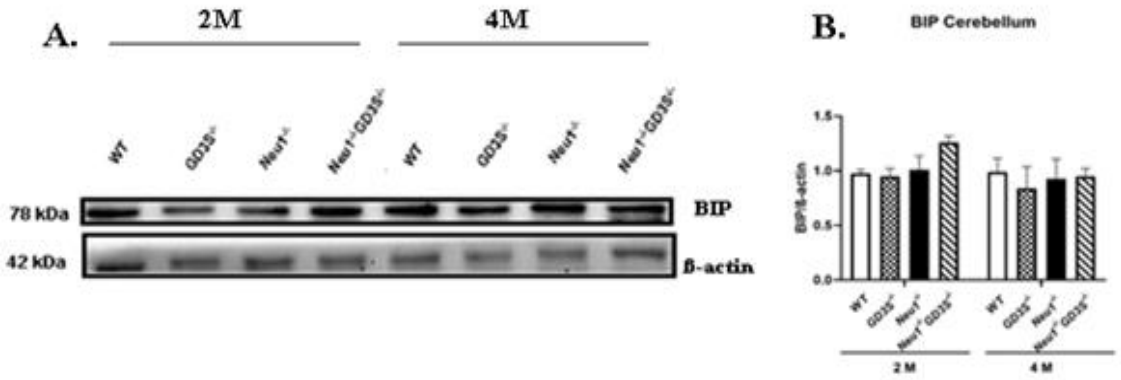

Figure 3.6. 6. Western Blot image of BIP antibody for the cerebellum region of 2- and 4-month-old WT, GD3S-/-, Neu1-/- and Neu1-/- mice. β-actin anti-body was used for control. (B) Protein bands were normalized with the ß-actin antibody. Significant levels in the data were presented by using the two-way ANOVA (n=3)

In cortex region, cleavage of caspase 9 was visible for all of the mice regardless of age although, cleaved caspase levels of 2- month old Neu1-/- and Neu1-/-GD3S-/- mice showed a significant increase compared to other genotypes at the same age. Increased levels of cleaved caspase 9 was also observed in the 4- month old Neu1-/- and Neu1-/-GD3S-/- mice for the cortex region (Figure 3.6.7 A and B).

In thalamus region, for the 2- month old mice, cleavage of caspase 9 observed in GD3S-/-, Neu1-/- and Neu1-/-GD3S-/- mice but it was less seen WT mice. 2- month old Neu1-/-GD3S-/- mice showed significantly increased levels of caspase 9 compared to WT mice at the same age. 4- month old mice, showed similar patterns of cleaved caspase 9 which did not show any significant difference among the genotypes. (Figure 3.6.8 A and B)

In cerebellum region, 2 month old mice cleavage of caspase 9 did not show any difference between genotypes. But when 4 month old mice were compared, Neu1-/- showed a significant increase in terms of cleaved caspase 9 levels compared to WT and Neu1-/-GD3S-/- mice at the same age (Figure 3.6.9 A and B).

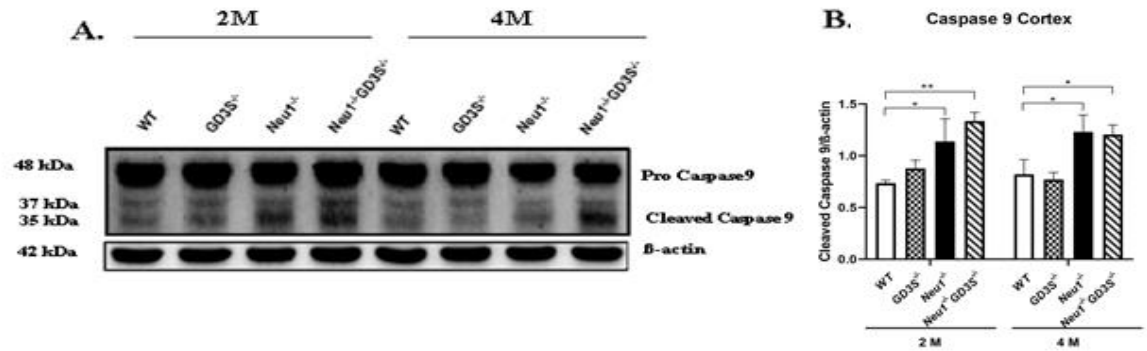

Figure 3.6. 7. Western Blot image of Caspase 9 antibody for the cortex region of 2- and 4-month-old WT, GD3S-/-, Neu1-/- and Neu1-/- mice. β-actin anti-body was used for control. (B) Protein bands were normalized with the ß-actin antibody. Significant levels in the data were presented by using the two-way ANOVA (*p<0.05 and **p<0.01). (n=3)

Cleaved Caspase 3 levels were visible for all of the mice in cortex region. 2-month old Neu1-/- mice showed significantly, increased levels of cleaved caspase 3 compared to GD3S-/- and WT mice with the same age. 2- month old Neu1-/-GD3S-/- mice also showed a significant increase compared to WT mice with the same age. When 4- month old mice were compared in terms of the cleavage of caspase 3, intensity of the bands were similar. (Figure 3.6.10 A and B)

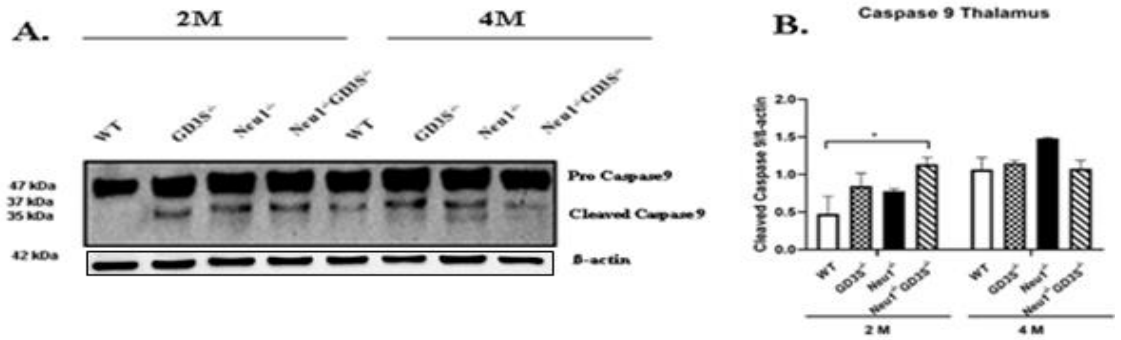

Figure 3.6. 8. Western Blot image of Caspase 9 for Thalamus antibody in the cortex region of 2- and 4-month-old WT, GD3S-/-, Neu1-/- and Neu1-/- mice. β-actin anti-body was used for control. (B) Protein bands were normalized with the ß-actin antibody. Significant levels in the data were presented by using the two-way ANOVA (*p<.05 and **p<.01). (n=3)

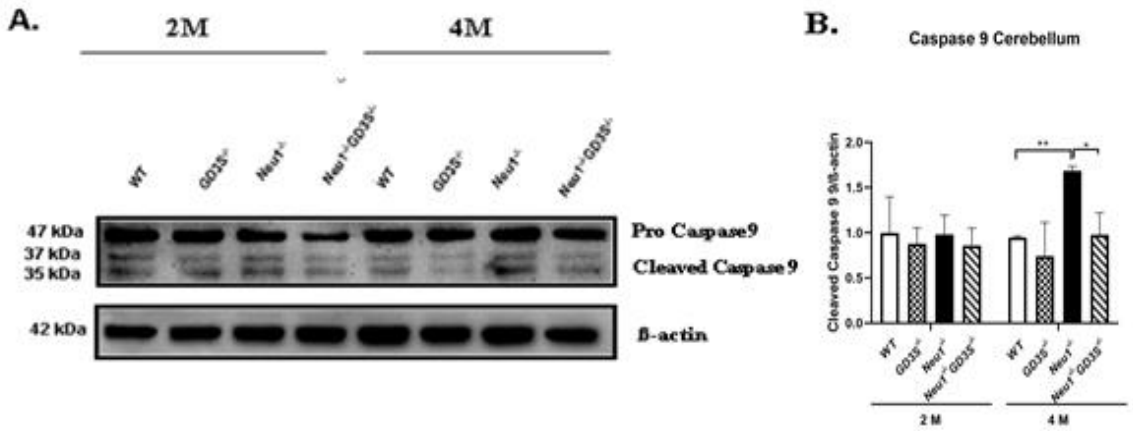

Figure 3.6. 9. Western Blot image of Caspase 9 antibody for the cerebellum region of 2- and 4-month-old WT, GD3S-/-, Neu1-/- and Neu1-/- mice. β-actin anti-body was used for control. (B) Protein bands were normalized with the ß-actin antibody. Significant levels in the data were presented by using the two-way ANOVA (*p<.05 and **p<.01). (n=3)

In thalamus region, cleaved caspase 3 levels of 2- month old Neu1-/- was the most intense band observed. Intensity of the cleaved caspase 3 for Neu1-/- mice in thalamus region was significantly higher compared to WT, GD3S-/- and Neu1-/-GD3S-/- mice. 4-month old micedid not show any significant diffrence between genotypes for the cleaved caspase (Figure 3.6.11 A and B)

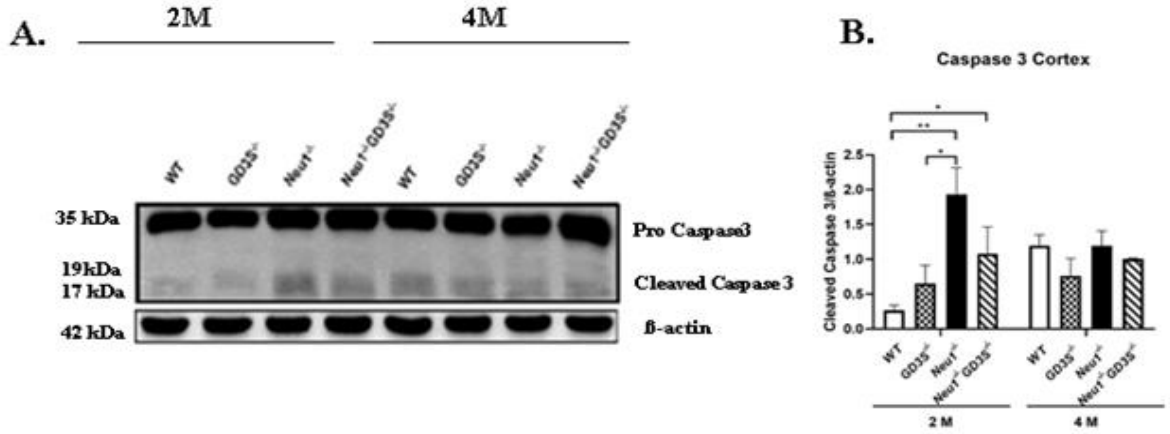

Figure 3.6. 10. Western Blot image of Caspase 3 antibody for the cortex region of 2- and 4-month-old WT, GD3S-/-, Neu1-/- and Neu1-/- mice. β-actin anti-body was used for control. (B) Protein bands were normalized with the ß-actin antibody. Significant levels in the data were presented by using the two-way ANOVA (*p<0.05 and **p<0.01). (n=3)

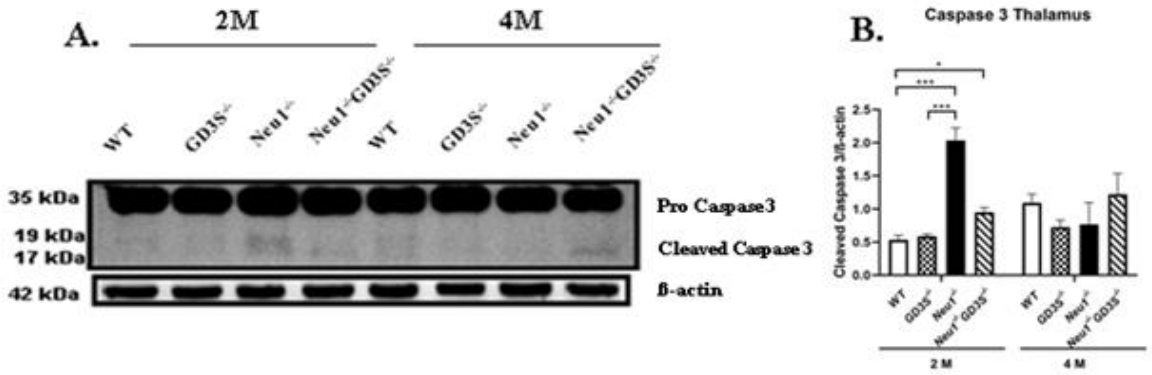

Figure 3.6. 11. Western Blot image of Caspase 3 antibody for the thalamus region of 2- and 4-month-old WT, GD3S-/-, Neu1-/- and Neu1-/- mice. β-actin anti-body was used for control. (B) Protein bands were normalized with the ß-actin antibody. Significant levels in the data were presented by using the two-way ANOVA (*p<.05 and **p<.01, ***p<.001). (n=3)

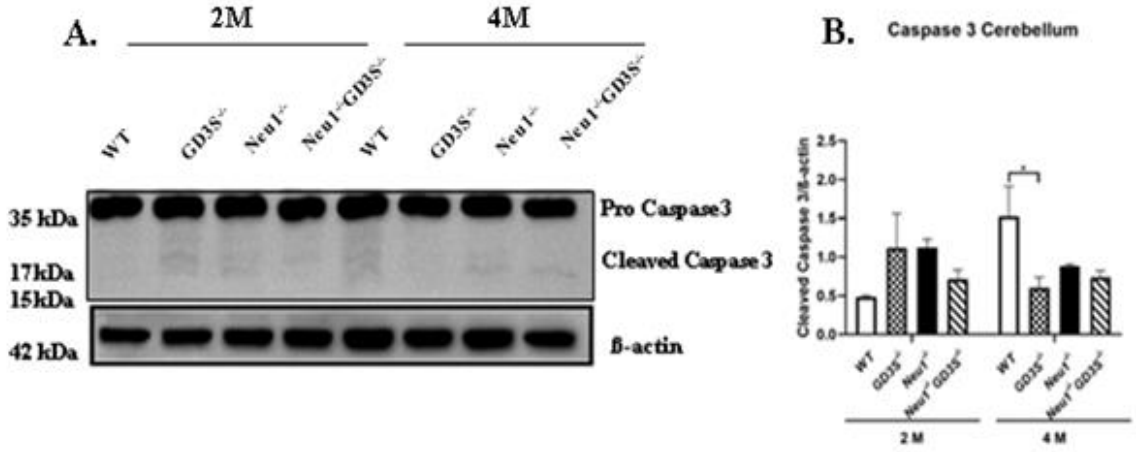

Figure 3.6. 12. Western Blot image of Caspase 3 antibody for the cerebellum region of 2- and 4-month-old WT, GD3S-/-, Neu1-/- and Neu1-/- mice. β-actin anti-body was used for control. (B) Protein bands were normalized with the ß-actin antibody. Significant levels in the data were presented by using the two-way ANOVA (*p<.05 and **p<.01). (n=3)

Cleaved caspase 3 levels in cerbellum region of 2- month old mice did not show a significant increase. Altough slightly visible cleaved bands of caspase 3 were present in GD3S-/-, Neu1-/- and Neu1-/-GD3S-/- mice. For the 4- month old mice, WT mice showed increased levels of cleaved caspase 3 which was significantly higher compared to GD3S-/- mice. Slightly visible bands of cleaved caspase was present for the Neu1-/- and Neu1-/-GD3S-/- mice (Figure 3.6.12 A and B).

3.7. DNA Fragmentation Analysis

A classical method used to detect apoptosis, DNA fragmentation analysis was performed to 2- and 4-month-old WT, GD3S-/-, Neu1-/- and Neu1-/- mice. Fragmented DNAs indicates apoptosis, which occurs after the cells are programmed to die after the activation of the DNases cleaves the DNA in to fragments.

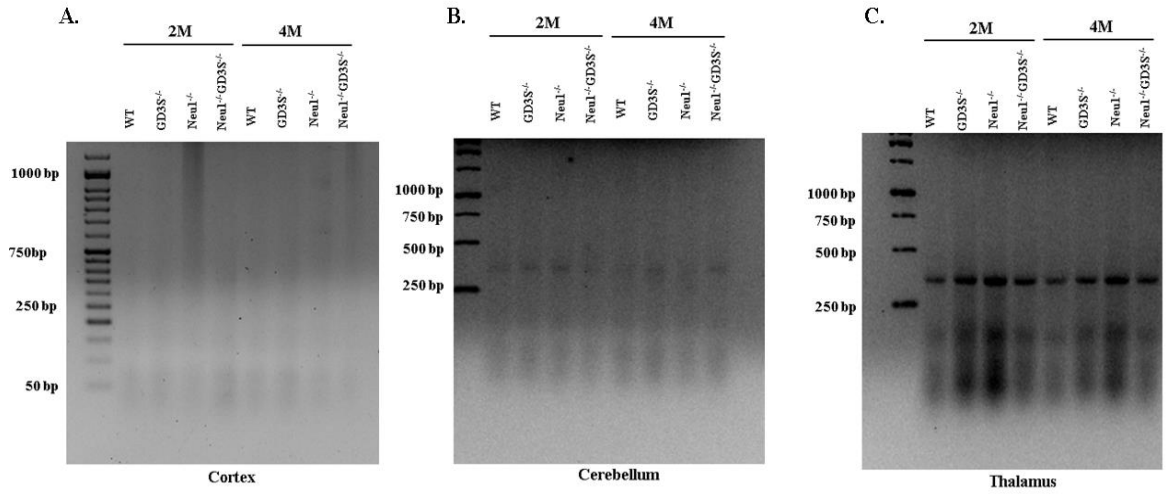

Figure 3.7. Visualized fragmented DNAs isolated from (A) cortex, (B) cerebellum and (C) thalamus region of 2- and 4-month-old WT, GD3S-/-, Neu1-/- and Neu1-/- mice. (n=3)

Separated fragmented DNAs on the agarose gel, mostly showed smear bands which were the fragmented DNAs. In thalamus region for the 2- month old mice, Neu1-/- mice showed very clear dark smear bands compared to other genotypes with the same age. Also smear bands were very clear in the thalamus region of 2 -month old GD3S-/- mice. Neu1-/-GD3S-/- mice showed less intense smear bands, although it was denser compared to WT which revealed the faintest bands in 2- month old mice. For the 4- month old mice, similar to 2- month old mice, Neu1-/- mice showed the most intense smear bands followed by GD3S-/- mice (Figure 3.7 C). The Neu1-/-GD3S-/- showed fainter bands compared to the Neu1-/- and GD3S-/- mice. In addition to this, near 350bp, unknown fragmented DNA bands were observed in the mice in thalamus region. And their intensities showed similar patterns with the smear bands seen with the mice (Figure 3.7 C). While observing such clear bands in the thalamus region, cortex and cerebellum regions showed less intense bands (Figure 3.7A and B).

3.8. NeuN- Staining

To evaluate the number of the neurons in different brain regions, 10µm coronal sections obtained from 4- month old WT, GD3S-/-, Neu1-/- and Neu1-/-GD3S-/- mice were stained with anti-NeuN antibody and their densities were normalized to WT mice (Figure3.8). NeuN is a neuronal protein which is expressed in neurons although its expression only limited to some certain types of cells in brain.(R. J. Mullen, Buck, and Smith 1992) Therefore Red signals observed with NeuN antibody only represent some portion of the cells in the brain but still its decrease can be correlated with cell death.

Neu1-/- and Neu1-/- GD3S-/- mice showed a severe decrease in terms of the red signals emitted from the neurons when compared with WT and GD3S-/- mice. Intensity analysis of NeuN antibody for Neu1-/- mice, showed about 60% for the cortex (Figure 3.8 C), 70% for the hippocampus (Figure 3.8 G), 75% for the thalamus (Figure 3.8 K) and 55% decrease in the cerebellum (Figure 3.8 O) regions in terms of red NeuN signals compared to WT mice. For Neu1-/-GD3S-/- mice for cortex region (Figure3.8 D) 65%, for hippocampus (Figure 3.8 H) 55%, for thalamus (Figure 3.8 L) 65% and for cerebellum region (Figure 3.8 P) neuron numbers were decreased about 65%. A significant loss in terms of red signals for the GD3S-/- mice was only observed in Thalamus region (Figure 3.8 T) which was about 33% compared but in other brain regions of GD3S-/- mice did not show a significant change compared to WT but a slight decrease about decrease was observed was observed (Figure 3.8 B, F and N).

3.9. Histopathological Results

Pathological analysis were performed with Hematoxylin and Eosin and Cresyl Violet stainings to study the morphology of the brain sections.

3.9.1. Hematoxylin and Eosin Staining

Histopathologic staining with hematoxylin and eosin staining was performed to examine the morphological changes of the brain tissues. 2- and 4- month old WT, GD3S-/-, Neu1-/- and Neu1-/-GD3S-/- mice were examined for this purpose. 2- and 4- month

old mice showed similar properties where an important group of cells were be altered in terms of their morphological structure. These cells are indicated with the green for normal, yellow for moderate and black for severe alterations of their structure.

Compared to WT mice 2 months GD3S-/- Neu1-/- and Neu1GD3S-/- mice differed in the pyramidal cell structure. For GD3-/- mice these cells were tend to be moderately changed compared to WT mice which can be seen in the cortex(Figure 3.9.1B) and thalamus (Figure 3.9.1 J) regions. For Neu1-/- (Figure 3.9.1C and K) and Neu1-/-GD3S-/- (Figure D and L) mice, most of the pyramidal cells in the cortex and thalamus regions were even in a smaller form compared to the one which GD3S-/- possess. For the hippocampus and cerebellum region with hematoxylin and eosin staining, no major abnormalities were found at 20X magnification between genotypes.

4 -month old-knock out mice did also displayed similar abnormalities with 2-month old knock out mice. Under 20x magnification. 4- month old GD3S-/- mice displayed smaller cells but moderately altered cells were still present in the cortex (Figure 3.9.2 B) and thalamus (Figure 3.9.2 J) region. Neu1-/- and Neu1-/-GD3S-/- mice displayed similar morphological structures in terms of the pyramidal neurons like their 2-months old littermates for the cortex (Figure 3.9.2 C and D) and thalamus (Figure 3.9.2 J and I) region.

3.9.2. Cresyl Violet Staining

Cresyl violet staining was performed to stain the neurons and observe their morphological structures. Axon relate Nissl bodies, which are the granular bodies of the neurons which were stained to blue color with cresyl violet staining .2- and 4- month old WT, GD3S-/-, Neu1-/- and Neu1-/-GD3S-/- mice sections were stained with cresyl violet dye and examinations were performed under 20x magnification. For the 2- month old mice for all genotypes showed similar images (Figure 3.9.3).

Examination of 4- month old Neu1-/- and Neu1-/-GD3S-/- mice displayed balloon like structures in their brain regions. These structures displayed paler color to other stained components of the brain compared to other genotypes at the same age. For Neu1-/- mice these structures can be seen in cortex (Figure 3.9.4 C) and thalamus (Figure 3.9.4K). These structures were also seen in the cortex (Figure 3.9.4 D) and thalamus (Figure 3.9.4 L) region of the Neu1-/-GD3S-/- mice.

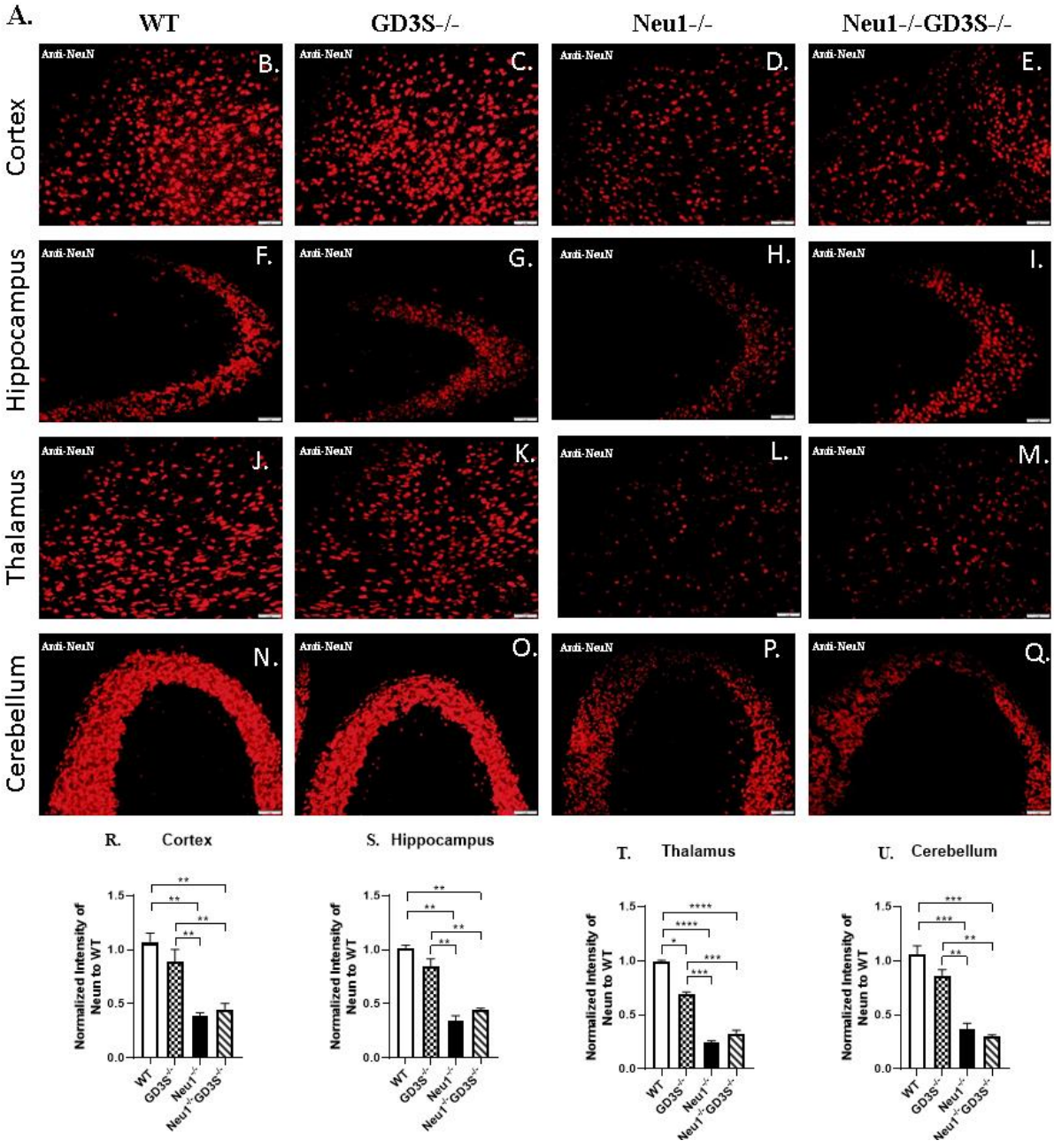

Figure 3.8. (A)Neuronal density analyses performed with the Anti-NeuN antibody stained for (B,C,D,E) cortex, (F,G,H,I) hippocampus, (J,K,L,M) thalamus, and (N,O,P,Q) cerebellum regions from 4-month-old WT, GD3S-/-, Neu1-/- and Neu1-/-GD3S-/- mice. Images were taken with the 20X magnification and the scale bar indicates 50μm. Intensity analysis was performed via Image J. Intensities were normalized to WT. Histograms below represents the intensity analysis of (R) cortex, (S) hippocampus, (T) Thalamus, (U). Data are represented as mean ± SEM of measurements. One-way ANOVA was used to determine the P-values. (*p<.05, **p<.025, ***p<.001 and ****p<.0001). (n=3)

3.10. Behavioral Analaysis

Behavioral analysis were conducted to reveal the behavioral changes of the 2- and 4- month old WT, GD3S-/-, Neu1-/-, Neu1-/-GD3S-/-

3.10.1. Open Field Test

Open field test was used to understand the anxiety levels and the locomotor activity of the mice. In this test, the time spent in the periphery, in the center and the total distance was for the 2- and 4-month-old WT, GD3S-/-, Neu1-/-, Neu1-/-GD3S-/- mice. Compared to 2- month old WT mice, all other genotypes spent significantly more time in the peripheral area (Figure 3.10.1 A). This type of increase was also observed in the 4 month old mice when they are compared with WT mice (Figure 3.10.1 A). When 2-month old mice were compared in terms of the time that they have spent in the center area, WT mice showed greater activity against other genotypes, especially for Neu1-/- and Neu1-/- mice (Figure 3.10.1 C).

When 4- months old mice were compared, the highest mice spent time in the center was WT mice. Although activity towards entering to the center area was increased for the 4- month old GD3S-/-, Neu1-/-, Neu1-/-GD3S-/- (Figure 3.10.1 C).

When mice were compared in terms of their total distance that they have during the test, 2- month old WT mice showed a significant increase compared to Neu1-/- and Neu1-/-GD3S-/- mice (Figure 3.10.1B). The total distance travelled of 2- month old GD3S-/- mice was higher compared to Neu1-/- and especially for Neu1-/-GD3S-/- mice with the same age (Figure 3.10.1B). At 4- months of age, knock out mice showed better performance and almost travelled the same distances as WT mice (Figure 3.10.1B).

3.9.2. Rotarod Test

Rotarod test was performed to the mice in order to understand the locomotor capabilities, balance adjustment and coordination. By forcing the mice to stand on an accelerating rod, their latency to fall was calculated. In 2 month old mice group, there were no significant changes compared when the genotypes are compared between each

other (Figure 3.10.3). However the time that 2- month old Neu1-/-GD3S-/- mice stayed on the rod was lower compared to other genotypes. In 4- month old mice, the most successful mice in terms of the time that stayed most on the rod was the WT mice (Figure 3.10.3). 4- month old WT mice stayed longer on the rod compared to GD3S-/- mice. 4-month old Neu1-/-GD3S-/- showed the worst performance. (Figure 3.10.3)

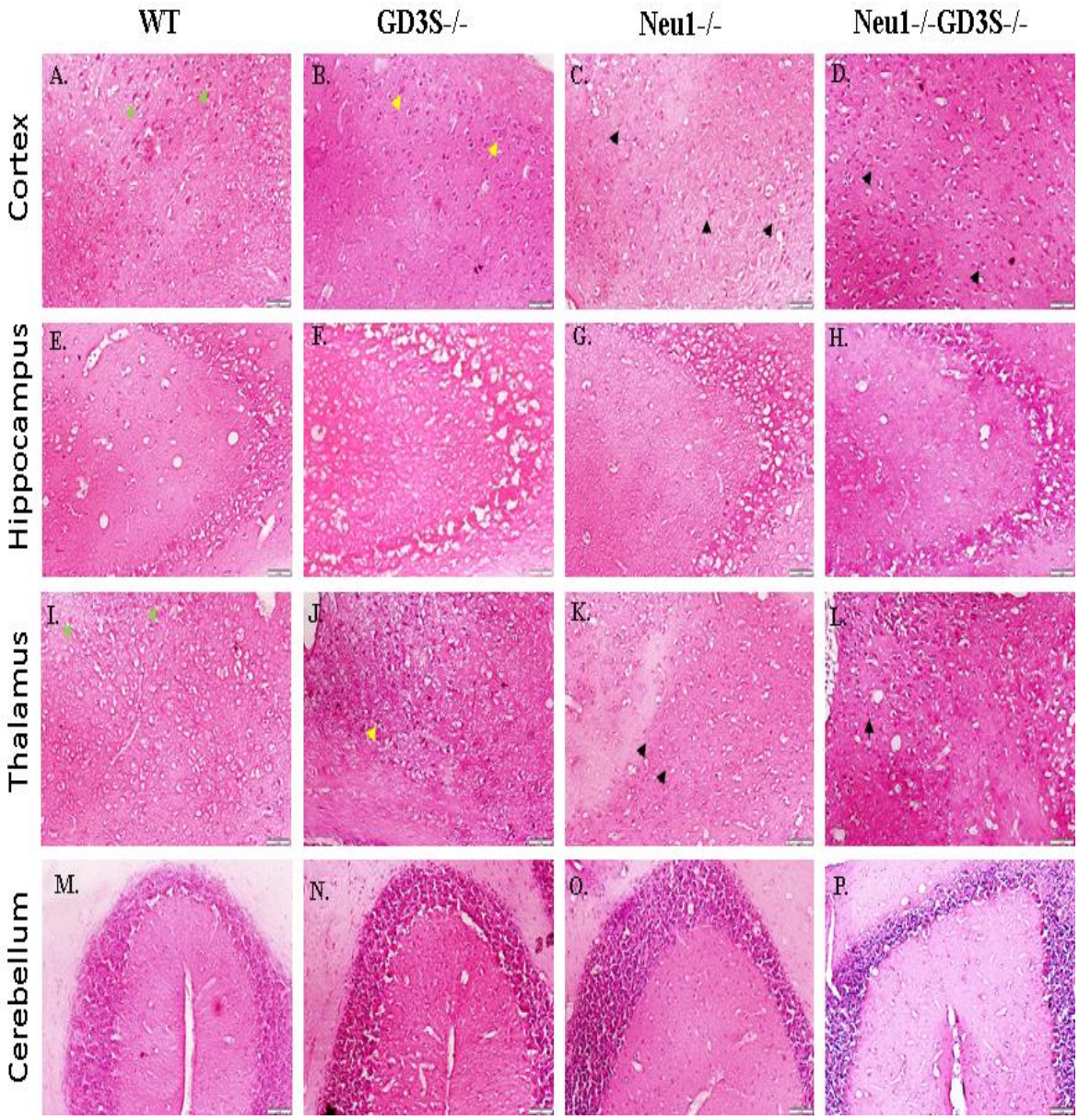

Figure 3.9. 1. Hematoxliyn & Eosin staining for cortex (A,B,C,D), hippocampus (E,F,G,H), thalamus (I,J,K,L), and cerebellum (M,N,O,P) regions of 2-month-old WT, GD3S-/- Neu1-/-, and Neu1-/- GD3S-/- mice stained with . 20x images were taken and the scale bar indicated 50μm. Arrow heads indicates the pyramidal cells (Condition. green for nomal, yellow for moderate, black severe)(n=3).

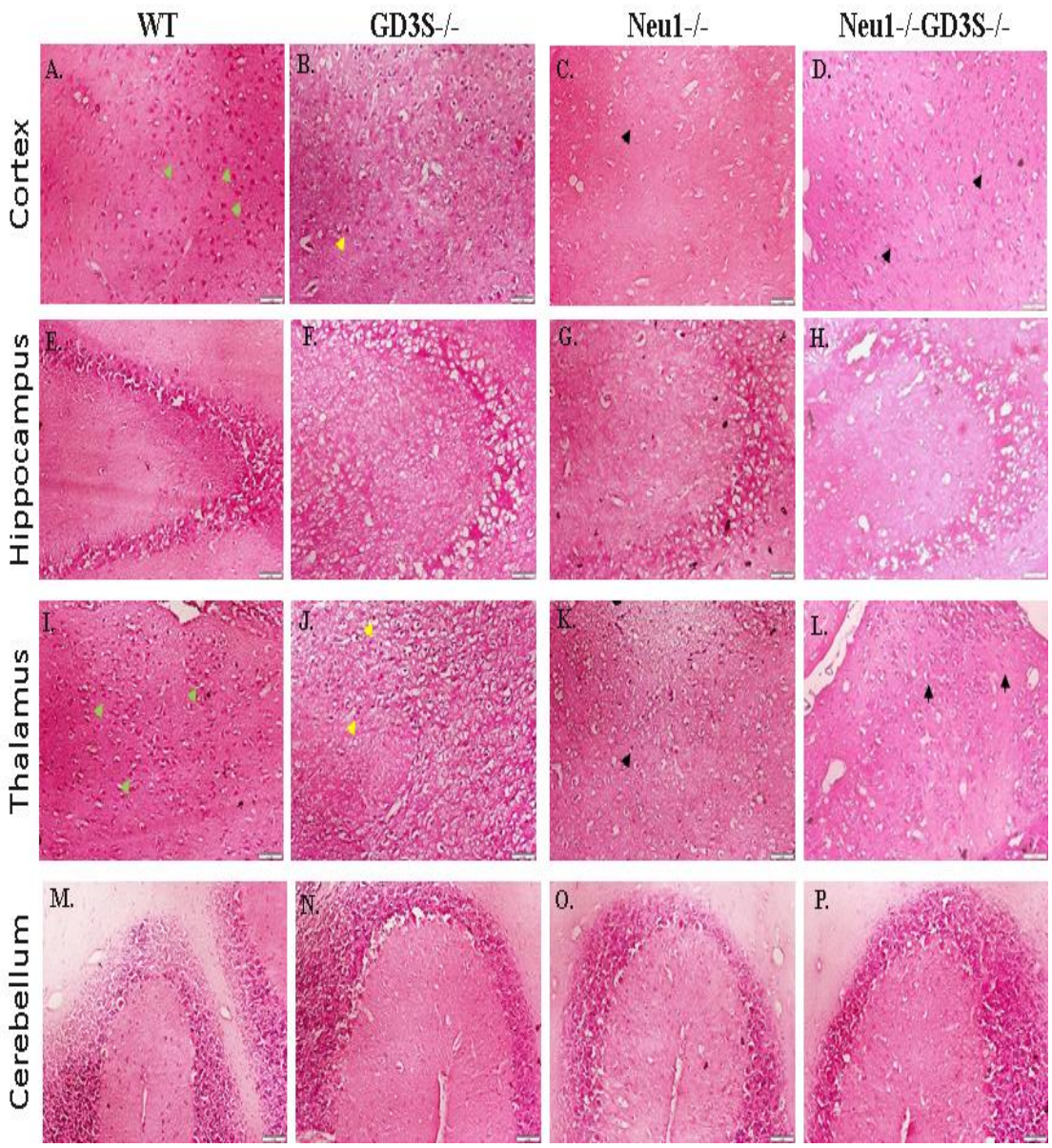

Figure 3.9. 2. Hematoxliyn & Eosin staining for cortex (A,B,C,D), hippocampus (E,F,G,H), thalamus (I,J,K,L), and cerebellum (M,N,O,P) regions of 4-month-old WT, GD3S-/- Neu1-/-, and Neu1-/- GD3S-/- mice stained with . 20x images were taken and the scale bar indicated 50μm. Arrow heads indicates the pyramidal cells (Condition. green for normal, yellow for moderate, black severe)(n=3)

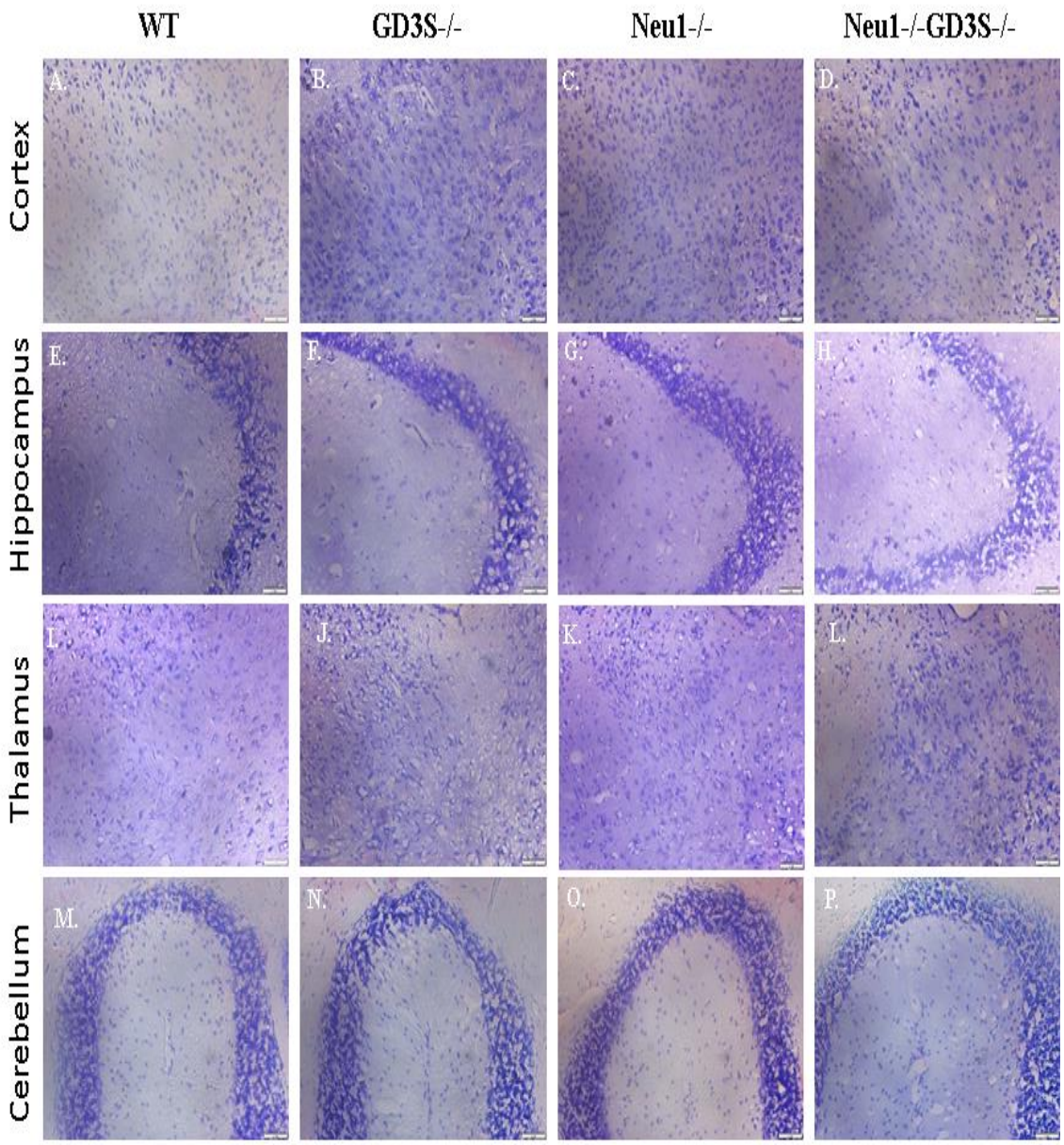

Figure 3.9.3. Cresyl violet staining for (A,B,C,D) cortex,(E,F,G,H) hippocampus, (I,J,K,L) thalamus, and (M,N,O,P) cerebellum regions 2-month-old WT, GD3S-/- Neu1-/-, and Neu1-/- GD3S-/- mice stained with . 20x images were taken and the scale bar indicated 50μm. (n=3)

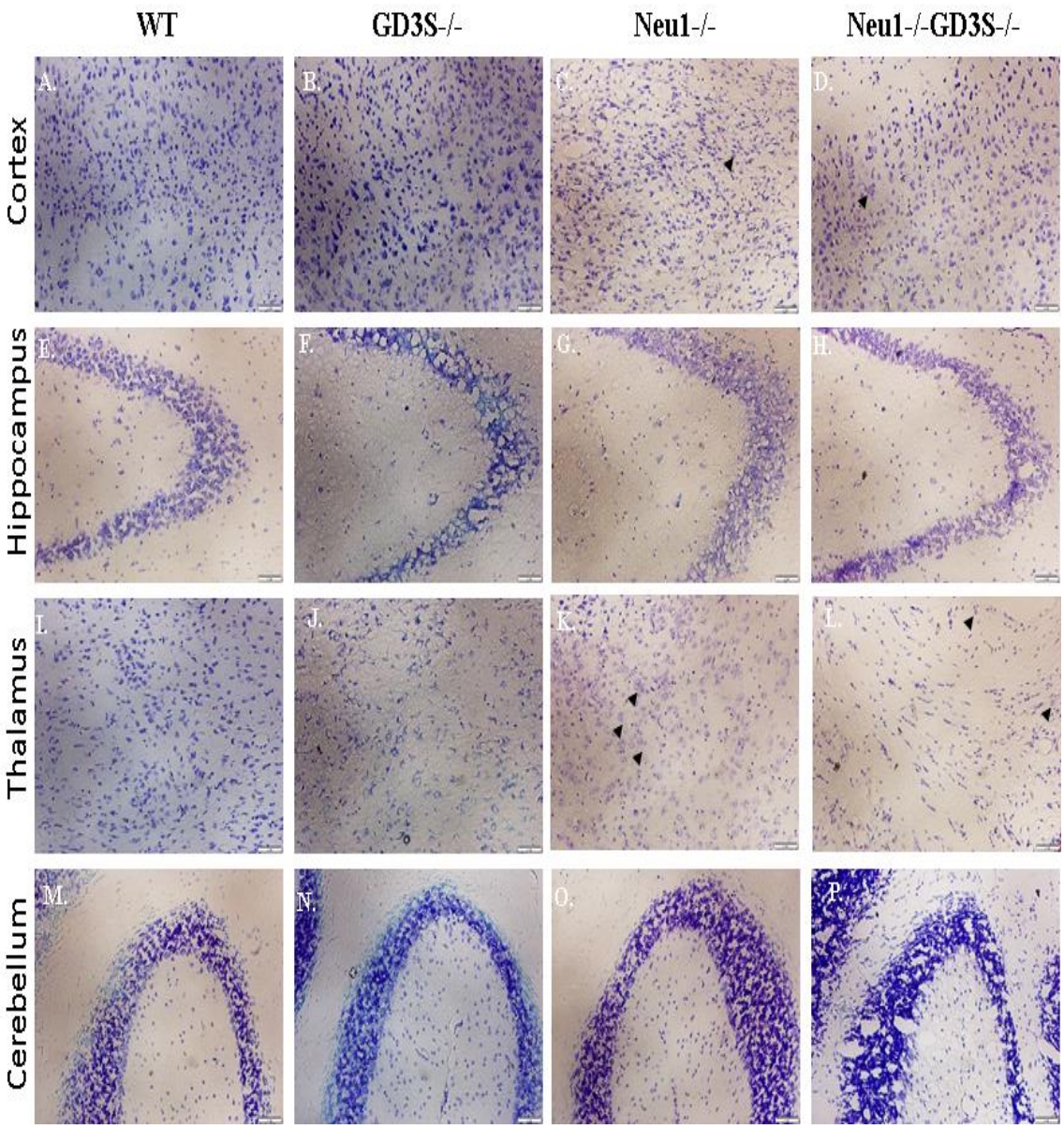

Figure 3.9.4. Cresyl violet staining for (A,B,C,D) cortex,(E,F,G,H) hippocampus, (I,J,K,L) thalamus, and (M,N,O,P) cerebellum regions 4-month-old WT, GD3S-/- Neu1-/-, and Neu1-/- GD3S-/- mice stained with . 20x images were taken and the scale bar indicated 50μm. (n=3)

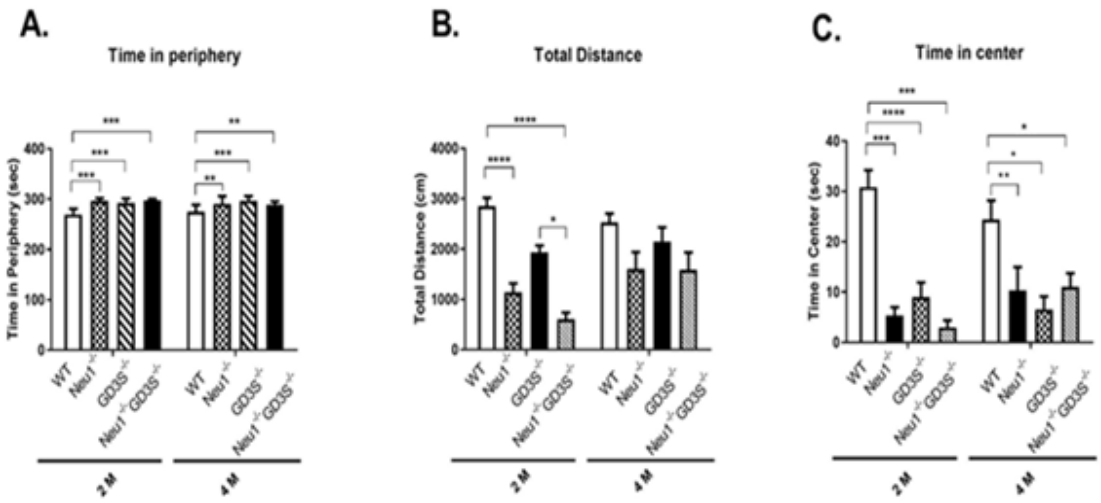

Figure 3.10.1. Open field results of 2- and 4-month-old WT (n=10), GD3S-/- (n=10), Neu1-/- (n=7), Neu1-/-GD3S-/-(n=5), mice. (A)Time in periphery, (B) total distance, and (C) time in center indicated with the histograms. (D) (Data were reported as means ± SE, *p<.05, **p<.005, ***p<.001, ****p<.000.1)

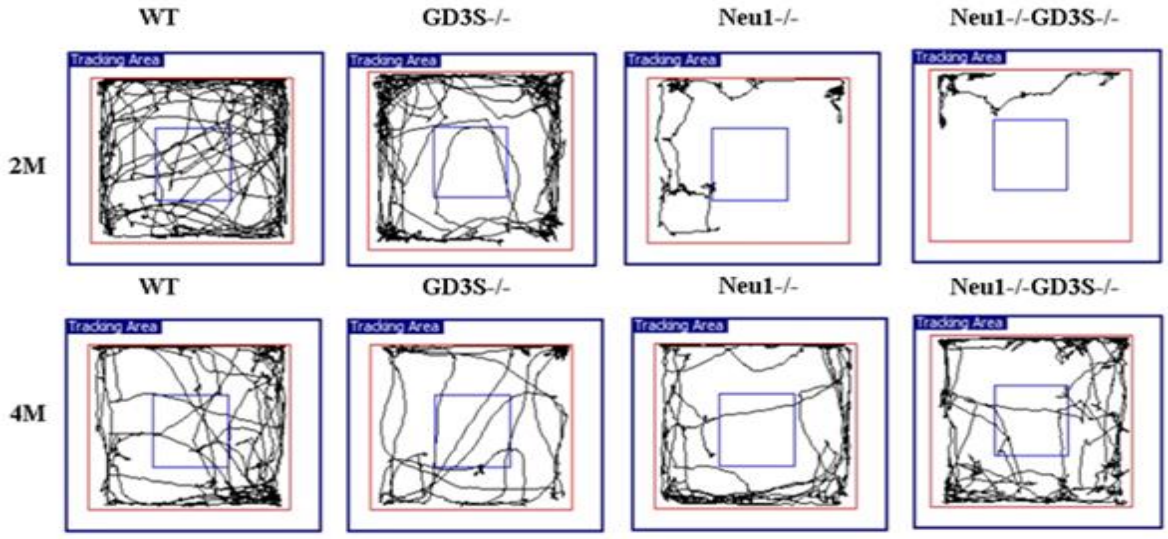

Figure 3.10.2. The representative movement patterns of 2- and 4-month-old WT, GD3S-/-, Neu1-/-, Neu1-/-GD3S-/- mice during the test inside the tracking area.

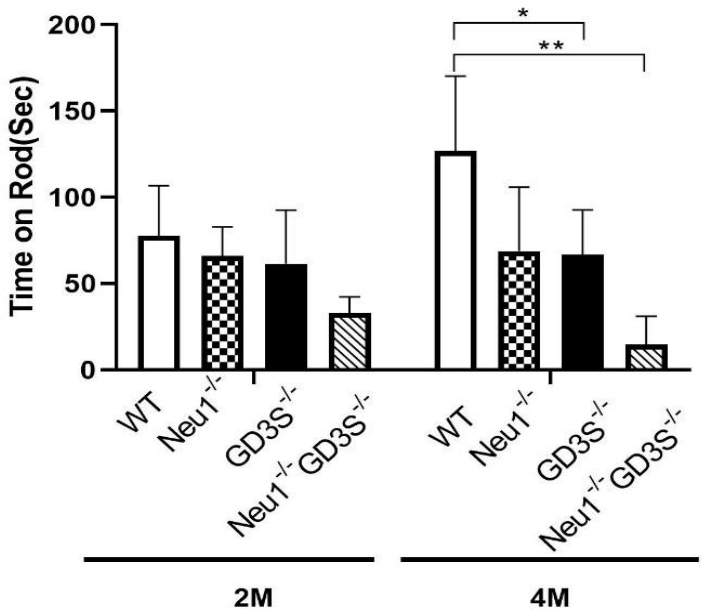

Figure 3.10.3. Rotarod test results of 2- and 4-month-old WT (n=10), GD3S-/- (n=10), Neu1-/- (n=7), Neu1-/-GD3S-/- (n=7), mice. P values obtained with two-way anova (*p<.05, **p<.005).

CHAPTER 4

DISCUSSION

Sialidases or neuraminidases are group of enzyme which have the ability to hydrolase the sialic acid conjugates from the glycoconjugates including glycoproteins, oligosaccharides and glycolipids. Sialic acids are composed of a 9-carbon structure and tend to form structures with glycoconjugates. Sialic acids plays important roles for the cell by providing interaction sites and cell signaling (Varki 1997; Laine 2008). Sialidases in vertebrates functions for many important biological processes like cell proliferation/differentiation, catabolism of sialic acid containing complexes(Miyagi et al. 2018). So far, 4 mammalian sialidases have been reported and named as Neu1, Neu2, Neu3 and Neu4. These enzymes are specialized for different roles and found to be differentially expressed in different subcellular localizations. Neu1 is an enzyme which its activity also includes other enzymes and forms a multienzyme complex including ß-Gal and PPCA (Van Der Spoel, Bonten, and D'Azzo 1998). Neu1 is one of the most important enzyme among sialidases which its absence or malfunctioned form is linked to severe clinical lysosomal storage disorders. These disorders includes sialidosis and galactosialidosis (Cantz and Ulrich-Bott 1990). Both sialidosis and galactosialidosis patients suffer from many severe pathological features, which can be life threatening. Sialidosis patients were classified in to two groups; sialidosis type I and II which showed different pathological features and severity depending on the mutations occurred in the Neu1 gene (Monti et al. 2010). Type II sialidosis was the severe form of the disease with patients suffering many physical abnormalities and a progressive neurodegenerative defects were observed (Monti et al. 2010). To understands more about the Neu1 enzyme its mice model was created by generating a mice with an non-functional Neu1 enzyme (N. de Geest 2002). Mice lack functioning Neu1 enzyme displayed a severe form of phenotype resembling the type II sialidosis patients. With further studies on Neu1 enzyme revealed important novel roles in many aspects. It was discovered that Neu1 had a crucial role in the process of lysosomal exocytosis where absence negatively affect the process due to oversialyated lysosomal associated protein1/Lamp1 accumulation which proved that Neu1 using Lamp1 as a substrate (Yogalingam et al. 2008). Also other

important roles of Neu1 was discovered by its related with muscle regeneration (Neves et al. 2015) and fibrosis(van de Vlekkert et al. 2019).

Glycosphingolipids (GSLs) are important types of lipids having many functions within the cell. Its ceramide (Cer) backbone structure is then further processed to generate many complex sugars within the GSLs pathway (MacCioni, Quiroga, and Ferrari 2011). Addition of glycans to the Cer in Endoplasmic Reticulum,is then transported to Golgi and further processed to form lactosylceramide (LacCer) (Proia 2003). With the addition of sialic acid residues to the LacCer, firstly forms the simple gangliosides which are then converted to form complex gangliosides via sialyltransferases (Schnaar 2019). Gangliosides are classified based on their additional groups in to 0-, a, b and c series terms of their sialic acid content.

Although having such important biological tasks in the cells, the role of Neu1 in the glycosphingolipid pathway is remain unclear. To provide more insight about its functions, we approached in an aspect of whether Neu1 has a biological role in the GSLs pathway.

To test our hypothesis, we used the sialidosis mice model, Neu1-/- mice and crossing it with another mice lacking b- and c- series of gangliosides, the GD3S-/- mice forming a Neu1-/-GD3S-/-double knock-out mice.

After obtaining the mice according to our breeding plan (Figure 2.1) we examined the mice by in terms of their weight. As reported in the previous studies on Neu1-/- mice revealed tend to be smaller and displayed less weight (N. de Geest 2002) compared to WT and GD3S-/- mice (Figure3.2A and B). In addition to this, Neu1-/-GD3S-/- mice showed even more severe loss of weight at the end of 20 weeks of examination (Figure 3.2 A and B). GD3S-/- mice tend to display a slightly increased weight compared to WT for the most of the individuals (Figure 3.2 A and B). The reason for this was unclear although a recent study reported that GD3S-/- had increased bone mass which displayed less bone attenuation with ageing compared to WT mice (Yo et al. 2019). But when combined with the Neu1-/- it instead reduced the weight of the mice and displayed an even worse phenotype compared to Neu1-/- mice. In this study our plan was to study 2-5- and 8- month old mice but because Neu1-/-GD3S-/- displayed a very unstable and a severe phenotype we saw many sudden deaths (data was not shown) before reaching 8-month old. The severity of the physical abnormalities, after the 5- months of age, worsened and only few of them could reach to 6.5 months of age. To avoid any unwanted

casualties we decided to change our experimental plan to 2 groups of age and collected the samples from 2 –and 4- month old mice.

To understand the pathology of the brain we dissected mice brain to cortex, cerebellum and thalamus regions to have a better understanding of the pathology of the disease. Although for only TLC method we used cortex and cerebellum due to very low size of the thalamus region which was difficult to detected gangliosides with TLC method.

Later on to reveal the ganglioside profile of the mice, we used TLC to separate the acidic and neutral gangliosides and orcinol staining for the visualization of the bands. As expected GD3S-/- and Neu1 -/-GD3S-/- mice was depleted in terms of b- and c-gangliosides and displayed increased amounts of GM1, GD1a for the both regions(Figure 3.3.1A and Figure 3.3.3A). Other studies on GD3S-/- mice showed increased amounts of GM1 and GD1a to compensate the lack of b-and-c series of gangliosides is consistent with other studies (Kawai et al. 2001). Surprisingly, in the cerebellum region of GD3S-/- and Neu1-/- mice we observed an unknown band right under the GM1 and very close to GD3 band (Figure 3.3.3 A). We couldn't identify the band but it might be a modified form of GM1 ganglioside. Due to differential expression of gangliosides in the tissue and organs to compensate the lack of other gangliosides, the cerebellum region in these mice might displayed such features. On the other hand, for the neutral gangliosides in cortex region for 4- month old Neu1-/- mice increased levels of LacCer. However this was only seen in the 4- month old mice. For the cerebellum region there weren't any changes in terms of LacCer. This type of change in terms of LacCer wasn't seen for the 2- month old Neu1-/- mice. Such events can be clarified with mass spectrometric analysis which would possibly identify the structure of the unknown band in the cerebellum region for the GD3S-/- and Neu1-/-GD3S-/- mice.

Because the urinary oligosaccharides are important for the diagnosis of the sialidosis patient which were also seen in the Neu1-/- mice (Natalie de Geest et al. 2002)s, we wanted to see if lack of b- and –c series of gangliosides would affect this profile. Low chained bands were visible for the 2-and 4- month old Neu1-/- and Neu1-/-GD3S-/-mice. Mice lack of GD3S-/- showed the lowest amounts of sugar which was also similar to 4-month old GD3S-/- mice. Neu1-/- GD3S-/- mice at 4- months of age had the highest sugar content in their urine but decreased within age this might be caused due to the lack of b- and c- series of gangliosides. However the same decrease was also observed for the

Neu1-/- mice which showed high levels of sugar in the 2- months of age but decreased at 4- months of age.

To observe the changes in the ER-Stress, oxidative stress and apoptosis expression analaysis were performed. ATF-6, calnexin and XBP-1 genes were chosen to evaluate the ER-stress in terms of their mRNA expressions.

Endoplasmic reticulum is the organelle where majority of the proteins are being secreted and their proper transport is provided to target sites with proper folding and modification. ATF-6 gene is responsible for the transcriptions which activates the target genes for the unfolded proteins (UPR). The increased production of proteins at a certain rate is critical to for maintaining the homeostasis of the cell. If these signals overwhelm the capacity of ER cells can go to programmed cell death, apoptosis (Schröder and Kaufman 2005). Calnexin is a type of chaperon protein which is responsible for the proper folding by binding to the partially or misfolded proteins, ensures their transport to the plasma membrane (Kim and Arvan 1995). In addition, X-box binding protein(XBP-1) is a transcription factor is spliced by activated IRE1 upon ER stress (Walter and Ron 2011). The XBP1 mRNA comprises of two overlapping reading frames; under normal conditions only unspliced variant is transcribed without translation and once the UPR is activated the unspliced variant converted to spliced XBP1 which promotes transcription of UPR target genes (Van Schadewijk et al. 2012). Recent studies revealed that some lysosomal storage disorders displayed such features including ER-stress. Increased expression of spliced XBP1 was reported in GD derived fibroblasts (Maor et al. 2013).

Expression levels of ATF-6 in our experiments show important features (Figure 3.5.1). For the cortex region increased levels of ATF-6 was observed in the 2 -month old mice GD3S-/- and Neu1-/-GD3S-/- compared to WT mice (Figure 3.5.1 A). Although 4 -month old mice Neu1-/-GD3S-/- mice showed a significant decrease in the levels of ATF-6 gene expression (Figure3.5.1 A). Also, when 4 -month old Neu1-/- was compared to WT mice, although it showed higher levels of ATF-6 compared to Neu1-/-GD3S-/-, it was significantly reduced (Figure 3.5.1 A). For the cerebellum region mice tend to show no significant change (figure 3.5.1 B). In thalamus region, between 2 month old mice, 4 month old GD3S-/- mice showed significant levels of ATF-6 compared to all other mice at the same age and increased its expression significantly within age For expression levels of calnexin, only GD3S-/- mice displayed an increase for the cortex region between 2-month old mice (Figure 3.5.2 A). In cerebellum, 4 month old knock-out mice, although it wasn't significant, showed a decrease compared to WT mice in terms of Calnexin levels

(Figure 3.5.2 B). Thalamus region was also seemed unaffected (Figure 3.5.2 C). Expression of XBP-1 did not show a significant change in any brain regions for all mice. To sum up these, for all of the knock out mice showed some features of increased ER-stress compared to WT mice in 2- months of age. Most significant changes were observed for the GD3S-/- mice. Due to lack of GD3S, these mice tend to compensate the required gangliosides by producing more, because they don't possess b- and c- series of gangliosides which was clearly seen that they had increased levels of GM1 and GD1a (Figure 3.3.1 and 3.3.3). There for it would be a logical feature to show such ER-stress markes, due to over production of certain gangliosides only, in terms of mRNA levels in these mice. In cerebellum region GD3S-/- did not differ maybe the additional ganglioside which we couldn't identified provided some support therefore for cerebellum region increased ER-stress was not crucial. Although for, it is clear that 4- month old Neu1-/- and Neu1-/-GD3S-/- mice showed decreased variable levels of ER-stress in terms of the mRNA levels and showed only a decrease for the ATF-6 for cerebellum and cortex regions (Figure 3.5.1 A and C). Mouse model of GM1 gangliosidosis which is a severe type of lysosomal storage disorders, displayed altered ER-stress and they suggested that this increased UPR triggered apoptosis (Tessitore et al. 2004). Although Neu1-/- and Neu1-/-GD3S-//- mice with severe phenotype did not show such increased levels of ER-stress markers instead displayed similar with the WT mice in terms of ER-stress markes for the mRNA levels.

Supeoxide Dismutase 2 is an enzyme that protects cells from the reactive oxygen species by maintaining the cellular and mitochondrial redox balance (Fukai and Ushio-Fukai 2011). Catabolisim of superoxides produced by mitochondria are targeted by SOD-2 and its conversion to less toxic forms such as H_2O_2 and O_2 is crucial for the cell (Miller, Brzezinska-Slebodzinska, and Madsen 1993). Catalase believed to have more than one function which decomposes the H2O2 in to H2o and O2 (catalytic activity). Another function is oxidation of H donors, like methanol, ethanol, formic acid, phenols (Kovačević et al. 2010). Thioltransferase-1 (Ttase1) is a member of glutaredoxin family proteins and involves in antioxidant defence mechanism (Lou et al. 1998) . Our results in terms of the expression levels of oxidative stress markers only showed a significant change for the Ttase 1 for the cortex region of 2 month old GD3S-/- mice compared to Neu1-/-GD3S-/- mice (Figure 3.5.6 A). ER-Stress and oxidative stress is linked in some manner. Increased ER-stress might also affect the reactive oxygen species amount (Malhotra and Kaufman 2007).

Apoptosis markers such as the Bcl-2 family proteins are highly related with apoptosis. Their roles are well studied and some members include the Bcl-2, Bcl-xl and Bax genes. They differ in terms of regulating the apoptosis. Bcl-2 and Bcl-xl are the anti-apoptotic proteins which their expression is related to suppress the apoptosis by binding to the pro-apoptotic proteins for their inhibition (Adams and Cory 1998). Our results for the expression of Bcl-2 differed among the brain regions. Where the most significant change was observed in cerebellum region in terms of Bcl-2 expressions belong to the 2-month old Neu1-/- mice (Figure 3.5.7). Bax levels showed clearly that Neu1-/- mice having a fight of anti- and- pro apoptotic markers for the 2- months old mice. In all of the regions it showed significant increase. For the cortex region Bax levels were only increased for the Neu1-/- mice whereas the other genotypes seemed normal compared to WT in 2- months old mice (Figure 3.5.9:). Cerebellum and thalamus regions were almost the same in terms of the expression of Bax where Neu1-/- was highly significant and decreased in its expression at 4- months of age (Figure 3.5.9B and C).

To conclude the data so far obtained from the mRNA expressions showed notable results where pro-apoptotic gene, Bax, showed increased expression for Neu1-/- mice in all brain regions of 2- month old mice showing the apoptotic signals are being expressed. Although 2- month old Neu1-/-GD3S-/- mice was also lack of Neu1 enzyme, Neu1-/-GD3S-/- mice did not expressed high levels of Bax together with lower levels of anti-apoptotic gene expressions were also noticeable which were at the same levels of GD3S-/- mice.

Our further analysis was to investigate the apoptosis in terms of protein levels. Fas-Ligand, BIP, Caspase 3 and Caspase 9 was used for western blotting. Fas-Ligand, a surface bound-receptor is known to trigger apoptosis with the activation of caspases through the extrinsic pathway of apoptosis. Fas-Ligand contains a domain (death domain) which is important and allows the recruitment of caspase 3 which then finalize with the caspase 8 (Volpe et al. 2016). The BIP chaperone is a protein founded that has interactions in the ER which is responsible for the maintenance of the permeable membrane of ER in various events like translocations, targeting misfolded proteins, and activating the UPR (Pobre, Poet, and Hendershot 2019). The intrinsic pathway of apoptosis can be triggered from various stimulus within the cell and also caspase 3 and caspase 9 are the well-known proteins for having a role in the intrinsic pathway. Although the roles of the caspases aren't fully understood, it is shown to have association with cell death (Li et al. 2017; Loreto et al. 2014).

We did not observe a change in the Fas-Ligand protein levels for all regions including all of the mice (Figure 3.6.1, Figure 3.6.2 and Figure 3.6.3).

For the 2- month old Neu1-/- and Neu1-/-GD3s-/- mice showed a significant increase in the level of BIP protein for cortex region which was higher for the double-knockout mice (Figure 3.6.4). At the 4 -months of age, BIP levels did not change between genotypes (Figure 3.6.4). For the thalamus region although it was clear that WT mice showed less BIP levels compared to 2- month mice with the other genotypes, which was not significant. 4- month old mice displayed similar amounts of BIP protein in the thalamus region (Figure 3.6.5). Also cerebellum region did not show a difference for the mice (Figure 3.6.6). The increased BIP protein levels in the cortex region for the Neu1-/- and Neu1-/-GD3S-/- showed the opposite results with the mRNA expression results for the markers of ER-stress.

Caspase 9 displayed significantly elevated cleaved levels of caspases and they were significant between WT mice for the cortex region (Figure 3.6.7). GD3S-/- mice showed similar intensity in terms of cleaved caspase 9 compared to WT mice for both ages (Figure 3.6.7). For the thalamus region, 2 month old Neu1-/-GD3S-/- mice displayed an increase in the caspase 9 cleavage but the levels were normal for the 4 month old mice (Figure 3.6.8). Cerebellum region 2 month old mice did not displayed a significant change but in the 4 months of age Neu1-/- showed significant levels of Cleaved caspase 9 (Figure 3.6.9).

To combine all of these, a considerable pattern was observed for the 2 month old mice group. Mice at developmental stages, requires such gangliosides and their expressions differ among the brain (Ngamukote et al. 2007). Most of the differences were observed in the 2 month old mice which they were still under development. Most interesting difference was that the western blot results in terms of BIP, caspase 3 and Caspase 9 showed the opposite with the RT-PCR analysis for GD3S-/- mice 2 month old in cortex region. Increased ER-stress was seen for the 2 month old GD3S-/- mice but with the western blot analysis we did not see such event. 2 month old Neu1-/- mice showed increased Bax expression level with also increased Bcl-2 in the cerebellum region. But for the caspase 3 and caspase 9 levels in cerebellum did not show a significant change but for the cortex region it showed very clear cleaved caspase 3 and caspase 9 levels indicating apoptosis. It is unclear that we expected to see the increased apoptosis signal in Neu1-/-GD3S-/- mice because of its phenotype was worse than Neu1-/-. Although some research indicates some gangliosides are important for the apoptosis signals.

Important notes which they indicate are the increased levels of GD3 in the mice. GD3 is only expressed in the developmental stages and it is associated with death signalling (Yamaguchi et al. 2005; Scorrano et al. 1999). These evidences are mostly related with the mitochondria and oxidative stress although our experimental plan only included oxidative stress for the RT-PCR and the data we have is not enough to explain this phenomenon. Although it is certain that the lack of b- and c- gangliosides altered the ER-stress and apoptotic signals for the mice lacking GD3S enzyme which includes the GD3S-/- and Neu1-/-GD3S-/- mice.

Later on, another study was made to show apoptosis which was the DNA fragmentation method. A classical method that was used for the fragmented DNA from the mice brain regions showed a quite different visual of apoptotic signals and the place where the bands were seen was mostly for the thalamus region (Figure 3.7 C). However the markers used to detect apoptosis and the most part of the brain which showed clear data was the cortex region where in this method the thalamus region showed clear and visible bands where 2-months old mice displayed apoptosis related fragmented DNAs. Although, for the thalamus region, Neu1-/-GD3S-/- mice showed more faint bands compared to GD3S-/- which was unusual, although Neu1 displayed the darkest bands. For cortex and cerebellum regions almost no significant bands were observed (Figure 3.7 A and B).

After such markers like apoptosis, ER-stress and oxidative stress we wanted to approach from an aspect that the data would provide a qualitative result instead. Therefore NeuN staining was applied to the 4- month old mice. NeuN - staining was not specific to every cell in the brain, although it would provide insight about the visual of cells. It gave a red signal with the antibody, where signals are counted as the places where neurons stained with NeuN would reside. It was clear that cells were severely depleted in the Neu1-/- mice and Neu1-/-GD3S-/- mice for all regions and they showed very similar results which can be interpreted as the mice had lost huge number of cells stained with NeuN compared with WT and GD3S-/- mice (Figure 3.8). For the loss of the neurons in terms of degeneration was also reported for the GD3S-/- mice which displayed low levels of cell loss compared to WT (Jing Wang et al. 2014). Although we only performed this experiment to 4-month old mice therefore the visual which 2-month old mice would show is very crucial to see more about the cell death related markers between age where most of the difference between genotypes were seen in 2-month old mice.

Next our aim was to examine the morphology of the mice with pathological staining. Haematoxylin and Eosin staining from 2- and 4- month old mice showed some important type of cells which were tend to be altered in terms of their physical structure. Pyramidal cells in the WT are showed with the green arrow head and their morphology was clearly normal. GD3S-/- mice also showed these pyramidal cells with normal size but, some of them were tend to be smaller. Neu1-/- and Neu1-/-GD3S-/- mice was also affected with the same structural deformation of pyramidal cells. For the both age these structure were the same and no age dependant change was observed. Also Cresyl violet staining was used to stain the Nissl particles found in the granular body of the neurons showed swollen balloon like structure for the 4-month old mice Neu1-/- mice and Neu1-/-GD3S-/- mice for the cortex and thalamus regions. Such altered morphology might belong to the lack Neu1 gene which wsuch altered structures was also shown before with 5-month old mice in their brain (N. de Geest 2002). Cerebellum of the Neu1-/- mice was earlier reported to have a normal purkinje layer which with these stainings they mostly tend to remain unharmed for the mice regardless of age and for all genotype.

To observe some behavioral information of the mice open field test was used for the mice and it shown dramatic results for the Neu1-/- and Neu1-/-GD3S-/- mice. While time in the periphery was the indication of anxiety like behavior, time in the center was the mice would normally appear to spend time. The GD3S-/- mice spent their time near the periphery and less time in the center was evident for anxiety like behavior. Although the 2- month old Neu1-/- and Neu1-/-G3S-/- mice might even displayed worse phenotype then GD3S-/- mice, which showed very low entry to the center and spent most of their time in the periphery, they didn't tend to move at all after their experiment started (Figure 3.10.1). This data can be interpreted as like a severe anxiety like behavior but also these mice tend to have physical abnormalities such as muscle and altered bone structure caused by Neu1 deficiency (Neves et al. 2015) might travel less distances (Tatem et al. 2014) . At the 4- months of age the time in the center which WT mice was still higher compared to other genotypes. Although the knock out mice showed more activity but still more anxiety like behavior was observed at 4-months of age (Figure 3.10.1).

Rotarod test was also applied to the animal which was to evaluate their motor coordination and balance on the accelerating rod. At 2- months of age mice did not differ significantly but the Neu1-/-GD3S-/- mice was the least successful. The 4- month old Neu1-/-GD3S-/- mice showed the worse success which was progressively worsened in terms of their balance and motor coordination. Previous studies on the GD3S-/- mice also

showed similar results (Ribeiro-Resende et al. 2014)Absence of the b- and c- series were clearly required for this task.

CHAPTER 5

CONCLUSION

Experiments conducted to understand more about the Role of Neu1 in the glycosphingolipid pathway showed very interesting results. Although we did not observe a change in the Neu1-/-GD3S-/- double knock out mice in terms of the GSLs. However, the Neu1-/-GD3S-/- mice displayed a severe phenotype which showed more fatality than Neu1-/- mice (data not shown). Lack of b- and c- series of gangliosides in mice did not show severe phenotype but when combined with a mouse model of a severe lysosomal storage disorder, Neu1-/- mice, displayed interesting features. Some very confusing data were obtained and remained to be further investigated. It was noteworthy that mice having such severe phenotype did not clearly show apoptosis. In addition, cortex, cerebellum and thalamus regions were investigated which displayed different results showing that the brain regions are affected differently for the Neu1-/-GD3S-/- mice. In terms of the gangliosides GD3S-/- and Neu1-/-GD3S-/-, due to the lack of GD3S, an interesting ganglioside was observed in the cerebellum where it was absent in the cortex region. The one of the most important feature of this mice was that although loss of cells in the brain was present showed with the NeuN antibody staining, it was really difficult to interpret the data because while Neu1-/- enzyme displaying apoptotic signals such as Bax for the mRNA levels, Neu1-/-GD3S-/- showed an expression pattern similar to GD3S-/- mice. Also similar event was observed for the GD3S-/- mice which showed increased ER-stress markers but low level of apoptotic Bax expression for the cortex region. These results indicate that, b- and –c series of gangliosides altered the apoptotic and ER-stress signals in the mRNA level. GD3S-/- mice can only possess certain types of gangliosides therefore it may cause the by the production of only certain types of GSLs might be a possible option for the increase in the ER-stress derived UPR in terms of mRNA expressions. In the developmental stage mice produces different GSLs in the lipids and it is also changes with ageing. The cerebellum region in terms of the ganglioside content of the GD3S-/- and Neu1-/-GD3S-/- mice also important seemed important and such interesting data will be planning to further studied.

5.1. Further Directions

Our study, to investigate the role of Neu1 in the glycosphingolipid pathway showed interesting features of the Neu1-/-GD3S-/- mice. After studying its role on the GSL pathway, we conducted a study design to observe the general pathological features of the Neu1-/-GD3S-/- mice. But there are still unclear results and features that are waiting to be studied.

Firstly, the mass spectrophotometric analysis of the brain samples should be performed to identify the ganglioside only seen in the cerebellum and even more can be found with such technique. Another topic is that to understand the cell-death related mechanism for the Neu1-/-GD3S-/- mice, cell culture studies can be carried out. Also, the alteration of bone structure which was recently reported that the deficiency of GD3S attenuated the bone loss with aging but the double knock-out mice that we possessed severe alterations in terms of their skeletal structure. In this respect, bone experiments can be further performed.

Especially the gangliosides which lacked in terms of b- and c- especially the GD3 ganglioside are related to be important for the mitochondria, therefore oxidative stress and ER- stress can be studied to understand the balance between these two events for the GD3S-/- and Neu1-/-GD3S-/- mice.

REFERENCES

Ada, G. L., and E. L. French. (1959) "Stimulation of the Production of Neuraminidase in Vibrio Cholerae Cultures by N-Acetylmannosamine." *Journal of General Microbiology*. https.//doi.org/10.1099/00221287-21-3-561.

Adams, Jerry M., and Suzanne Cory. (1998) "The Bcl-2 Protein Family. Arbiters of Cell Survival." *Science*. https.//doi.org/10.1126/science.281.5381.1322.

Annunziata, Ida, and Alessandra d'Azzo. (2017) "Galactosialidosis. Historic Aspects and Overview of Investigated and Emerging Treatment Options." *Expert Opinion on Orphan Drugs*. https.//doi.org/10.1080/21678707.2016.1266933.

Bieberich, Erhard, Sarah MacKinnon, Jeane Silva, and Robert K. Yu. (2001) "Regulation of Apoptosis during Neuronal Differentiation by Ceramide and B-Series Complex Gangliosides." *Journal of Biological Chemistry*. https.//doi.org/10.1074/jbc.M107239200.

Bigi, Alessandra, Lavinia Morosi, Chiara Pozzi, Matilde Forcella, Guido Tettamanti, Bruno Venerando, Eugenio Monti, and Paola Fusi. (2009) "Human Sialidase NEU4 Long and Short Are Extrinsic Proteins Bound to Outer Mitochondrial Membrane and the Endoplasmic Reticulum, Respectively." *Glycobiology*. https.//doi.org/10.1093/glycob/cwp156.

Bonten, E J, and A D'Azzo. (2000) "Lysosomal Neuraminidase. Catalytic Activation in Insect Cells Is Controlled by the Protective Protein/Cathepsin A." *The Journal of Biological Chemistry* 275 (48). 37657–63. https.//doi.org/10.1074/jbc.M007380200.

Breiden, Bernadette, and Konrad Sandhoff. (2018) “Ganglioside Metabolism and Its Inherited Diseases.” In *Methods in Molecular Biology*. https.//doi.org/10.1007/978-1-4939-8552-4_5.

Burnet, F M, J F McCrea, and J D Stone. (1946) “Modification of Human Red Cells by Virus Action; the Receptor Gradient for Virus Action in Human Red Cells.” *British Journal of Experimental Pathology* 27 (4). 228–36. http.//www.ncbi.nlm.nih.gov/pubmed/21002128.

Caciotti, Anna, Serena Catarzi, Rodolfo Tonin, Licia Lugli, Carmen Rodriguez Perez, Helen Michelakakis, Irene Mavridou, et al. (2013) “Galactosialidosis. Review and Analysis of CTSA Gene Mutations.” *Orphanet Journal of Rare Diseases*. https.//doi.org/10.1186/1750-1172-8-114.

Cantz, M., and B. Ulrich-Bott. (1990) “Disorders of Glycoprotein Degradation.” *Journal of Inherited Metabolic Disease*. https.//doi.org/10.1007/BF01799510.

Demarco, Mari I., and Robert J. Woods. (2009) “Atomic-Resolution Conformational Analysis of the GM3 Ganglioside in a Lipid Bilayer and Its Implications for Ganglioside-Protein Recognition at Membrane Surfaces.” *Glycobiology*. https.//doi.org/10.1093/glycob/cwn137.

Fukai, Tohru, and Masuko Ushio-Fukai. (2011) “Superoxide Dismutases. Role in Redox Signaling, Vascular Function, and Diseases.” *Antioxidants and Redox Signaling*. https.//doi.org/10.1089/ars.2011.3999.

Gault, Christopher R., Lina M. Obeid, and Yusuf A. Hannun. (2010) “An Overview of Sphingolipid Metabolism. From Synthesis to Breakdown.” *Advances in Experimental Medicine and Biology*. https.//doi.org/10.1007/978-1-4419-6741-1_1.

Geest, N. de. (2002) “Systemic and Neurologic Abnormalities Distinguish the Lysosomal Disorders Sialidosis and Galactosialidosis in Mice.” *Human Molecular*

Genetics. https.//doi.org/10.1093/hmg/11.12.1455.

Geest, Natalie de, Erik Bonten, Linda Mann, Jean de Sousa-Hitzler, Christopher Hahn, and Alessandra D'Azzo. (2002) "Systemic and Neurologic Abnormalities Distinguish the Lysosomal Disorders Sialidosis and Galactosialidosis in Mice." *Human Molecular Genetics* 11 (12). 1455–64. http.//www.ncbi.nlm.nih.gov/pubmed/12023988.

Hasegawa, Takafumi, Naoto Sugeno, Atsushi Takeda, Michiko Matsuzaki-Kobayashi, Akio Kikuchi, Katsutoshi Furukawa, Taeko Miyagi, and Yasuto Itoyama.(2007) "Role of Neu4L Sialidase and Its Substrate Ganglioside GD3 in Neuronal Apoptosis Induced by Catechol Metabolites." *FEBS Letters*. https.//doi.org/10.1016/j.febslet.2006.12.046.

Hasegawa, Takafumi, Kazunori Yamaguchi, Tadashi Wada, Atsushi Takeda, Yasuto Itoyama, and Taeko Miyagi. (2000) "Molecular Cloning of Mouse Ganglioside Sialidase and Its Increased Expression in Neuro2a Cell Differentiation." *Journal of Biological Chemistry*. https.//doi.org/10.1074/jbc.275.11.8007.

Hidari, K I-P J, S Ichikawa, K Furukawa, M Yamasaki, and Y Hirabayashi. (1994) "B1-4N-Acetylgalactosaminyltransferase Can Synthesize Both Asialoglycosphingolipid GM2 and Glycosphingolipid GM2in Vitro and in Vivo. Isolation and Characterization of a B1-4N-Acetylgalactosaminyltransferase CDNA Clone from Rat Ascites Hepatoma Cell Line A." *Biochemical Journal* 303 (3). 957–65. https.//doi.org/10.1042/bj3030957.

Hinek, Aleksander, Alexey V. Pshezhetsky, Mark Von Itzstein, and Barry Starcher. (2006) "Lysosomal Sialidase (Neuraminidase-1) Is Targeted to the Cell Surface in a Multiprotein Complex That Facilitates Elastic Fiber Assembly." *Journal of Biological Chemistry*. https.//doi.org/10.1074/jbc.M508736200.

Holthuis, J. C.M., T. Pomorski, R. J. Raggers, H. Sprong, and G. Van Meer. (2001)

"The Organizing Potential of Sphingolipids in Intracellular Membrane Transport." *Physiological Reviews*. https://doi.org/10.1152/physrev.2001.81.4.1689.

Kawai, Hiromichi, Maria Laura Allende, Ryuichi Wada, Mari Kono, Kazunori Sango, Chuxia Deng, Tsuyoshi Miyakawa, et al. 2001. "Mice Expressing Only Monosialoganglioside GM3 Exhibit Lethal Audiogenic Seizures." *Journal of Biological Chemistry*. https://doi.org/10.1074/jbc.C000847200.

Kim, P. S., and P. Arvan. (1995) "Calnexin and BiP Act as Sequential Molecular Chaperones during Thyroglobulin Folding in the Endoplasmic Reticulum." *Journal of Cell Biology*. https://doi.org/10.1083/jcb.128.1.29.

Kiss, A., P. R.G. Zen, V. Bittencourt, G. A. Paskulin, R. Giugliani, A. D'Azzo, and I. V. Schwartz. (2008) "A Brazilian Galactosialidosis Patient given Renal Transplantation. A Case Report." *Journal of Inherited Metabolic Disease*. https://doi.org/10.1007/s10545-008-0730-3.

Kovačević, Goran, Sandra Radić, Biserka Jelenčić, Mirjana Kalafatić, Hrvoje Posilović, and Branka Pevalek-Kozlina. (2010) "Catalase in Vitro." *Plant Systematics and Evolution = Entwicklungsgeschichte Und Systematik Der Pflanzen*. https://doi.org/10.3989/scimar.2004.68n2211.

Laine, Roger A. (2008) "The Information-Storing Potential of the Sugar Code." In *Glycosciences*. https://doi.org/10.1002/9783527614738.ch1.

Li, Ping, Libin Zhou, Ting Zhao, Xiongxiong Liu, Pengcheng Zhang, Yan Liu, Xiaogang Zheng, and Qiang Li. (2017) "Caspase-9. Structure, Mechanisms and Clinical Application." *Oncotarget*.

https.//doi.org/10.18632/oncotarget.15098.

Loreto, Carla, Giampiero La Rocca, Rita Anzalone, Rosario Caltabiano, Giuseppe Vespasiani, Sergio Castorina, David J. Ralph, et al. (2014) "The Role of Intrinsic Pathway in Apoptosis Activation and Progression in Peyronie's Disease." *BioMed Research International*. https.//doi.org/10.1155/2014/616149.

Lou, Marjorie F., Guo Ming Wang, Fine Wu, Nalini Raghavachari, and John R. Reddan. (1998) "Thioltransferase Is Present in the Lens Epithelial Cells as a Highly Oxidative Stress-Resistant Enzyme." *Experimental Eye Research*. https.//doi.org/10.1006/exer.1997.0464.

Lukong, Kiven E., Volkan Seyrantepe, Karine Landry, Stéphanie Trudel, Ali Ahmad, William A. Gahl, Stéphane Lefrancois, Carlos R. Morales, and Alexey V. Pshezhetsky. (2001) "Intracellular Distribution of Lysosomal Sialidase Is Controlled by the Internalization Signal in Its Cytoplasmic Tail." *Journal of Biological Chemistry*. https.//doi.org/10.1074/jbc.M104547200.

MacCioni, Hugo J.F., Rodrigo Quiroga, and Mariana L. Ferrari. (2011) "Cellular and Molecular Biology of Glycosphingolipid Glycosylation." *Journal of Neurochemistry*. https.//doi.org/10.1111/j.1471-4159.2011.07232.x.

Malhotra, Jyoti D., and Randal J. Kaufman. (2007) "Endoplasmic Reticulum Stress and Oxidative Stress. A Vicious Cycle or a Double-Edged Sword?" *Antioxidants and Redox Signaling*. https.//doi.org/10.1089/ars.2007.1782.

Maor, Gali, Sigal Rencus-Lazar, Mirella Filocamo, Hermann Steller, Daniel Segal, and Mia Horowitz. (2013) "Unfolded Protein Response in Gaucher Disease. From Human to Drosophila." *Orphanet Journal of Rare Diseases* 8 (1). https.//doi.org/10.1186/1750-1172-8-140.

Meer, Gerrit Van, Dennis R. Voelker, and Gerald W. Feigenson. (2008) "Membrane Lipids. Where They Are and How They Behave." *Nature Reviews Molecular Cell Biology*. https.//doi.org/10.1038/nrm2330.

Miller, J. K., E. Brzezinska-Slebodzinska, and F. C. Madsen. 1993. "Oxidative Stress, Antioxidants, and Animal Function." *Journal of Dairy Science*. https.//doi.org/10.3168/jds.S0022-0302(93)77620-1.

Miyagi, Taeko, Kohta Takahashi, Koji Yamamoto, Kazuhiro Shiozaki, and Kazunori Yamaguchi. (2018) "Biological and Pathological Roles of Ganglioside Sialidases." In *Progress in Molecular Biology and Translational Science*. https.//doi.org/10.1016/bs.pmbts.2017.12.005.

Miyagi, Taeko, Tadashi Wada, Akihiro Iwamatsu, Keiko Hata, Yuko Yoshikawa, Satoru Tokuyama, and Masashi Sawada. (1999) "Molecular Cloning and Characterization of a Plasma Membrane-Associated Sialidase Specific for Gangliosides." *Journal of Biological Chemistry*. https.//doi.org/10.1074/jbc.274.8.5004.

Mochizuki, Atsuko, Yasufumi Motoyoshi, Megumi Takeuchi, Masahiro Sonoo, and Teruo Shimizu. (2000) "A Case of Adult Type Galactosialidosis with Involvement of Peripheral Nerves [2]." *Journal of Neurology*. https.//doi.org/10.1007/s004150070116.

Monti, Eugenio, Erik Bonten, Alessandra D'Azzo, Roberto Bresciani, Bruno Venerando, Giuseppe Borsani, Roland Schauer, and Guido Tettamanti. (2010) "Sialidases in Vertebrates. A Family Of Enzymes Tailored For Several Cell Functions." In *Advances in Carbohydrate Chemistry and Biochemistry*. https.//doi.org/10.1016/S0065-2318(10)64007-3.

Mullen, R. J., C. R. Buck, and A. M. Smith. (1992) "NeuN, a Neuronal Specific Nuclear Protein in Vertebrates." *Development*.

Mullen, Thomas D., Yusuf A. Hannun, and Lina M. Obeid. (2012) "Ceramide Synthases at the Centre of Sphingolipid Metabolism and Biology." *Biochemical Journal*. https.//doi.org/10.1042/BJ20111626.

Mütze, Ulrike, Friederike Bürger, Jessica Hoffmann, Helmut Tegetmeyer, Jens Heichel, Petra Nickel, Johannes R. Lemke, Steffen Syrbe, and Skadi Beblo. (2017) "Multigene Panel next Generation Sequencing in a Patient with Cherry Red Macular Spot. Identification of Two Novel Mutations in NEU1 Gene Causing Sialidosis Type I Associated with Mild to Unspecific Biochemical and Enzymatic Findings." *Molecular Genetics and Metabolism Reports*. https.//doi.org/10.1016/j.ymgmr.2016.11.004.

Neves, Juliana de Carvalho, Vanessa Rodrigues Rizzato, Alan Fappi, Mariana Miranda Garcia, Gerson Chadi, Diantha van de Vlekkert, Alessandra d'Azzo, and Edmar Zanoteli. (2015) "Neuraminidase-1 Mediates Skeletal Muscle Regeneration." *Biochimica et Biophysica Acta - Molecular Basis of Disease*. https.//doi.org/10.1016/j.bbadis.2015.05.006.

Ngamukote, Sathaporn, Makoto Yanagisawa, Toshio Ariga, Susumu Ando, and Robert K. Yu. (2007) "Developmental Changes of Glycosphingolipids and Expression of Glycogenes in Mouse Brains." *Journal of Neurochemistry*. https.//doi.org/10.1111/j.1471-4159.2007.04910.x.

Okada, Masahiko, Michi Ichiro Itoh, Masashi Haraguchi, Tetsuya Okajima, Masahiro Inoue, Hideto Oishi, Yoichi Matsuda, et al. (2002) "B-Series Ganglioside Deficiency Exhibits No Definite Changes in the Neurogenesis and the Sensitivity to Fas-Mediated Apoptosis but Impairs Regeneration of the Lesioned Hypoglossal Nerve." *Journal of Biological Chemistry*. https.//doi.org/10.1074/jbc.C100395200.

Pan, Xuefang, Camila De Britto Pará De Aragão, Juan P. Velasco-Martin, David A. Priestman, Harry Y. Wu, Kohta Takahashi, Kazunori Yamaguchi, et al. (2017) "Neuraminidases 3 and 4 Regulate Neuronal Function by Catabolizing Brain Gangliosides." *FASEB Journal*.

https.//doi.org/10.1096/fj.201601299R.

Papini, Nadia, Luigi Anastasia, Cristina Tringali, Gianluigi Croci, Roberto Bresciani, Kazunori Yamaguchi, Taeko Miyagi, et al. (2004) "The Plasma Membrane-Associated Sialidase MmNEU3 Modifies the Ganglioside Pattern of Adjacent Cells Supporting Its Involvement in Cell-to-Cell Interactions." *Journal of Biological Chemistry*. https.//doi.org/10.1074/jbc.M400881200.

Pasquel-Dávila, Daniela S, Sabrina A. Yanez-Vaca, Nicole D Espinosa-Hidalgo, and Evelin G Cuadros Buenaventura. (2019) "Gangliosides Generalities and Role in Cancer Therapies." *Bionatura*. https.//doi.org/10.21931/rb/cs/2019.02.01.28.

Pobre, Kristine Faye R., Greg J. Poet, and Linda M. Hendershot. (2019) "The Endoplasmic Reticulum (ER) Chaperone BiP Is a Master Regulator of ER Functions. Getting by with a Little Help from ERdj Friends." *Journal of Biological Chemistry*. https.//doi.org/10.1074/jbc.REV118.002804.

Privitera, Salvatore, Catherine A. Prody, John W. Callahan, and Aleksander Hinek. (1998) "The 67-KDa Enzymatically Inactive Alternatively Spliced Variant of β-Galactosidase Is Identical to the Elastin/Laminin-Binding Protein." *Journal of Biological Chemistry*. https.//doi.org/10.1074/jbc.273.11.6319.

Proia, Richard L. (2003) "Glycosphingolipid Functions. Insights from Engineered Mouse Models." In *Philosophical Transactions of the Royal Society B. Biological Sciences*. https.//doi.org/10.1098/rstb.2003.1268.

Ribeiro-Resende, Victor Túlio, Tiago Araújo Gomes, Silmara De Lima, Maiara Nascimento-Lima, Michele Bargas-Rega, Marcelo Felipe Santiago, Ricardo Augusto De Melo Reis, and Fernando Garcia De Mello. (2014) "Mice Lacking GD3 Synthase Display Morphological Abnormalities in the Sciatic Nerve and Neuronal Disturbances during Peripheral Nerve Regeneration." *PLoS ONE*. https.//doi.org/10.1371/journal.pone.0108919.

Saito, Megumi, and Robert K. Yu. (1995) “Biochemistry and Function of Sialidases.” In *Biology of the Sialic Acids*. https://doi.org/10.1007/978-1-4757-9504-2_8.

Sato, Kaoru, and Taeko Miyagi. (1996) “Involvement of an Endogenous Sialidase in Skeletal Muscle Cell Differentiation.” *Biochemical and Biophysical Research Communications*. https://doi.org/10.1006/bbrc.1996.0681.

Schadewijk, Annemarie Van, Emily F A Van'T Wout, Jan Stolk, and Pieter S. Hiemstra. (2012) “A Quantitative Method for Detection of Spliced X-Box Binding Protein-1 (XBP1) MRNA as a Measure of Endoplasmic Reticulum (ER) Stress.” *Cell Stress and Chaperones* 17 (2). 275–79. https://doi.org/10.1007/s12192-011-0306-2.

Schnaar, Ronald L. (2019) “The Biology of Gangliosides.” In *Advances in Carbohydrate Chemistry and Biochemistry*. https://doi.org/10.1016/bs.accb.2018.09.002.

Schröder, Martin, and Randal J. Kaufman. (2005) “ER Stress and the Unfolded Protein Response.” *Mutation Research - Fundamental and Molecular Mechanisms of Mutagenesis*. https://doi.org/10.1016/j.mrfmmm.2004.06.056.

Scorrano, Luca, Valeria Petronilli, Fabio Di Lisa, and Paolo Bernardi. (1999) “Commitment to Apoptosis by GD3 Ganglioside Depends on Opening of the Mitochondrial Permeability Transition Pore.” *Journal of Biological Chemistry*. https://doi.org/10.1074/jbc.274.32.22581.

Sewell, A. C., B. F. Pontz, D. Weitzel, and C. Humburg. (1987) “Clinical Heterogeneity in Infantile Galactosialidosis.” *European Journal of Pediatrics* 146 (5). 528–31. https://doi.org/10.1007/BF00441610.

Seyrantepe, Volkan, Maryssa Canuel, Stéphane Carpentier, Karine Landry, Stéphanie Durand, Feng Liang, Jibin Zeng, et al. (2008) "Mice Deficient in Neu4 Sialidase Exhibit Abnormal Ganglioside Catabolism and Lysosomal Storage." *Human Molecular Genetics*. https.//doi.org/10.1093/hmg/ddn043.

Seyrantepe, Volkan, Secil Akyildiz Demir, Zehra Kevser Timur, Johanna Von Gerichten, Christian Marsching, Esra Erdemli, Emin Oztas, et al. (2018) "Murine Sialidase Neu3 Facilitates GM2 Degradation and Bypass in Mouse Model of Tay-Sachs Disease." *Experimental Neurology*. https.//doi.org/10.1016/j.expneurol.2017.09.012.

Seyrantepe, Volkan, Karine Landry, Stéphanie Trudel, Jacob A. Hassan, Carlos R. Morales, and Alexey V. Pshezhetsky. (2004) "Neu4, a Novel Human Lysosomal Lumen Sialidase, Confers Normal Phenotype to Sialidosis and Galactosialidosis Cells." *Journal of Biological Chemistry*. https.//doi.org/10.1074/jbc.M404531200.

Seyrantepe, Volkan, Pablo Lema, Aurore Caqueret, Larbi Dridi, Samar Bel Hadj, Stephane Carpentier, Francine Boucher, et al. (2010) "Mice Doubly-Deficient in Lysosomal Hexosaminidase a and Neuraminidase 4 Show Epileptic Crises and Rapid Neuronal Loss." *PLoS Genetics*. https.//doi.org/10.1371/journal.pgen.1001118.

Shiozaki, Kazuhiro, Koichi Koseki, Kazunori Yamaguchi, Momo Shiozaki, Hisashi Narimatsu, and Taeko Miyagi. (2009) "Developmental Change of Sialidase Neu4 Expression in Murine Brain and Its Involvement in the Regulation of Neuronal Cell Differentiation." *Journal of Biological Chemistry*. https.//doi.org/10.1074/jbc.M109.012708.

Spoel, Aarnoud Van Der, Erik Bonten, and Alessandra D'Azzo. (1998) "Transport of Human Lysosomal Neuraminidase to Mature Lysosomes Requires Protective Protein/Cathepsin A." *EMBO Journal*. https.//doi.org/10.1093/emboj/17.6.1588.

Suzuki, Naoki, Masashi Aoki, Yuji Hinuma, Toshiaki Takahashi, Yoshiaki Onodera, Aya Ishigaki, Masaaki Kato, Hitoshi Warita, Maki Tateyama, and Yasuto Itoyama. (2005) "Expression Profiling with Progression of Dystrophic Change in Dysferlin-Deficient Mice (SJL)." *Neuroscience Research*. https.//doi.org/10.1016/j.neures.2005.01.006.

Tatem, Kathleen S., James L. Quinn, Aditi Phadke, Qing Yu, Heather Gordish-Dressman, and Kanneboyina Nagaraju. (2014) "Behavioral and Locomotor Measurements Using an Open Field Activity Monitoring System for Skeletal Muscle Diseases." *Journal of Visualized Experiments*. https.//doi.org/10.3791/51785.

Tessitore, Alessandra, Maria Del P. Martin, Renata Sano, Yanjun Ma, Linda Mann, Angela Ingrassia, Eric D. Laywell, Dennis A. Steindler, Linda M. Hendershot, and Alessandra D'Azzo. (2004) "GM1-Ganglioside-Mediated Activation of the Unfolded Protein Response Causes Neuronal Death in a Neurodegenerative Gangliosidosis." *Molecular Cell*. https.//doi.org/10.1016/j.molcel.2004.08.029.

Varki, Ajit. (1997) "Sialic Acids as Ligands in Recognition Phenomena." *The FASEB Journal*. https.//doi.org/10.1096/fasebj.11.4.9068613.

Vlekkert, Diantha van de, Jeroen Demmers, Xinh Xinh Nguyen, Yvan Campos, Eda Machado, Ida Annunziata, Huimin Hu, et al. (2019) "Excessive Exosome Release Is the Pathogenic Pathway Linking a Lysosomal Deficiency to Generalized Fibrosis." *Science Advances*. https.//doi.org/10.1126/sciadv.aav3270.

Volpe, Elisabetta, Manolo Sambucci, Luca Battistini, and Giovanna Borsellino. (2016) "Fas-Fas Ligand. Checkpoint of t Cell Functions in Multiple Sclerosis." *Frontiers in Immunology*. https.//doi.org/10.3389/fimmu.2016.00382.

Walter, Peter, and David Ron. (2011) “The Unfolded Protein Response. From Stress Pathway to Homeostatic Regulation.” *Science*. https.//doi.org/10.1126/science.1209038.

Wang, Jianfeng, Gusheng Wu, Taeko Miyagi, Zi Hua Lu, and Robert W. Ledeen. (2009) “Sialidase Occurs in Both Membranes of the Nuclear Envelope and Hydrolyzes Endogenous GD1a.” *Journal of Neurochemistry*. https.//doi.org/10.1111/j.1471-4159.2009.06339.x.

Wang, Jing, Allison Cheng, Chandramohan Wakade, and Robert K. Yu. (2014) “Ganglioside GD3 Is Required for Neurogenesis and Long-Term Maintenance of Neural Stem Cells in the Postnatal Mouse Brain.” *Journal of Neuroscience*. https.//doi.org/10.1523/JNEUROSCI.2275-14.2014.

Wu, Gusheng, Zi Hua Lu, Xin Xie, Bin Li, and Robert W. Ledeen. (2001) “Mutant NG108-15 Cells (NG-CR72) Deficient in GM1 Synthase Respond Aberrantly to Axonogenic Stimuli and Are Vulnerable to Calcium-Induced Apoptosis. They Are Rescued with LIGA-20.” *Journal of Neurochemistry*. https.//doi.org/10.1046/j.1471-4159.2001.00036.x.

Yamaguchi, Kazunori, Keiko Hata, Koichi Koseki, Kazuhiro Shiozaki, Hirotoshi Akita, Tadashi Wada, Setsuko Moriya, and Taeko Miyagi. (2005) “Evidence for Mitochondrial Localization of a Novel Human Sialidase (NEU4).” *Biochemical Journal*. https.//doi.org/10.1042/BJ20050017.

Yamanaka, Shoji, Mark D. Johnson, Alex Grinberg, Heiner Westphal, Jacqueline N. Crawley, Masako Taniike, Kinuko Suzuki, and Richard L. Proia. (1994) “Targeted Disruption of the Hexa Gene Results in Mice with Biochemical and Pathologic Features of Tay-Sachs Disease.” *Proceedings of the National Academy of Sciences of the United States of America*. https.//doi.org/10.1073/pnas.91.21.9975.

Yanagisawa, Hiromi, and Elaine C. Davis. (2010) "Unraveling the Mechanism of Elastic Fiber Assembly. The Roles of Short Fibulins." *International Journal of Biochemistry and Cell Biology*. https.//doi.org/10.1016/j.biocel.2010.03.009.

Yo, Shoyoku, Kazunori Hamamura, Yoshitaka Mishima, Kosuke Hamajima, Hironori Mori, Koichi Furukawa, Hisataka Kondo, et al. (2019) "Deficiency of GD3 Synthase in Mice Resulting in the Attenuation of Bone Loss with Aging." *International Journal of Molecular Sciences*. https.//doi.org/10.3390/ijms20112825.

Yogalingam, Gouri, Erik J. Bonten, Diantha van de Vlekkert, Huimin Hu, Simon Moshiach, Samuel A. Connell, and Alessandra d'Azzo. (2008) "Neuraminidase 1 Is a Negative Regulator of Lysosomal Exocytosis." *Developmental Cell*. https.//doi.org/10.1016/j.devcel.2008.05.005.

Yu, Robert K., Yoshihiko Nakatani, and Makoto Yanagisawa. (2009) "The Role of Glycosphingolipid Metabolism in the Developing Brain." *Journal of Lipid Research*. https.//doi.org/10.1194/jlr.R800028-JLR200.

Yu, Robert K., Yi Tzang Tsai, and Toshio Ariga. (2012) "Functional Roles of Gangliosides in Neurodevelopment. An Overview of Recent Advances." *Neurochemical Research*. https.//doi.org/10.1007/s11064-012-0744-y.

Zanoteli, Edmar, Diantha van de Vlekkert, Erik J. Bonten, Huimin Hu, Linda Mann, Elida M. Gomero, A. John Harris, Giulio Ghersi, and Alessandra d'Azzo. (2010) "Muscle Degeneration in Neuraminidase 1-Deficient Mice Results from Infiltration of the Muscle Fibers by Expanded Connective Tissue." *Biochimica et Biophysica Acta - Molecular Basis of Disease*. https.//doi.org/10.1016/j.bbadis.2010.04.002.